THERMOPLASTIC-FREE PAPER COATINGS AS SUSTAINABLE ALTERNATIVES FOR SINGLE-USE PLASTIC PACKAGING

By

Dhwani Kansal

A DISSERTATION

Submitted to
Michigan State University
in partial fulfillment of the requirements
for the degree of

Chemistry-Doctor of Philosophy

2021

ABSTRACT

THERMOPLASTIC-FREE PAPER COATINGS AS SUSTAINABLE ALTERNATIVES FOR SINGLE-USE PLASTIC PACKAGING

By

Dhwani Kansal

Plastics are one of the most widely used classes of synthetic products due to their lightweight nature, affordability, and versatility. However, commonly used plastics are non-biodegradable and have low recycling rates that have created environmental issues. Paper is considered to be an excellent alternative to plastics in certain packaging applications due to its biodegradability, low-cost, and good mechanical properties. However, the porous texture and polar chemistry of paper make them unfit for containing liquid products and thus limit its applicability. This problem is circumvented by applying plastic and per- and polyfluoroalkyl substances (PFAS) coatings onto paper. However, plastic is non-biodegradable, and PFAS is harmful, and their accumulation in ecosystems poses threats to human health and the environment.

This thesis work is aimed to address the current non-sustainable challenges associated with coated paper. Three approaches were used to develop environmentally friendly and sustainable coatings. The aim of **Approach 1** is to develop chitosan- and zein-based dual-layer coatings as novel paper coating materials because both chitosan and zein are biobased, biodegradable, and food safe materials. Kraft paper was coated with an oil-resistant chitosan solution as the first layer and subsequently by a hydrophobic zein solution as the top layer. The resultant chitosan-zein-coated paper showed significant water resistance (Cobb 60 value of 4.88 g/m²) and oil repellency (kit rating of 12/12). Scanning electron microscopy (SEM) analysis showed that the pores were masked upon coating with chitosan and zein dual-layer coating that led to the improvement in

water- and oil- resistance. The desirable mechanical properties of the coated paper were retained after the coating treatment. In addition, the pulp was recovered from the chitosan-zein-coated paper to validate the recyclability of this novel approach percentage of recovery and properties of recoverable materials. Approach 2 is aimed to replace chitosan with a less expensive material such as starch in the dual layer paper coating. Again, starch is widely available, and due to the similar chemical structure with that of chitosan, it shows the same oil resistance as chitosan. Accordingly, starch and zein dual-layer coatings were applied onto a Kraft paper and yielded a low Cobb 60 value of 4.81 g/m². In addition, the coated paper exhibited excellent grease resistance with a kit rating of 12/12. SEM characterization confirmed that the dual-layer coating filled the pores of the paper substrate. The mechanical properties, as well as the thermal stability of the paper, remained essentially unchanged after the coating treatments. Approach 3 is focused on the use of single-layer coating to obtain water and oil resistant coatings. Here, sunflower oils were first modified and then grafted onto chitosan using industry-relevant epoxidation chemistry. The obtained chitosan-graft-oil was coated onto paper for the water and oil resistance properties. Cobb 60 and kit rating values were determined to be 8.00 g/m² and 7.66, respectively, for the optimal formulations. Considering the excellent sustainability i.e., ability to be reused without depletion of natural resources, of our developed paper (e.g., thermoplastic-free, PFAS-free, repulpable, and biodegradable), this work offers a multitude of packaging applications with invaluable benefits for human, animal health, the environment, as well as industry.

Copyright by DHWANI KANSAL 2021 This thesis is dedicated to my parents Pawan K. Kansal and Neeraj Kansal Thank you

ACKNOWLEDGEMENTS

I would like to express my deepest thanks to my Ph.D. supervisor Dr. Muhammad Rabnawaz. I truly believe this journey would not have been possible without his efforts. He has been extremely supportive and understanding throughout my Ph.D. I would also like to thank my committee members Dr. Karen Draths, Dr. Gary Blanchard and Dr. Donatien Kamdem for their valuable comments and suggestions on my research work.

Special thanks to Dr. Gary Blanchard for supporting my career my giving continuous financial support through teaching assistant position. Thanks to Anna Osborn who was always ready to give quick suggestions and a helping hand. I would also like to thank all the staff members of the Department of Chemistry, who have been helpful in keeping the resources handy.

My heart filled acknowledgement to all the members of the research group. They have made the research fun and interesting over the years. The time spent with them has been extremely memorable and close to my heart.

I would like to extend my acknowledgement to my parents who have been very supportive when I did not believe in myself. They have made me capable in every way to be able to finish this journey.

Lastly, I would like to thank my amazing friends and colleagues who have supported me and made all these years of hectic studies and work, a memorable journey. I have spent some amazing times with you all. Special thanks to Meenal, Brijen, Aditya for always boosting my moral.

TABLE OF CONTENTS

LIST OF TABLES	X
LIST OF FIGURES	xi
LIST OF SCHEMES	xiv
KEY OF ABBREVATIONS	XV
Chapter 1: INTRODUCTION	1
1.1 Background and Motivation:	
1.2 Goals and Objectives	5
REFERENCES	8
Chapter 2: LITERATURE REVIEW	14
2.1 Biobased polymers and its importance	
2.1.1 Polysaccharides	
2.1.2 Zein- Properties and paper coating applications	
2.2 Industrially used Paper Coating methods	21
2.2.1 Multi-layer and lamination method	
2.2.2 Blending or emulsion	
2.2.3 Chemical modification	
2.3 Coating Methods	22
2.3.1 Rod coating	22
2.3.2 Dip coating	
2.3.3 Spray coating	
REFERENCES	25
Chapter 3: MATERIALS AND CHARACTERIZATION	30
3.1 Materials	
3.2 Coating Procedure	
3.3 Characterization	
3.3.1 Wettability	
3.3.2 Barrier properties	
3.3.3 Mechanical properties	
3.3.4 Recyclability	
3.3.5 Basis weight, coating load and material thickness	
3.3.6 Scanning electron microscopy (SEM)	
3.3.7 Thermogravimetric analysis (TGA)	
3.3.8 Attenuated-Total-Reflection Fourier-Transform Infrared ATR-FTIR	analysis
2.2.0 C.1	
3.3.9 Gel permeation chromatography (GPC)	
3.3.10 Differential scanning calorimetry (DSC)	44 44
a a la nuclear magnetic resonance	44

REFERENCES	45
Chapter 4: FOOD-SAFE CHITOSAN-ZEIN DUAL-LAYER COATING FOR WA	TER- AND
OIL-REPELLANT PAPER SUBSTRATES	
4.1 Summary	
4.2 Experimental	
4.2.1 Materials	
4.3 Methods and Characterization	
4.3.1 Preparation of chitosan and zein stock solutions	
4.3.2 Characterization	
4.3.3 Recyclability	
4.3.4 Mechanical Properties	
4.4 Results and Discussion	
4.5 Conclusions	
REFERENCES	
Chapter 5: STARCH AND ZEIN BIOPOLYMERS AS A SUSTAINABLE REPLACE	CEMENT
FOR PFAS, SILICONE OIL AND PLASTIC-COATED PAPER	
5.1 Summary	
5.2 Experimental	
5.2.1 Materials	
5.3 Methods and Characterization	77
5.3.1 Solution preparation of starch and zein and coating method	77
5.3.2 Characterization	
5.3.3 Recyclability	
5.3.4 Mechanical Properties	
5.4 Results and Discussion	
5.5 Conclusion	95
REFERENCES	97
CL C EADDICATION OF OUR AND WATER REGISTANT RARER WITHOUT	T I'M
Chapter 6: FABRICATION OF OIL- AND WATER-RESISTANT PAPER WITHO	
CREATING MICROPLASTICS ON DISPOSAL	
6.1 Summary	
6.2 Experimental	
6.2.1 Materials	
6.3 Methods and Characterization	
6.3.1 Synthesis of epoxidized sunflower oil (ESO)	
6.3.2 Preparation of the chitosan stock solution	
6.3.3 Synthesis of chitosan- <i>graft</i> -sunflower oil	
6.4 Coating Procedure	
6.5 Characterization	
6.6 Results and Discussion	
6.7 Conclusions	
REFERENCES	120
Chapter 7: CONCLUSIONS AND FUTURE OUTLOOK	122
A DIZURGE E CALING A CINICANA PANTA POLITICA PARTA DALLA JAMA	1//

7.1 Conclusions	122
7.2 Future Outlook	123
APPENDICES	125

LIST OF TABLES

Table 2.1: Summary of previously reported data on biopolymers in coatings and its properties24
Table 3.1: Instruments and TAPPI standards used for measuring tensile strength, compressing strength on the edge, bending stiffness and internal tearing resistance
Table 4.1: Comparison of the Cobb 60 values and Kit ratings for various coated paper substrates 55
Table 4.2: Basis weight, thickness and coating load of uncoated and coated paper 56
Table 5.1: Comparison of Cobb 60 values and kit ratings for S5Z10-coated paper, reverse coated Z10S5 paper and mix coated S5Z10 paper 82
Table 5.2: Coating content and thickness of uncoated and coated paper 83
Table 6.1: Amounts of the different starting materials. 101
Table 6.2: (a) Cobb 60 (g/m²) and (b) kit ratings of paper samples bearing CS-g-SO copolymers with various compositions
Table 6.3: Material thickness, basis weight and coating load for uncoated and coated paper 111

LIST OF FIGURES

Figure 2.1: Overview of classification of bio-based polymers
Figure 3.1: Coating procedure (a) bar coating machine (b) blank Kraft paper attached with a rod (c) even coating of solution with rod (d) final coated paper
Figure 3.2: Depiction of three contact surface line for a water droplet on a solid surface 33
Figure 3.3: (a) Cassie state, (b) Wenzel state for a liquid droplet on solid surface
Figure 4.1: Illustration of various coatings on paper with respect to their water and oil repellency. a) Zein-coated paper exhibits water resistance but prone to permeation by oils; b) Chitosan-coated paper is oil resistant but allows the passage of water; c) a zein and chitosan blend coating allows the passage of both water and oil; and d) a dual-layer coating (with a chitosan bottom and zein top layer) prevents the passage of both water and oils
Figure 4.2: ATR-FTIR spectra of uncoated paper (U-p), 2% chitosan-coated paper (C2-p), 20% zein-coated paper (Z20-p), and dual-layer-coated paper (C2Z20-p). Two IR portions are zoom-in for clarity
Figure 4.3: Permeability $(g \cdot \mu m/m^2 \cdot day \cdot Pa)$ and Cobb 60 values (g/m^2) of coated and uncoated paper samples at 50% RH and 25 °C. The average thickness of all coated papers was $\sim 200~\mu m$.
Figure 4.4: Sliding angles and CAs (after 30 s) of: a) water b) castor oil
Figure 4.5: Kit ratings of coated and uncoated paper samples. A kit rating of '12' corresponds to the maximum oil-resistance, while a value of '0' corresponds to a complete lack of oil resistance.
the maximum oil-resistance, while a value of '0' corresponds to a complete lack of oil resistance.
the maximum oil-resistance, while a value of '0' corresponds to a complete lack of oil resistance. 65 Figure 4.6: SEM images (200×) of unmodified paper U-p (a), chitosan-coated paper C2-p (b), zein-coated paper Z20-p (c), as well as the chitosan and zein bilayer-coated paper C2Z20-p (d).
the maximum oil-resistance, while a value of '0' corresponds to a complete lack of oil resistance. 65 Figure 4.6: SEM images (200×) of unmodified paper U-p (a), chitosan-coated paper C2-p (b), zein-coated paper Z20-p (c), as well as the chitosan and zein bilayer-coated paper C2Z20-p (d). 66 Figure 4.7: TGA (a) and DTG (b) plots of uncoated paper (U-p) and coated paper (C2, Z20, C2Z20). Also shown are TGA (c) and DTG (d) plots of the chitosan coating (C2), Zein coating

and e) unwashed pulp. The brown color of the paper is primarily due to the use of unbleached Kraft paper
Figure 5.1: Illustration of various coating on paper substrate and their anticipated water and oil repellencies. a) A zein-starch blend coating allows the passage of both water and oil. b) A dual-layer coating with zein comprising the bottom layer and starch forming the top layer only retains oil but permits the passage of water. c) A dual-layer coating in which starch comprises the bottom layer and zein forms the top layer offers a barrier against both oil and water
Figure 5.2: ATR-FT-IR spectra of uncoated paper (U-p), 5% (w/v) starch-coated paper (S5-p), 10% (w/v) zein-coated paper (Z10-p), and bilayer-coated paper (S5Z10-p)
Figure 5.3: Permeability (g·μm/m²·day·Pa) and Cobb 60 values (g/m²) of coated and uncoated paper samples at 25 °C and 50% RH
Figure 5.4: Contact angles (at 30 s and 5 min) and sliding angles of a) water b) castor oil. [WCA: Water contact angle and OCA: Oil contact angle]
Figure 5.5: Kit ratings of coated paper and control. Higher number denotes higher oil-resistance and vice versa
Figure 5.6: SEM images (200×) of: (a) unmodified paper (U-p); (b) starch-coated paper (S5-p); (c) zein-coated paper (Z10-p); and (d) starch-zein dual-layer-coated (S5Z10-p)91
Figure 5.7: Mechanical properties of the uncoated paper (U-p), and coated paper (S5, Z10 and S5Z10) including a) The tensile strength, b) ring crush test, c) bending stiffness, and d) internal tearing.
Figure 5.8: Photographs of repulped paper samples after various washing treatments. (a) Uncoated paper pulp that had been washed with distilled water; (b) S5Z10-coated paper pulp that had been washed with distilled water; (c) S5Z10-coated paper pulp that had been washed first with distilled water and then with an 85% ethanol solution; and (d) S5Z10-coated paper pulp that had washed with first with distilled water and then with 85% ethanol
Figure 6.1: ¹ H NMR spectrum of sunflower oil (a) before epoxidation. Also shown are ¹ H NMR spectra of epoxidized sunflower oil, including (b) ESO1 and (c) ESO2
Figure 6.2: ATR-FTIR spectra of un-epoxidized sunflower oil (SO), epoxidized sunflower oil (ESO1 and ESO2), and chitosan-g-sunflower oil (CS-g-SO2)
Figure 6.3: ¹ H NMR spectra of: (a) 2 wt% chitosan, (b) chitosan-g-SO1 after heating at 70 °C for 3 h, and (c) chitosan-g-SO2 after heating at 70 °C for 3 h
Figure 6.4: ATR-FTIR spectra of uncoated paper (U-p), 2% w/v chitosan-coated paper (CS2-p), and chitosan-g-sunflower oil-coated paper (CS-g-SO1-p and CS-g-SO2-p)
Figure 6.5: Permeability (g·μm/m²·day·Pa) and Cobb 60 values of coated and uncoated paper samples

Figure 6.6: Kit ratings of coated and uncoated paper samples.
Figure 6.7: (a) Water contact angles and water sliding angles (°) as well as (b) oil contact angles and oil sliding angles (°) of coated and uncoated paper samples. The water and oil contact angles were recorded 30 s after the droplet had been placed on each surface
Figure 6.8: SEM images of (a) uncoated paper (U-p), (b) chitosan-coated paper (CS2-p), (c chitosan-g-SO1-coated paper (CS-g-SO1-p), and (d) chitosan-g-SO2-coated paper (CS-g-SO2-p)

LIST OF SCHEMES

Scheme 2.1: Chemical structures of chitin, chitosan, starch and backbone of zein	16
Scheme 6.1: Depection of interaction of chitosan-g-sunflower oil with paper substrate	100
Scheme 6.2: Synthetic route toward the epoxidized sunflower oil.	105
Scheme 6.3: Proposed opening of oxirane ring of epoxidized sunflower oil with chitosan to chitosan-g-sunflower oil.	

KEY OF ABBREVATIONS

LDPE Low Density Polyethylene

PVDC Polyvinylidene chloride

PLA Polylactic acid

EU European Union

PFAS Per- and polyfluoro Alkyl Substabces

PDMS Polydimethyl siloxane

WVTR Water Vapor Transmittance Rate

USDA United States Department of Agriculture

PHAs Polyhydroxy alkanoates

PBS Poly (butylene succinate)

PET Polyethylene Terepthalate

WCA Water Contact Angle

HDPE High Density Polyethylene

DI Deionized

RH Relative Humidity

TAPPI Technical Association of the Pulp and Paper Industry

ACA Advancing Contact Angle

RCA Receding Contact Angle

CAH Contact Angle Hysteresis

ISO International Organization for Standardization

ASTM American Society for Testing and Materials

SCCM Standard Cubic Centimeter per Minute

MD Machine Direction

CD Cross Direction

RCT Ring Crush Test

BS Bending Stiffness

SEM Scanning Electron Microscopy

TGA Thermogravimetric Analysis

FTIR Fourier-transform Infrared

ATR Attenuated Total Reflectance

GPC Gel Permeation Chromatography

DSC Differential Scanning Calorimetry

NMR Nuclear Magnetic Resonance

CS Chitosan

OCA Oil Contact Angle

Chapter 1: INTRODUCTION

1.1 Background and Motivation:

With increase in the use of single-use plastics, the proliferation of microplastics in the ocean and other water bodies is becoming an alarming issue. Microplastics are plastic particles with diameters <5 mm that can reside in the environment (e.g., water bodies, soil, and air). ¹⁻⁴ These microplastics are created due to the UV light and mechanical degradation of plastics in the environment. The plastics used today are predominantly non-biodegradable, and as a result microplastics accumulate in the environment and they are million times more than previously thought. ⁵ To address these problems associated with microplastics, it is necessary to replace non-biodegradable plastics with biodegradable alternatives. Paper can prove to be a great alternative as it can be recycled again for use.

Paper has been known for more than two thousand years now and has been an essential part of our civilization. The paper is reported to be invented by the Chinese in around 105 A.D. by reducing the fibrous matter of the wood to a pulp in water and then forming it into a long network. Since then, it has been used in day to day life, with almost 42% used for newspapers, printing, and writing and nearly 46% used for packaging applications. By mass, paper contributes >51% of all materials used in the US packaging sector. The high demand of paper in packaging applications, is due to several factors. First, the raw materials for paper are inexpensive compared to synthetic plastic and are derived from renewable source. Paper is not renewable itself, but materials used to make paper, make it renewable. Second, paper is lightweight (compared to glass, metals) thus less energy required for transportation. Third, due to the long network of the fibers paper shows good mechanical property such as stiffness, tensile strength, compression, tear, burst, optical, porosity.

Fourth, excellent biodegradability and highest rate of recyclability among all packaging materials.^{6–8} Paper is made from natural plant fibers (mainly wood), which leads to the biodegradability of the paper in the environment (e.g., soil, ocean). Also, after usage, paper can be recycled easily to get back the raw paper. Despite of all the great benefits, paper in its native form is unfit for many packaging applications primarily due to their tendency to absorb water (hydrophilic) and oils (oleophilic).

In order to understand how paper can be modified to achieve water and oil repellency, it is essential to understand the chemical nature of the paper. Paper is derived from plants, which are mainly fibers. These fibers are mostly composed of carbohydrates (e.g., cellulose, hemi-cellulose, and lignocellulose). Carbohydrates has numerous hydroxyl groups with a strong tendency to form hydrogen bonds with water, making them strong water absorbents Paper is known to be porous material with pores of different sizes. These pores lead to the absorption of water and other similar liquids in it.

Over the years, research has been done to improve the water and oil resistance of paper-based products. Chemical modification of the surface of the paper using grafting, 9-11 layer-by-layer 12,13 coatings etc. approaches have been developed along with physicochemical modification like paper sizing/coating, plasma etching 14 etc. Paper sizing and paper refining 15-18 have been widely used by the industry in order to improve the water- and oil- resistance of the paper products. However, limited success is achieved in this direction towards robust water and oil resistance paper. 19 On the other hand, coatings, and laminations are the surface modification approaches that have been commercialized and are widely used in our daily lives (e.g., LDPE laminated paper coffee cup). However, these coatings/liners are mostly non-biodegradable, and their separation from the paper is challenging, and accordingly, they end up in landfills/oceans with problems of

microplastics. Though in some cases biologically available wax from honeybee is used for coffee cups, however, wax is challenging to remove from paper during repulping process.

Latex based coatings have been used to achieve water-repellent paper²⁰. Most commonly used latex is styrene-butadiene latex which is non-biodegradable and ends up as microplastics in oceans and landfills after usage of the paper.²¹ In addition, latexes are water-based coatings and require surfactants and other polar groups for dispersion in water prior to application on paper substrate.²² The presence of these polar groups renders the performance of latex-based coated papers towards water absorption and leaves the coated paper more hydrophilic. Polyvinylidene chloride (PVDC)^{23,24} latex are also used for paper coating to impart great water- and oil-repellency; however, their non-biodegradable nature and difficulties in their separation from paper, has created landfilling and ocean pollution.

In summary, the presence of non-biodegradable thermoplastic coated paper single-use packaging has created significant environmental challenges. Recently, the EU parliament also voted to ban single-use plastics from cutlery, plates, and straws and urged reduced use of single-use cups and beverage containers.²⁵ Laminated and waxed based coatings have also proved to be a great alternative for water- and oil- resistance in paper coatings for food packaging applications, however difficulties have been faced to separate them from the paper pulp after recycling of paper.^{26,27}

Per- and polyfluoroalkyl substances (PFAS) are compounds containing fluorine atoms. Owing to low surface energies of fluorochemicals, the PFAS coated papers show excellent waterand oil- repellency. PFAS coated papers are widely used in food takeout containers, disposal plates, food wrappers, etc. However, PFAS are harmful, and their leakage into environment has adverse effects on the environment.^{28,29} For example, EPA has also called for strategies for analysis

and separation from the environment.³⁰ Bans are being implemented PFAS uses in non-critical applications (e.g., packaging).

Apart from synthetic non-biodegradable polymers there has been an advancement in the use of polylactide (PLA), a biobased thermoplastic for coatings in paper products. PLA is derived from renewable sources like corn starch, cassava roots, sugarcane. PLA has shown good waterand oil- repellency, however PLA does not biodegrade in the natural environment and like other thermoplastics is difficult to separate form coated paper. A low degradation temperature (thermal/hydrolytic instability) of PLA also limits its uses.

To overcome the problems with aforementioned coating methods, biopolymers like proteins, ³⁷⁻⁴⁰ polysaccharides ^{13,41,42} and lipids ⁴³⁻⁴⁵ have been studied for their applications in paper coatings. The biopolymers are of great attention due to their biocompatibility, biodegradability, and renewability. For example, chitosan is a polysaccharide derived from deacetylation of chitin has been studied for use as edible films, coating for packaging materials as they have good barrier properties against moisture. 46-49 However, due to the presence of hydroxyl groups chitosan coated papers tend to form hydrogen bonds quickly with water and leads to absorption of water.⁵⁰ On the other hand, chitosan due to the presence of polar groups shows good oil repellency.⁵¹ Starch is another polysaccharide that can be derived from highly renewable sources like potato, corn, cassava, etc. Starch has a similar chemical structure to chitosan with hydroxyl groups on its surface and therefore is known to impart similar hydrophilic properties like chitosan. However, starch is much cheaper as compared to chitosan and therefore can be commercialized without adding any extra cost to the coated paper products.⁵² Starch is widely used in paper industries as an intern and external sizing as glue to retain fine short fibers in the paper network and additives in paper and for surface improvements for improvement of stiffness.

Lipids are a class of organic compounds such as waxes and fatty acids that are known to have great hydrophobicity. The hydrophobic properties of lipids come from the long alkyl chains, such as in oils. Oils can be produced as a co-product from bioethanol industry. It was also reported in a 2017 report by the Renewable Fuels Association, that almost 375 million pounds of corn oil was produced by the bioethanol industry in the USA alone. Proteins are another class of good source of bio-based polymers. Proteins are usually made up of amino acids and depending on the Renewable Fuels are usually made up of amino acids and depending on the report in amino acid, they can be either hydrophilic or hydrophobic in nature. For example, zein is protein found in corn, that is known to possess 55% hydrophobic and 45% hydrophilic groups. The majority of hydrophobic groups in zein renders it to be hydrophobic in nature and therefore is known to repel water.

Polydimethylsiloxane (PDMS) is a prominent member of polysiloxanes with siliconoxygen backbone and two methyl pendant groups. PDMS has been receiving attention in the field of coating due to their hydrophobic nature. PDMS has low surface energy (second lowest surface energy after fluorochemicals) but are considered environment friendly and has low cost compared to PFAS chemicals. Therefore, PDMS has proved be a great alternative to fluorochemicals in recent times.⁵⁸ Chemical grafting of PDMS onto chitosan has also been previously studied and it may be used to achieve both water- and oil- repellency for paper coatings.^{59,60}

1.2 Goals and Objectives

The overall goal of this study is to develop sustainable water and oil-resistant paper coatings without thermoplastic- nor PFAS, inexpensive, renewable, and biodegradable.

The above stated goals will be accomplished by the following objectives:

- 1. Develop a thermoplastic free chitosan-zein dual layer coated paper for both water- and oil- resistant: Our hypothesis is that a dual layer coating of the paper substrates with water- and oil- resistant materials could perform better as opposed to single layer coated papers with the same materials. The overall thickness of the coated paper will be higher than a single layer coated paper. Chitosan and zein are both bio-based, biodegradable and food-safe materials that may ensure the low-cost of the coated papers. To test the hypothesis a paper will be first coated with chitosan to control oil migration, followed by a second layer of zein as the top coating to control the migration of polar liquid like water. The coated papers will be tested for water- and oil- resistance and the repulpability.
- 2. Develop starch and zein dual layer coated paper for low cost of coated papers: In this hypothesis we are trying to bring the cost of the coated paper down using a dual-layer coating method. Here, food-grade chitosan which is an oil- resistant polysaccharide and relatively expensive has been replaced with starch. Starch is a polysaccharide with chemical structure similar to chitosan, hence we anticipate a similar performance of starch compared to chitosan as coating material. The first coating will be an oil- resistant starch followed with a second layer of zein, a water-resistant material. The coated papers will be tested using Cobb60 and kit rating for water and oil-resistance, respectively. The water barrier (such as WVTR values), repulpability, mechanical properties will also be evaluated.
- 3. Develop water- and oil- resistant paper from oil grafted chitosan with zero plastic waste: Here, we will develop a single layer paper coating that will be focus on the modification of chitosan with plants oil. The oil is a triglyceride with long alkyl chain and reactive groups such as hydroxyl, carboxyl etc. In this case, sunflower oil will be chemically grafted onto chitosan. The prepared solution will be coated on paper as a single layer. Our hypothesis is that this coating will

impart water- resistance due to the presence of long alkyl chains from sunflower oil and oil-resistance due to the hydroxyl groups present on chitosan.

REFERENCES

REFERENCES

- 1. Gallowaya, T. S. & Lewisa, C. N. Marine microplastics spell big problems for future generations. *Proceedings of the National Academy of Sciences of the United States of America* **2016**, *113*, 2331–2333.
- 2. Gandara e Silva, P. P., Nobre, C. R., Resaffe, P., Pereira, C. D. S. & Gusmão, F. Leachate from microplastics impairs larval development in brown mussels. *Water Res.* **2016**, *106*, 364–370.
- 3. Chubarenko, I., Bagaev, A., Zobkov, M. & Esiukova, E. On some physical and dynamical properties of microplastic particles in marine environment. *Mar. Pollut. Bull.* **2016**, *108*, 105–112.
- 4. Underwood, A. J., Chapman, M. G. & Browne, M. A. Some problems and practicalities in design and interpretation of samples of microplastic waste. *Analytical Methods* **2017**, *9*, 1332–1345.
- 5. Microplastics million times more abundant in the ocean than previously thought *NSF National Science Foundation*. **2019**. https://www.nsf.gov/discoveries/disc_summ.jsp?cntn_id=299718&org=NSF&from=news.
- 6. Deshwal, G. K., Panjagari, N. R. & Alam, T. An overview of paper and paper based food packaging materials: health safety and environmental concerns. *Journal of Food Science and Technology* **2019**, *56*, 4391–4403 (2019).
- 7. Nicu, R., Lupei, M., Balan, T. & Bobu, E. Alkyl-Chitosan as Paper Coating Material to Improve Water Barrier Properties. *Cellulose Chem. Technol.*, **2013** *47* (7), 623-630.
- 8. William E. Scott and James C. Abbott. *Properties of paper: An Introduction*. (1989).
- 9. Gryuter, D. Chemical modification of pulp fibers by TEMPO-mediated oxidation. *Nordic Pulp & Paper Research Journal* **1999**, *14(4)*.
- 10. Hon, D. S. *Chemical Modification of Lignocellulosic Materials*. New York: Routledge, 1996. doi:doi.org/10.1201/9781315139142.
- 11. Roy, D., Semsarilar, M., Guthrie, J. T. & Perrier, S. Cellulose modification by polymer grafting. *Chem. Soc. Rev.* **2009**, *38*, 2046–2064.
- 12. Chuan-Fu, L., Ai-Ping, Z., Wei-Ying, L., Feng-Xia, Y. & Run-Cang, S. Homogeneous modification of cellulose in ionic liquid with succinic anhydride using n-bromosuccinimide as a catalyst. *J. Agric. Food Chem.*, **2009**, *57*, 1814–1820.
- 13. Yang, J., Li, H., Lan, T., Peng L., Cui, R., Yang, H. Preparation, characterization, and

- properties of fluorine-free superhydrophobic paper based on layer-by-layer assembly. *Carbohydr. Polym.* **2017,** *78*, 228–237.
- 14. Dimitrakellis, P., Travlos, A., Psycharis, V. P. & Gogolides, E. Superhydrophobic Paper by Facile and Fast Atmospheric Pressure Plasma Etching. *Plasma Process. Polym.* **2017**, *14*, 1600069.
- 15. Guo, Y. H., Guo, J. J., Miao, H., Teng, L. J. & Huang, Z. Properties and paper sizing application of waterborne polyurethane emulsions synthesized with isophorone disocyanate. *Prog. Org. Coatings* **2014**, 77, 988–996.
- 16. Kiuru, J., Sievänen, J., Tsitko, I., Pajari, H. & Tukiainen, P. A new dual biocide concept for fine papermaking. *Paper Conference and Trade Show 2010, PaperCon 2010* **2010**, *1*, 598–629.
- 17. Hubbe, M.A. Paper's Resistance to Wetting-A Review of Internal Sizing Chemicals and their Effects. *BioResources* **2006**, *2*(*1*), 106-145.
- 18. Dang, C., Xu, M., Yin, Y. & Pu, J. Preparation and Characterization of Hydrophobic Non-Crystal Microporous Starch (NCMS) and its Application in Food Wrapper Paper as a Sizing Agent. *BioRes.* **2017**, *12*(*3*), 5775-5789.
- 19. Samyn, P. Wetting and hydrophobic modification of cellulose surfaces for paper applications. *Journal of Materials Science* **2013**, *48*, 6455–6498.
- 20. Lee, D. I. Latex Applications in Paper Coating. *Polymeric Dispersions: Principles and Applications*, **1997**, *335*.
- 21. Lee D.I. Latex Applications in Paper Coating. Asua Polymeric Dispersions: Principles and Applications. NATO ASI Series (Series E: Applied Sciences), 1997, 335, Springer, Dordrecht. doi.org/10.1007/978-94-011-5512-0 32
- 22. Du, Y., Zang, Y.-H. & Du, J. Effects of Starch on Latex Migration and on Paper Coating Properties. *Ind. Eng. Chem. Res.***2011**, *50*, 9781–9786.
- 23. Martin, L. L., Minn., S., Paper Laminate and Method for Producing the Laminate for Paperboard Containers. United States Pat., US4806398, **1989**, *427*, 391.
- 24. Rastogi, V. & Samyn, P. Bio-Based Coatings for Paper Applications. *Coatings* **2015**, *5*, 887–930.
- 25. US EPA, O. O. of R. C. and R. Municipal Solid Waste, https://archive.epa.gov/epawaste/nonhaz/municipal/web/html/index.html.
- 26. B. Shoot, EU Parliament Votes to Ban Single-Use Plastics, Including Plates, Cutlery, and Straws, Http://Fortune.Com/2018/10/24/Eu-Ban-Single-Use-Plastic-Pollution/(Accessed

- 4-2, 2019).
- 27. Oswald R. G., Harvey, W. T., Johnson, H. L. Wax-coated paper United States Pat., US3231462A, 1961.
- 28. Knights, E. F. Wax coated paper of improved water resistance. United States Pat., US3874905. 1973.
- 29. Zhang, X., Wang, H., Liu, Z., Zhu, Y., Wu, S., Wang, C., Zhu, Y. Fabrication of durable fluorine-free superhydrophobic polyethersulfone (PES) composite coating enhanced by assembled MMT-SiO 2 nanoparticles. *Appl. Surf. Sci.* **2017**, *396*, 1580–1588.
- 30. Rosenmai, A. K., Taxvig, C., Svingen, T., Trier, X., Vugt-Lussenburg, B. M. A., Pedersen, M., Lesne, L., Jegou, B., Vinggaard, A. M. Fluorinated alkyl substances and technical mixtures used in food paper-packaging exhibit endocrine-related activity in vitro. *Andrology* **2016**, *4*, 662–672.
- 31. Paper and Paperboard: Material-Specific Data, Facts and Figures about Materials, Waste and Recycling. US EPA. https://www.epa.gov/facts-and-figures-about-materials-waste-and-recycling/paper-and-paperboard-material-specific-data.
- 32. Rastogi, V. K. & Samyn, P. Bio-based coatings for paper applications. *Coatings* **2015**, *5*, 887–930.
- 33. Clevelan, C. S., Reighard T. S., Marchman, J. I. Biodegradable paper-based laminate with oxygen and moisture barrier properties and method for making biodegradable paper-based laminate. United States Pat., US8637126B2 **2006**.
- 34. Uemura, M. Yamamatsu, T. Paper Cup Compromising a Shet of Polylactic Acid Laminated Paper. United States Pat., US20080176015A1, **2007**.
- 35. Uemura, M. Yamamatsu, T. Paper Cup Compromising a Shet of Polylactic Acid Laminated Paper. United States Pat., US20080176015A1, **2007**.
- 36. Khwaldia, K., Arab-Tehrany, E. & Desobry, S. Biopolymer Coatings on Paper Packaging Materials. *Compr. Rev. Food Sci. Food Saf.* **2010,** *9*, 82–91.
- 37. C. K. Wong and L. C. Wadsworth. European Pat., EP 2913361 A1. 2015.
- 38. Guillaume, C., Pinte, J., Gontard, N. & Gastaldi, E. Wheat gluten-coated papers for biobased food packaging: Structure, surface and transfer properties. *Food Res. Int.* **2010**, *43*, 1395–1401.
- 39. Han, J., Salmieri, S., Le Tien, C. & Lacroix, M. Improvement of Water Barrier Property of Paperboard by Coating Application with Biodegradable Polymers. *J. Agric. Food Chem.* **2010**, *58*, 3125–3131.

- 40. Khanzadi, M.; Jafari, S. M.; Mirzaei, H.; Chegini, F. K.; Maghsoudlou, Y.; Dehnad, D. Physical and Mechanical Properties in Biodegradable Films of Whey Protein Concentrate-Pullulan by Application of Beeswax. *Carbohydr. Polym.* **2015**, *118*, 24–29.
- 41. Rhim, J. W., Lee, J. H. & Hong, S. I. Water resistance and mechanical properties of biopolymer (alginate and soy protein) coated paperboards. *LWT Food Sci. Technol.* **2006**, 39, 806–813.
- 42. Jost, V., Kobsik, K., Schmid, M. & Noller, K. Influence of plasticiser on the barrier, mechanical and grease resistance properties of alginate cast films. *Carbohydr. Polym.* **2014**, *110*, 309–319.
- 43. Kopacic, S., Walzl, A., Zankel, A., Leitner, E. & Bauer, W. Alginate and chitosan as a functional barrier for paper-based packaging materials. *Coatings* **2018**, *8*, 235.
- 44. Tambe, C., Graiver, D. & Narayan, R. Moisture resistance coating of packaging paper from biobased silylated soybean oil. *Prog. Org. Coatings* **2016**, *101*, 270–278.
- 45. Sothornvit, R. Effect of hydroxypropyl methylcellulose and lipid on mechanical properties and water vapor permeability of coated paper. *Food Res. Int.* **2009**, *42*, 307–311.
- 46. Morillon, V., Debeaufort, F., Blond, G., Capelle, M. & Voilley, A. Factors affecting the moisture permeability of lipid-based edible films: A review. *Crit. Rev. Food Sci. Nutr.* **2002**, 42, 67–89.
- 47. Bordenave, N., Grelier, S. & Coma, V. Hydrophobization and antimicrobial activity of chitosan and paper-based packaging material. *Biomacromolecules* **2010**, *11*, 88–96.
- 48. Reis, A. B., Yoshida, C. M., Reis, A. P. C. & Franco, T. T. Application of chitosan emulsion as a coating on Kraft paper. *Polym. Int.* **2011**, *60*, 963–969.
- 49. Ham-Pichavant, F., Sèbe, G., Pardon, P. & Coma, V. Fat resistance properties of chitosan-based paper packaging for food applications. *Carbohydr. Polym.* **2005** *61*, 259–265.
- 50. Zhang, Y., Liu, B.-L., Wang, L.-J., Deng, Y.-H., Zhou, S.-Y., Feng, J.-W. Preparation, structure and properties of acid aqueous solution plasticized thermoplastic chitosan. *Polymers* **2019**, *11*(5), 818.
- 51. Zhang, W., Xiao, H. & Qian, L. Enhanced water vapour barrier and grease resistance of paper bilayer-coated with chitosan and beeswax. *Carbohydr. Polym.* **2014**, *101*, 401–406.
- 52. Li, H., Qi, Y., Zhao, Y., Chi, J. & Cheng, S. Starch and its derivatives for paper coatings: A review. *Progress in Organic Coatings* **2019**, *135*, 213–227.
- 53. Ethanol Co-Products, Renewable Fuels Association. https://ethanolrfa.org/co-products/.

- 54. Thakur, S., Misra, M. & Mohanty, A. K. Sustainable Hydrophobic and Moisture-Resistant Coating Derived from Downstream Corn Oil. *ACS Sustain. Chem. Eng.* **2019**, *7*, 8766–8774.
- 55. Kasaai, M. R. Zein and zein -based nano-materials for food and nutrition applications: A review. *Trends in Food Science and Technology* **2018**, *79*, 184–197.
- 56. Parris, N. & Dickey, L. C. Extraction and Solubility Characteristics of Zein Proteins from Dry-Milled Corn. *J. Agric. Food Chem.* **2001**, *49*(*80*), 3757-3760.
- 57. Argos, P., Pedersen, K., Marks, M. D. & Larkins, B. A. A structural model for maize zein proteins. *J. Biol. Chem.* **1982**, *257*, 9984–9990.
- 58. Rabnawaz, M., Liu, G. & Hu, H. Fluorine-Free Anti-Smudge Polyurethane Coatings. *Angew. Chemie Int. Ed.* **2015**, *54*, 12722–12727.
- 59. Li, Z. et al. A closed-loop and sustainable approach for the fabrication of plastic-free oil-And water-resistant paper products. *Green Chem.* **2019**, *21*, 5691–5700.
- 60. Li, Z. & Rabnawaz, M. Oil- and Water-Resistant Coatings for Porous Cellulosic Substrates Oil- and Water-Resistant Coatings for Porous Cellulosic Substrates. *ACS Appl. Polym. Mater.* **2018**, *I*(*I*), 103-111.

Chapter 2: LITERATURE REVIEW

This chapter gives a brief overview of paper coating methods that have been developed over the years. The focus will be on paper coating techniques that includes the use of biobased materials like polysaccharides, proteins, and lipids for elimination of microplastics.

2.1 Biobased polymers and its importance

Plastic pollution in water streams is alarming for a large number of marine inhabitants. These plastic polymers are known to degrade to smaller pieces or into microplastics. Microplastics are plastic particles with size less than 5mm. Microplastics due to their small size are ingested planktons which in turn become food for fish and eventually enters our food chain. ¹⁻⁴ Accordingly, there is an urgent need to eliminate non-biodegradable plastics with biodegradable alternatives. Therefore, current coatings with synthetic polymers like polyethylene are getting banned from certain single-use applications because they enter the environment and are carriers for microplastics. Therefore, looking for more biobased and biodegradable alternatives becomes a necessity to eliminate plastics from paper coatings.⁵

In the mid-20th century, the polymer industry was completely dependent on petroleum-derived products. However, unpredictable oil prices and the recent push for sustainable practices,, it became important to find an alternative strategy for the polymer industry. One method was to move to biobased products.⁶ As per United States Department of Agriculture (USDA), biobased products are defined as the products derived from plants and other renewable agricultural, marine and forestry materials. Biobased products generally provide an alternative to conventional petroleum derived products and include a diverse range of offerings such as lubricants, detergents, inks, fertilizers and bioplastics.⁷ Biobased polymers have lot of advantages including recycling,

reusing, biodegradability, lower CO₂ footprint, derived from renewable sources, sustainable, they find applications in numerous fields. Generally, biobased polymers are classified into three main categories (shown in **Figure 2.1**):^{6,8,9}

- Natural derived biomass polymers like polysaccharides such as cellulose, chitosan, starch, and proteins like zein, etc. These are usually used without any further purification.
- 2. Polymers that are synthesized by microorganisms and plants, for example, poly (hydroxy alkanoates (PHAs), poly (glutamic acid), etc.
- 3. Synthetic polymers like polylactide (PLA), bio-polyolefins, poly (butylene succinate) (PBS), bio-poly(ethylene terephthalic acid) (bio-PET)¹⁰. These polymers are produced from naturally derived monomers or by the breakdown of naturally derived macromolecules.

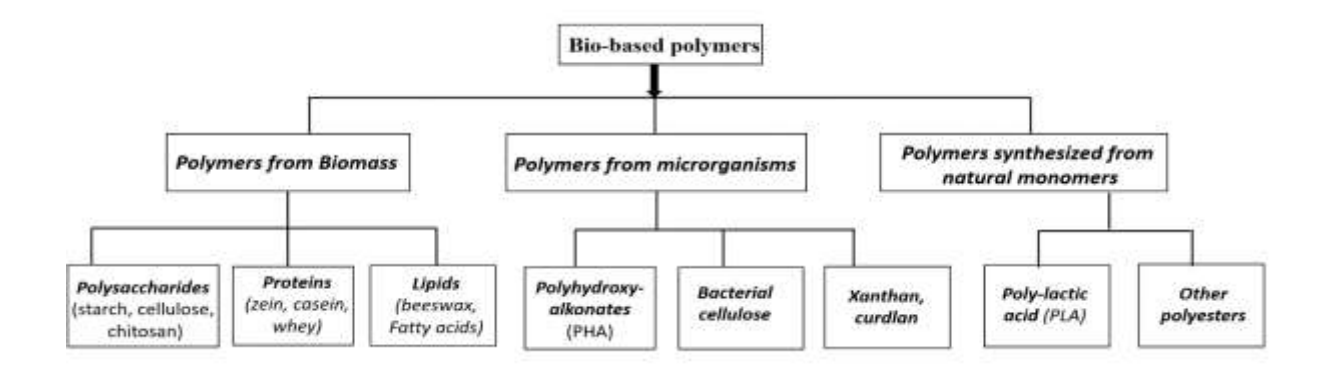


Figure 2.1: Overview of classification of bio-based polymers¹¹

2.1.1 Polysaccharides

The most abundant biobased polymers are polysaccharides that are extracted from plants or marine animals. Polysaccharides are long chain carbohydrate molecules that are made of monomers called monosaccharides bonded by glycosidic linkages. Over the years, a variety of

polysaccharides have been used for applications such as in membranes, biodegradable films, coatings etc, due to their grease, gas and aroma barrier properties.¹¹ Here we will discuss chitosan and starch polysaccharides and their application for paper coatings in detail.

Scheme 2.1: Chemical structures of chitin, chitosan, starch and backbone of zein

2.1.1.1 Chitosan- Properties and paper coating applications

Chitin, which is derived from shells of prawns and crabs, is one of the most abundant natural amino polysaccharides. Production of chitin includes demineralization by acid and deproteination by an alkali. Further deacetylation of purified chitin leads to the production of chitosan. The structure of chitin and deacetylated chitosan is shown in **Scheme 2.1**.^{9,12,13} Chitin can also be produced by processes like fermentation or hydrolysis by enzymes. However, these processes are not practical on an industrial scale.¹⁴

Chitosan is widely used in practical applications like in pharmaceutical, cosmetic products, water treatment due to its biodegradability, biocompatibility, chemical inertness, mechanical strength, low cost and good film-forming properties. Fully deacetylated chitosan is a homopolymer of deacetylated 2-amino-2-deoxy-β-D-glucopyranose and is a naturally occurring

cationic biopolymer. 17,18 Structurally, chitosan is similar to cellulose and is insoluble in water and most organic solvents. However, the presence of primary aliphatic amine groups with a pKa=9-10 can be protonated by some weak acids. The formed salt then becomes soluble in water and can be used for further water-based applications. 19,20 Commercially used chitosan has a molecular weight in the range of 50,000-300,000 Daltons with degree of deacetylation between 60 to 100%.

Chitosan, as mentioned earlier, is the deacetylated form of chitin that is cationic in nature. Chitosan is known to show excellent oxygen-barrier of (1.4-5.8) × 10-8 cc/m day atm at 25 °C and 0% RH and grease resistance due to its semi-crystalline nature and hydrogen bonds between the intermolecular chains. The antibacterial and antifungal properties of chitosan coated papers have also been studied. It has been studied that the mechanical properties of the paper increase / coating with chitosan. Kjellgren et. al. studied that on coating paper and paperboards with chitosan the oxygen transmission rate decreased to a value of 1.6 cm³mm/(m².day.atm) and grease resistance increased to 1800 s, when the coating weight was 5 g/m². However, Cobb 60 values remained the same, implying that water resistance did not change on the coating with chitosan owing to hydrophilic nature of chitosan.²¹ Chitosan has also been applied by means of size press where oil/grease resistance was found to be comparable to PFAS coated papers.²² Reis et. al. studied the water vapor transmission rate and found that WVTR values improved (by ca. 43%) when Kraft paper was coated with coating weight of 3.5 g/m² of chitosan and a reduction in water absorption capacity (by ca.35%) was also observed. Also, when palmitic acid with coating weight of 1.8 g/m² was blended with chitosan, a further reduction of WVTR by ca. 51% and water absorption capacity by 41% was observed.²³ The fat resistance has also been found to improve on addition of sodium alginate to chitosan because of the ionic nature of sodium alginate. Zhang et. al. studied a beeswax and chitosan bilayer coated papers that showed to improve the WVTR and

grease resistance due to oleophobicity of chitosan and filling of pores by both beeswax and chitosan.²⁴ Raluca et. al. prepared various alkyl groups grafted onto chitosan by chemical reaction of aldehydes with different chain lengths (octyl, decyl, dodecyl) with amino groups of chitosan with two different degrees of substitutions. It was observed that with increase in the alkyl chain length, the WCA decreases. The trend was reversed in the case of water absorptivity (Cobb 60) and WVTR, the values were found to increase with increase in the alkyl chain length. It was due to the tight packing of small alkyl chains in case of octyl group, that repels water from the surface. However, with increase in the length of the chain, the chains are not tightly packed and not well arranged in the matrix leading to cavities that in the film that allows the penetration of liquid or vapor. ¹⁰ Li et. al. successfully explored the chemical grafting of chitosan and polydimethylsiloxane (PDMS) in a number of papers.

2.1.1.2 Starch- Properties and paper coating applications

Starch is another polysaccharide that is abundantly available in nature. The sources of starch include wheat, rice, corn and potato. Starch consists of two polysaccharides, the linear amylose and the highly branched amylopectin. The linear amylose is made of glucose units joined by α (1-4) linkages. represents the amorphous fraction of starch. The branched structure of amylopectin has glucose units joined by α (1-6) linkages represents the crystalline fraction due to the movement restriction of highly branched chains.²⁵ The structure of starch is shown in **Scheme** 2.1. Depending on the source, starch can have different ratios of amylose and amylopectin in it. Starch is insoluble in cold water and forms a suspension on mixing. However, when the suspension is heated to 100 °C it leads to swelling of the starch granules and forms a paste. Amylose and amylopectin are both insoluble in cold water, but when solubilized starch solution is allowed to stand for some time, the amylose chains start to self-associate known as retrogradation that leads

to formation of gel if the starch solution is left standing for a long period of time. Due to linear chains of amylose as compared to amylopectin, retrogradation is often due to amylose. To minimize the retrogradation, plasticizers are often added to starch that to affects its thermal and mechanical properties such as improvement of mechanical strength and flexibility of starch coatings.

Starch is known to have excellent film forming abilities. Unlike chitosan, starch films are brittle due to the semi-crystalline nature owing to the branched structure of amylopectin. Therefore, the mechanical properties like tensile strength, flexural strength have not been good enough for practical purposes.²⁶ Matsui et. al. studies show that coated starch improves the surface smoothness, physical strength such as tensile strength and elongation at break, oil resistance and optical properties of the paper. However, the barrier properties do not improve due to crack formation in starch coatings.²⁷ Due to the semi-crystalline nature, starch has been either modified chemically and blends have been prepared using plasticizers (like glycerol, sorbitol, etc.) that help in improving the flexibility of starch. Hydrophobically modified starch-acetate have found to reduce the water vapor permeability and also improves the barrier properties. The mechanical and barrier properties of starch has also been improved by cross-linking it with citric acid.²⁸ Starch has also been oxidized chemically that leads to a reduction in chain length and molecular weight, that in turn leads to lower viscosity and minimal retrodegradation of starch solution.[50] The oil resistance of potato starch with coating weight of 3.5 g/m² has been found to improve on treatment of starch with an alkali.²⁹ Due to hydrophilic nature of starch, the moisture sensitivity of starchcoated papers is found to be bad. For this, starch has been hydrophobically modified with chemical grafting or mixing with hydrophobic lignin. 30–32

2.1.2 Zein- Properties and paper coating applications

Zein is the major protein found in corn and comprises of $\sim 45\text{-}50\%$ of the protein in corn. Unlike polysaccharides, zein is insoluble in water but is soluble in alcohol, high concentrations of alkali, anionic detergents and high concentrations of urea. The reason for this discrepancy in the solubility of zein is attributed to the amino acid composition in zein. The main functionalities of zein is shown in **Scheme 2.1**. Zein is mainly composed of glutamic acid (21-26%), leucine (20%), proline (10%) and alanine (10%). However, zein is found to be deficit in tryptophane and lysine. The presence of these non-polar amino acids leads to its insolubility in water.³³

Zein protein is water insoluble and therefore has advantages like improving water resistance and the gloss of zein coated paper. The grease resistance was found to be comparable to polyethylene coated paper used for sandwich packaging.³⁴ In another study the water vapor permeability and grease resistance was found to improve on paper coated with a soft-bristled brush to form a uniform coating of zein.³⁵ Parris et. al. also discovered that on spray coating Kraft paper with zein solution, the grease resistance and water vapor permeability can be improved. Zein coated papers also helps in easy recycling of the coated paper as compared to plastic or waxed coated paper that ends up in landfills because zein can be recovered by washing with benign solvents such as water and ethanol mixture.³⁶ Lipids- Properties and paper coating applications

Lipids are defined as compounds that are hydrophobic in nature due to the presence of long alkyl chains and hence are found to be insoluble in water but soluble in organic solvents.³⁷ Oils are a class of lipids that find numerous applications in biodegradable packaging, paints, coatings, inks, lubricants, plasticizers etc. due to its low-toxicity, abundant availability, non-volatility, biodegradability and non-depletability.³⁸ In this thesis we will focus specifically on vegetable oils and their applications in paper coatings. Vegetable oils are triacylglycerols of fatty acids that

contain functionalities such as double bonds, hydroxyl, epoxide, ester groups, etc. in the backbone that are capable of undergoing several chemical reactions. Some of the common chemical reactions that are being carried out are hydrogenations, trans-esterification, epoxidation, hydroxylation, acylation etc. These so-modified vegetable oils can be used as monomers or polymers for coating applications.

2.2 Industrially used Paper Coating methods

Here are some of the approaches that have been used to improve the barrier properties of paper and paperboards

2.2.1 Multi-layer and lamination method

Lamination is the method of incorporating two or more layers together with abio-based adhesive mainly starch. Multi-layer coating method is achieved by subsequently coating the paper with two or more layers in multi steps. Generally, in multi-layer coatings the paper is coated with a hydrophilic and hydrophobic material that are spread uniformly on the paper which in turn helps in improving water and oil resistance at the same time. Both lamination and multi-layer coating method have shown good barrier towards oil and water. In case of multi-layer coating, chitosan or starch is applied as the first layer on paper or paper board layer subsequently with some hydrophobic material. Chitosan or starch are cationic polymers and therefore show good adhesion with cellulose in paper. Solids are also used to alter paper surface properties such as titanium oxide, chalks, styrene, HDPE, phenol formaldehyde, melamine, styrene butadiene and a lot of other additives to modify surface properties such as hardness, antimicrobial, tensile strength, contact angle.

2.2.2 Blending or emulsion

Blending is a technique in which two or more polymers are mixed together to form blend or emulsion that is being coated on paper to form a single layer of coating. In this case chitosan and starch are blended with other materials and coated on paper to form a single layer on paper surface. However, this method of single layer coating only leads to a minor improvement in the water barrier of paper and paper boards because of non-uniformity of hydrophilic and hydrophobic coating material on the paper surface. Blending or emulsion technique depends on the affinity of hydrophobic and hydrophilic components, phase separation in case of emulsions and the surfactant used. The use of surfactants makes the coating more susceptible to water due to the presence of polar groups on surfactant that absorbs water.

2.2.3 Chemical modification

Polysaccharides consist of a six-membered ring with hydroxyl groups, in case of (cellulose and starch) and hydroxyl and amine groups (in case of chitosan). The hydroxyl and amine groups act as nucleophiles that can be modified with reactive electrophilic groups including ester, ether, epoxides, etc. to modify the properties of polysaccharides used to coat papers

2.3 Coating Methods

Dip coating, rod coating and spray coating are the three most commonly used coating methods used for paper coating.

2.3.1 Rod coating

Rod coating as the name implies involves the use of a rod to coat the paper. The three steps involved in rod coating method are coating, drying, and curing. The thickness of the coating can be adjusted by using rods of different groove depths. This method of coating is common in both labs and industry due to its easy application.

2.3.2 Dip coating

Dip coating in paper industry refers to the process of coating a paper substrate by dipping the paper into the coating material solution, leaving it to dry and cure afterwards. This technique is commonly used in industry and at lab scale. Though easy processing and low cost are some of the advantages of dip coating, however, there is no control over the thickness of the coating, especially when the coating solution is very viscous.

2.3.3 Spray coating

Spray coating involves spraying the coating solution onto the paper substrate depositing a layer of coating on paper. The thickness and coating load can be controlled by varying the concentration of the solution to be sprayed.

 Table 2.1:
 Summary of previously reported data on biopolymers in coatings and its properties.

Coated biopolymer	coating	WVTR (g/m²-d)	Cobb 60 (g/m ²)	Kit rating	WCA °	Coating method
	load (g/m²)	(decreased %)	(decreased %)			
chitosan	6.0	220 (68)	54 (-116)	6	70	-
chitosan ²³	3.5	606 (44)	30.1 (23)	-	-	-
chitosan-palmitic acid ²³	5.3	553 (48)	23 (41)	-	-	emulsion
chitosan-beeswax ²⁴	12.0	60 (98)	-	-	-	bilayer
chitosan-caseinate ³⁹	16.0	5 (71)	-	-	-	bilayer
chitosan-curdlan ⁴⁰	5.0	500 (17)	3.2 (33)	-	-	emulsion
chitosan ³⁰	1.6	241 (62)	-	7	75	-
0,0'-	1.6	441 (31)	-	6	117	Chemical grafting
dipalmitoylchitosan ³⁰						6 6
chitosan-palmitic acid ³⁰	1.6	239 (63)	-	6	110	emulsion
chitosan ⁴¹	5.2	-	33.9	2000 s	_	rod
chitosan ²²	5.4	-	-	10-11	-	
Chitosan-g-octyl ¹⁰	1.0	475	20 (83)	-	132.6	rod
Chitosan-g-decyl ¹⁰	1.0	575	50	_	125.3	rod
Chitosan-g-dodecyl ¹⁰	1.0	620	70 (26-34)	-	106.7	rod
chitosan-g-HDIT-	109.8	716 (1.4)	65 (31.5)	12	107.2	rod and dip
PDMS ⁴²			()		(5 min)	1
chitosan-g-HDIT-	4.2	850	9.9	11.7	120.53	rod
PDMS ⁴³						
chitosan-g-IPDI-castor		734.6			92.9	rod
oil ⁴⁴		, , , , ,				
chitosan-g-PDMS/zein	7.2	1000	21	11	100.7	rod
filler ⁴⁵	,	1000			10007	104
Chitosan-starch ⁴⁶	5	495 (18)	2.8 (39)	_	_	emulsion
Starch triacetate ⁴⁷	10	2340	-	_		rod
Starch-citric acid ²⁸	15-18	16-41	_	_	_	rod
Zein ³⁶	10	881	_	_	_	spray

REFERENCES

REFERENCES

- 1. Gallowaya, T. S. & Lewisa, C. N. Marine microplastics spell big problems for future generations. *Proceedings of the National Academy of Sciences of the United States of America* **2016**, *113*, 2331–2333.
- 2. Gandara e Silva, P. P., Nobre, C. R., Resaffe, P., Pereira, C. D. S. & Gusmão, F. Leachate from microplastics impairs larval development in brown mussels. *Water Res.* **2016**, *106*, 364–370.
- 3. Chubarenko, I., Bagaev, A., Zobkov, M. & Esiukova, E. On some physical and dynamical properties of microplastic particles in marine environment. *Mar. Pollut. Bull.* **2016** *108*, 105–112.
- 4. Underwood, A. J., Chapman, M. G. & Browne, M. A. Some problems and practicalities in design and interpretation of samples of microplastic waste. *Analytical Methods* **2017**, *9*, 1332–1345.
- 5. Microplastics million times more abundant in the ocean than previously thought. NSF National Science Foundation. https://www.nsf.gov/discoveries/disc_summ.jsp?cntn_id=299718&org=NSF&from=news.
- 6. Nakajima, H., Dijkstra, P. & Loos, K. The Recent Developments in Biobased Polymers toward General and Engineering Applications: Polymers that are Upgraded from Biodegradable Polymers, Analogous to Petroleum-Derived Polymers, and Newly Developed. *Polymers (Basel)*. **2017**, *9*, 523.
- 7. Biobased Chemicals American Chemical Society. chemicals.html.
- 8. Avérous, L. & Pollet, E. Biodegradable Polymers. *Green Energy Technol.* **2012**, *50*, 13–39.
- 9. Babu, R. P., O'Connor, K. & Seeram, R. Current progress on bio-based polymers and their future trends. *Prog. Biomater.* **2013**, *2*, 8.
- 10. Nicu, R., Lupei, M., Balan, T. & Bobu, E. Alkyl-Chitosan as Paper Coating Material to Improve Water Barrier Properties *Cellulose Chem. Technol.*, **2013** *47* (7), 623-630.
- 11. Rastogi, V. & Samyn, P. Bio-Based Coatings for Paper Applications. *Coatings* **2015**, *5*, 887–930.
- 12. Roberts, G. A. F. Chitosan production routes and theirrole in determining the structure and properties of the product. *European Chitin Society International conference 7th, Chitin and chitosan* **1997**, 22–31.

- 13. Rinaudo, M. Chitin and chitosan: Properties and applications. *Progress in Polymer Science* **2006**, *31*, 603–632.
- 14. Win, N. N. & Stevens, W. F. Shrimp chitin as substrate for fungal chitin deacetylase. *Appl. Microbiol. Biotechnol.* **2001**, *57*, 334–341.
- 15. Liu, M., Zhang, Y., Wu, C., Xiong, S. & Zhou, C. Chitosan/halloysite nanotubes bionanocomposites: Structure, mechanical properties and biocompatibility. *Int. J. Biol. Macromol.* **2012**, 51, 566–575.
- 16. Epure, V., Griffon, M., Pollet, E. & Avérous, L. Structure and properties of glycerol-plasticized chitosan obtained by mechanical kneading. *Carbohydr. Polym.* **2011**, *83*, 947–952.
- 17. Cissé, M., Montet, D., Tapia, M. S., Loiseau, G. & Ducamp-Collin, M. N. Influence of temperature and relative humidity on the immobilized lactoperoxidase system in a functional chitosan film. *Food Hydrocoll.* **2012**, *28*, 361–366.
- 18. Liu, Z. *et al.* Effects of chitosan molecular weight and degree of deacetylation on the properties of gelatine-based films. *Food Hydrocoll.* **2012**, *26*, 311–317.
- 19. Zargar, V., Asghari, M. & Dashti, A. A Review on Chitin and Chitosan Polymers: Structure, Chemistry, Solubility, Derivatives, and Applications. *ChemBioEng Rev.* **2015**, *2*, 204–226.
- 20. Kumar, M. N. V. R., Muzzarelli, R. A. A., Muzzarelli, C., Sashiwa, H. & Domb, A. J. Chitosan chemistry and pharmaceutical perspectives. *Chem. Rev.* **2004**, *104*, 6017–6084.
- 21. Kjellgren, H., Gällstedt, M., Engström, G. & Järnström, L. Barrier and surface properties of chitosan-coated greaseproof paper. *Carbohydr. Polym.* **2006**, *65*, 453–460.
- 22. Ham-Pichavant, F., Sèbe, G., Pardon, P. & Coma, V. Fat resistance properties of chitosan-based paper packaging for food applications. *Carbohydr. Polym.* **2005**, *61*, 259–265.
- 23. Reis, A. B., Yoshida, C. M., Reis, A. P. C. & Franco, T. T. Application of chitosan emulsion as a coating on Kraft paper. *Polym. Int.* **2011**, *60*, 963–969.
- 24. Zhang, W., Xiao, H. & Qian, L. Enhanced water vapour barrier and grease resistance of paper bilayer-coated with chitosan and beeswax. *Carbohydr. Polym.* **2014**, *101*, 401–406.
- 25. Finch, C. A. Modified starches: Properties and uses Edited by O. B. Wurzburg, CRC Press, Boca Raton, Florida, *Br. Polym. J.* 1989, 21, 87–88.
- 26. Perry, P. A. & Donald, A. M. The role of plasticization in starch granule assembly.

- *Biomacromolecules* **2000**, *1*, 424–432.
- 27. Matsui, K. N. *et al.* Cassava bagasse-Kraft paper composites: Analysis of influence of impregnation with starch acetate on tensile strength and water absorption properties. *Carbohydr. Polym.* **2004**, *55*, 237–243.
- 28. Menzel, C. & Koch, K. Impact of the coating process on the molecular structure of starch-based barrier coatings. *J. Appl. Polym. Sci.* **2014**, *131(23)*.
- 29. Gryuter, D. Chemical modification of pulp fibers by TEMPO-mediated oxidation. *Nordic Pulp & Paper Research Journal* **1999**, *14(4)*.
- 30. Bordenave, N., Grelier, S. & Coma, V. Hydrophobization and antimicrobial activity of chitosan and paper-based packaging material. *Biomacromolecules* **2010**, *11*, 88–96.
- 31. Yang, X. -W., Shen, Y., -D., Li, P. -Z., Huang, F. Study on the performance and of hydrophobic starch modified by ASA and its application as surface sizing agent. *Journal of Functional Materials* **2013**, *44*(2), 212-215.
- 32. Maximova, N., Österberg, M., Laine, J. & Stenius, P. The wetting properties and morphology of lignin adsorbed on cellulose fibres and mica. in *Colloids and Surfaces A: Physicochemical and Engineering Aspects* **2004**, *239*, 65–75.
- 33. Shukla, R. & Cheryan, M. Zein: The industrial protein from corn. *Ind. Crops Prod.* **2001**, *13*, 171–192.
- 34. Trezza, T. A., Wiles, J. L., Vergano, P. J. Water vapor and oxygen barrier properties of corn zein coated paper. *TAPPI Journal* **1998**, *81*(*8*), 171-176.
- 35. Trezza, T. A., Vergano, P. J. Grease Resistance of Corn Zein Coated Paper. *J. Food Sci.* **1994**, *59*, 912–915.
- 36. Parris, N., Dickey, L. C., Wiles, J. L., Moreau, R. A. & Cooke, P. H. Enzymatic hydrolysis, grease permeation, and water barrier properties of zein isolate coated paper. *J. Agric. Food Chem.* **2000**, *48*, 890–894.
- 37. Fahy, E. *et al.* A comprehensive classification system for lipids. *Eur. J. Lipid Sci. Technol.* **2005**, *107*, 337–364.
- 38. Alam, M., Akram, D., Sharmin, E., Zafar, F. & Ahmad, S. Vegetable oil based eco-friendly coating materials: A review article. *Arabian Journal of Chemistry* **2014**, *7*, 469–479.
- 39. Khwaldia, K., Basta, A. H., Aloui, H. & El-Saied, H. Chitosan-caseinate bilayer coatings for paper packaging materials. *Carbohydr. Polym.* **2014**, *99*, 508–516.

- 40. Brodnjak, U. V. Experimental investigation of novel curdlan/chitosan coatings on packaging paper. *Prog. Org. Coatings* **2017**, *112*, 86–92.
- 41. Kjellgren, H., Gällstedt, M., Engström, G. & Järnström, L. Barrier and surface properties of chitosan-coated greaseproof paper. *Carbohydr. Polym.* **2006**, *65*, 453–460.
- 42. Li, Z. & Rabnawaz, M. Oil- and Water-Resistant Coatings for Porous Cellulosic Substrates Oil- and Water-Resistant Coatings for Porous Cellulosic Substrates. *ACS Appl. Polym. Mater.* **2018**, *1*(1), 103-111.
- 43. Li, Z., Rabnawaz, M., Sarwar, M. G., Khan, B., Nair, A. K., Sirinakbumrung, N., Kamdem, D. P. A closed-loop and sustainable approach for the fabrication of plastic-free oil- And water-resistant paper products. *Green Chem.* **2019**, *21*, 5691–5700.
- 44. Li, Z., Rabnawaz, M. & Khan, B. Response Surface Methodology Design for Biobased and Sustainable Coatings for Water-and Oil-Resistant Paper. *ACS Appl. Polym. Mater.* **2020**, *2(3)*, 1378-1387.
- 45. Hamdani, S. S., Li, Z., Rabnawaz, M., Kamdem, D. P. & Khan, B. A. Chitosan –Graft Poly(dimethylsiloxane)/Zein Coatings for the Fabrication of Environmentally Friendly Oiland Water-Resistant Paper . *ACS Sustain. Chem. Eng.* **2020**, *8*, 5147–5155.
- 46. Vrabič Brodnjak, U. Influence of ultrasonic treatment on properties of bio-based coated paper. *Prog. Org. Coatings* **2017**, *103*, 93–100.
- 47. Fringant, C., Rinaudo, M., Gontard, N., Guilbert, S., Derradji, H. A Biodegradable Starch Based Coating to Waterproof Hydrophilic Materials. *Biosynthesis Nutrition Biomedical* **1998**, *50 (7)*, 292-296.

Chapter 3: MATERIALS AND CHARACTERIZATION

This chapter gives detailed information related to the materials used for paper coating in this thesis work and also the methods used for the paper coating and various characterization techniques employed.

3.1 Materials

Chitosan of molecular weight $M_n = 50,000$ -190,000 g/mol with 100% deacetylation, zein (purity 96%) and corn starch were purchased from Sigma-Aldrich. 3-Cloroperbenzoic acid was also purchased from Sigma-Aldrich with a purity >77%. Ethanol (95%) was purchased from Koptec. Deionized (DI) water was used in all experiments described herein. Glacial acetic acid was purchased from Macron Fine Chemicals. Dichloromethane and acetone solvent of ACS reagent grade were purchased from Sigma-Aldrich. All the chemicals were used without further purification. Deionized (DI) water was used for all the experiments. Paper (35 liner Kraft) was purchased from Uline (United States).

3.2 Coating Procedure

The coating technique used here is bar coating for which a K303 Multi Coater (RK PrintCoat Instruments Ltd., UK) was used. The coating procedure is shown in **Figure 3.1**. The Kraft paper was cut into a ~29 cm x 21 cm size and attached to the bar coater with the rod. Then nearly 5 mL solution of the coating material was spread on top, that spreads on the paper with a rod. Once the paper is coated it was dried at room temperature for 24 h. For bilayer coated papers, the same step was repeated with another coating material solution. After the samples were dried

for 24 h, they were pre-conditioned at 23 °C under 50 % relative humidity (RH) before carrying out any further tests.

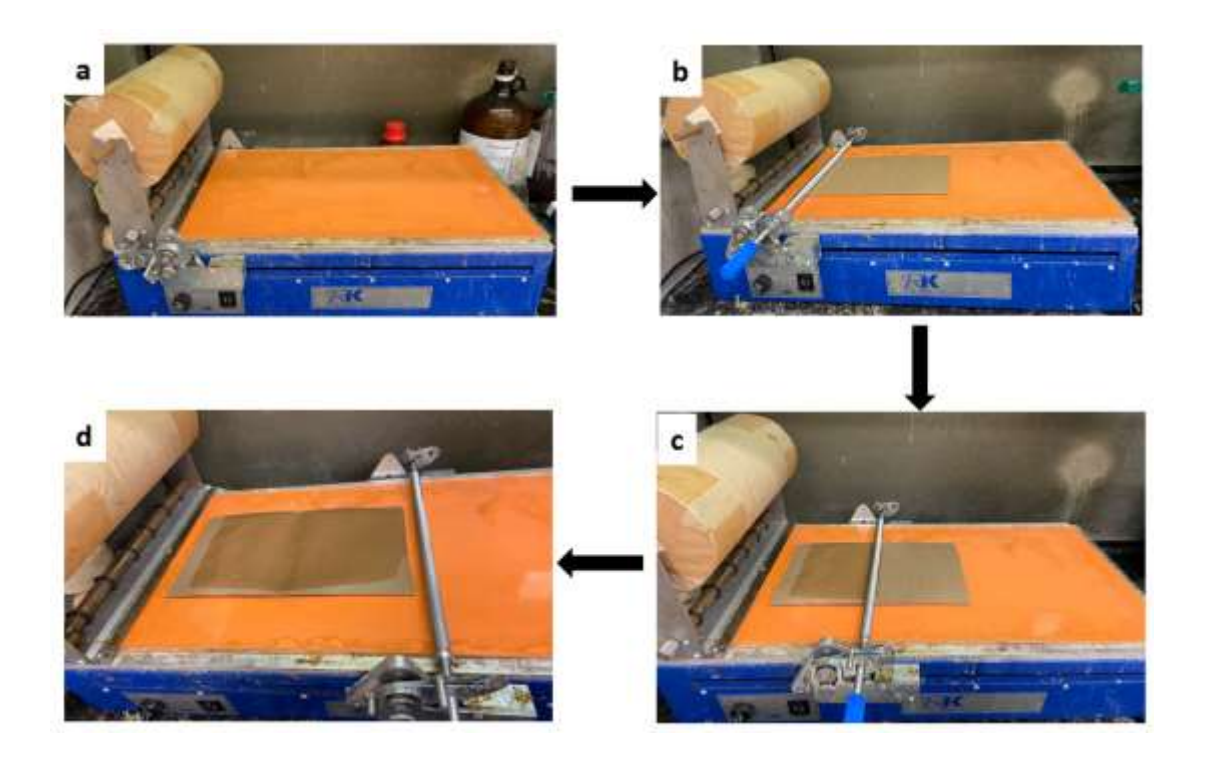


Figure 3.1: Coating procedure (a) bar coating machine (b) blank Kraft paper attached with a rod (c) even coating of solution with rod (d) final coated paper

3.3 Characterization

3.3.1 Wettability

3.3.1.1 Water contact angle

Wetting is the process of interaction of a liquid (generally water) with a solid surface.¹ Surface wettability plays an important role in various processes of day-to-day life. For example, in printing and packaging applications, in order to attain good adhesion of liquid to the solid, it is

important to understand the factors affecting the surface tension or surface free energy of both liquid probe and solid surface.²

Wetting is characterized by various methods like contact angle, sessile drop,³ Wilhelmy, wicking,⁴ inverse gas chromatography.^{5,6} However, the most commonly used method is contact angle method which is defined as the angle between the tangent to the liquid-vapor interface and the solid surface at the three-phase contact line (**Figure 3.2**). The value of contact angle indicates the tendency of the surface to get wet when liquid comes in contact with the solid surface. Young equation defines the contact angle between the liquid and solid surface, assuming the solid surface to be atomically smooth, homogeneous, non-reactive and non-deformable by the liquid, as shown in equation 1,¹

$$cos\theta_{Young} = \frac{\gamma_{SV} - \gamma_{Sl}}{\gamma}$$
 (Eq.1)

where, θ_{Young} is the Young contact angle, γ is the surface tension of liquid, γ_{SV} and γ_{SI} are solid-vapor and solid-liquid interfacial tensions, respectively. Surfaces with high energy show a low contact angle, implying the liquid droplet spreads and adheres to the surface. On the other hand, surfaces with low energy show a high contact angle, implying surface tends to repel the liquid.

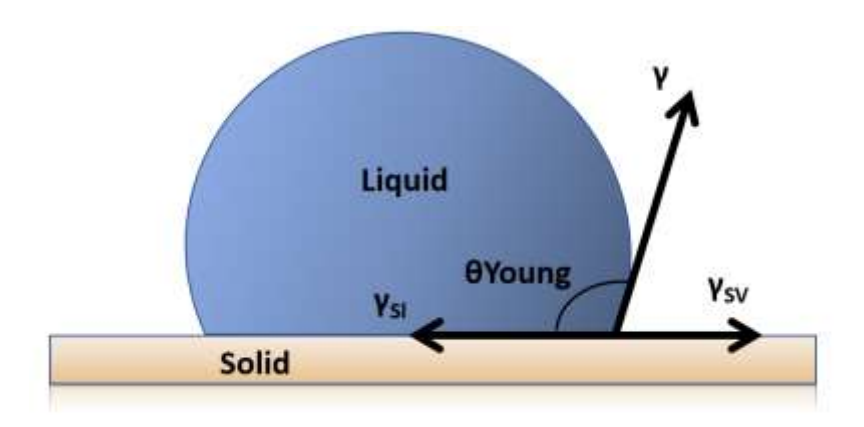


Figure 3.2: Depiction of three contact surface line for a water droplet on a solid surface¹

The conventional theory assumes a straight boundary between the liquid and the vapor phase despite of the three-phase contact line or the droplet size. However, in real cases the solid surfaces are rarely smooth, instead they have some roughness which makes them heterogeneous. In this case, the surface energy can be described by two states: Wenzel and Cassie-Baxter states as shown in **Figure 3.3**. In Cassie-Baxter wetting state, air gets trapped in the grooves of the solid surface which makes a composite hydrophobic surface of solid/air. The liquid then sits on top of the solid-air composite and results in a larger contact angle, as opposed to the contact angle if the surface was flat as shown in equation 2.

$$\cos \theta_{C-B} = f - 1 + f \cos \theta \quad (Eq. 2)$$

where $\theta_{C\text{-B}}$ is the Cassie-Baxter contact angle, f is the fraction of solid/liquid interface in the entire composite surface beneath the liquid. On the other hand, in Wenzel wetting state, the liquid goes into the groves of the solid surface and results in a lower contact angle due to the increase in contact area. The Wenzel state is represented by equation 3, where θ_W is the Wenzel contact angle and R represents the ratio of actual area of solid/liquid interface to normally projected

area. The transition from stable Wenzel state to metastable Cassie-Baxter state becomes reversible if both states are thermodynamically stabilized by changing thermodynamic variables like, temperature, pressure or applying electric field or external forces.⁸

$$\cos \theta_W = R \cos \theta$$
 (Eq. 3)

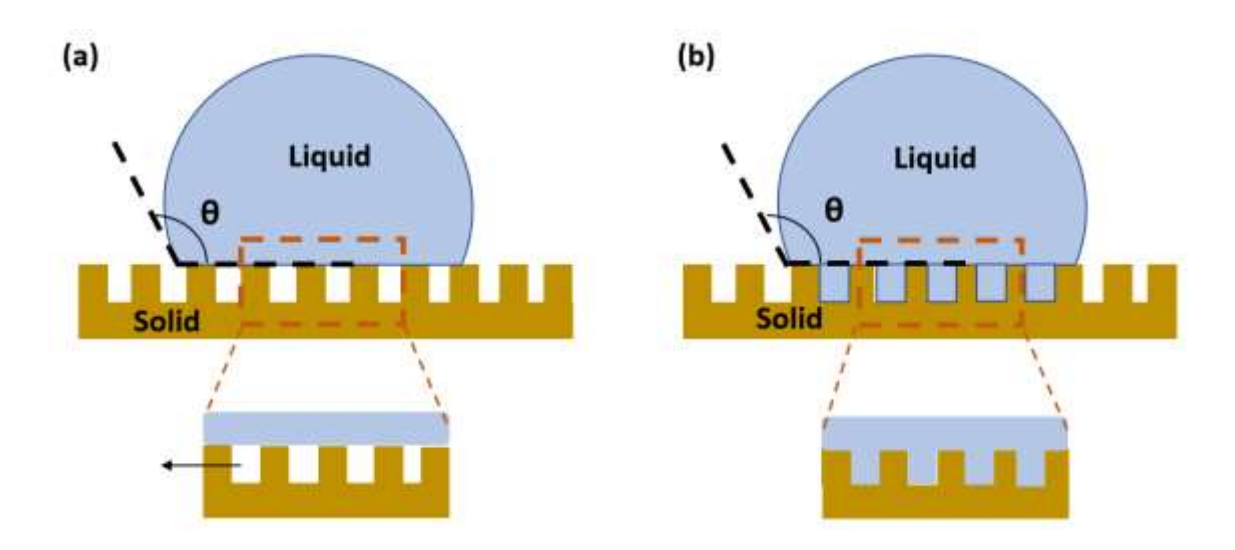


Figure 3.3: (a) Cassie state, (b) Wenzel state for a liquid droplet on solid surface

Paper consists of pores made up of cellulosic fiber networks. The penetration of liquid can be predicted to take place by any or all of the following mechanisms: (a) penetration of liquid into the capillary system of the paper, (b) diffusion of the liquid through the fibers of the paper, (c) surface diffusion along capillary walls and (d) the transfer of vapor phase through the fibers. However, generally when water meets the paper surface it gets absorbed by the fiber networks, which causes the hydrogen bonds to break leading to the swelling of fibers and hence an expansion of the fiber network. However, paper can be modified in order to reduce the absorption of liquid into the pores of the paper by creating a paper with low surface energy.^{3,9} In practice, the duration

of the contact of water with paper surface is also necessary to understand. The contact angles are found to be larger initially which gradually decreases over time due to the penetration through the pores. Therefore, a standard method TAPPI (T458 and T558) has been used for the scientific purposes to study the wettability of the paper. A droplet of deionized water with a pH 7 size of 10 μ L was dropped on the surface at room temperature to measure the contact angle recorded after 5s and 60s.

3.3.1.2 Sliding angle and contact angle hysteresis

In this thesis, contact angles have been determined by sessile-drop goniometry, where a video is recorded of the angle formed at the liquid-solid interface and the static contact angle is determined by a fitting procedure. However, this approach presumes drop to be in a global energy minimum, i.e. in a stable state that in turns corresponds to Young contact angle and hence the results are non-reproducible. However, the drop can be any local minimum within the hysteresis range. ACA or advancing contact angle is the highest and RCA or receding contact angle is the lowest angle in the hysteresis range that are reproducible. ¹⁰

In case of ACA, as the volume of the drop increases, the contact angle increases but the contact line remain pinned until ACA is reached. After that point, further increase in the volume of the drop leads to the change in contact line while the angle remains the same. In case of RCA, as the volume of the drop decreases, the contact angle decreases with the contact line being pinned until RCA is reached. Further decrease in the volume leads to a change in the contact line, while the angle remains constant. Contact angle hysteresis (CAH) is then calculated as shown in equation 4. The higher the CAH value, the lower the mobility of the drop and vice versa.¹

$$CAH = cos\theta_r - cos\theta_a$$
 (Eq. 4)

Another method to obtain CAH is the sliding angle method. The angle of the solid surface at which the liquid droplet starts to slide down is defined as the sliding angle. CAH and sliding angle are related by equation 5.

$$mgsin\theta_{slide} = kw\gamma_{LV}(cos\theta_r - cos\theta_a)$$
 (Eq. 5)

where g is the gravity, m is the mass, k is a constant, θ_{slide} is the sliding angle, w is the contact diameter of the droplet, θ_{a} is advanced contact angle, θ_{r} is receding contact angle, γ_{LV} is the liquid-vapor surface tension.

3.3.2 Barrier properties

3.3.2.1 Cobb test/ water absorption

Paper is made of cellulose fibers, that tend to form hydrogen bonds with water through the hydroxyl groups present on its surface. Due to this, the fibers swell, and the paper becomes less useful for practical applications. Therefore, its necessary to have a quantitative estimate of amount of water being absorbed by the paper.

Cobb test gives a deeper understanding of resistance of water by the paper by measuring the amount of liquid water (in grams) being absorbed by the paper when the paper is being exposed to a certain amount of water for a specific amount of time as per standard tests TAPPI 441om-09 and ISO 535. For carrying out the test, the paper is cut into a 100 cm² size. Then paper specimen is exposed to 100 mL deionized water or 1-cm depth for 60 seconds. The weight of the paper specimen is recorded before exposing to water for 60 s. Water absorptiveness or Cobb value is

then calculated as shown in equation 6, reported in g/m². This method is widely used in industry to quantify the liquid water absorption by paper specimen.

Cobb value =
$$Final\ weight - Initial\ weight$$
 (Eq. 6)

3.3.2.2 Water vapor transmission rate

The protection of the product from external factors like moisture, gas permeation, light etc. is a critical function of packaging. Coatings prove to be great at improving the barrier properties of the packaging material that helps in reducing the permeability of water vapor or other gas molecules. Gas or liquid permeation through the coated films usually takes places by one of the two modes mentioned below:¹¹

1. The permeate gets absorbed by the surface, diffuses through the coated film and desorbs on the other side. The driving force for this is the difference in concentration on either side of the coated film. Permeation defined as the amount of permeate transported through a unit area of coated film in a given time is given by equation 7.

$$Permeation = \frac{(Quantity\ of\ permeant)(Film\ thickness)}{(area)(time)(pressure\ difference))} \quad (Eq.\ 7)$$

2. The permeation of gas molecules through cracks and other deficits in the coated film.

This mode of permeation common in glass-coated or metal coated films.

The factors that are known to determine the permeation of gas molecules through the films are: 11

a) Coated polymer factors: The diffusion of permeate molecules depends greatly on the properties of polymer material that paper is coated with and the pores sizes. If the

material posses' polar groups, it tends to form hydrogen bonds with water and leads to greater permeability for polar molecules like water vapors. Other properties like crystallinity, packing density, glass transition temperature, and free volume also affects the amount of permeability.

- b) *Permeant factors*: The permeability also depends on size, shape, chemistry and concentration of the permeate. For example, larger molecules are known to diffuse slowly. The interaction of permeate with the coated polymer can lead to swelling or plasticization effects, which leads to higher permeation due to increase in free volume.
- c) *Environmental effects*: Factors like temperature, pressure, relative humidity are also known to greatly affect the permeability. Higher the relative humidity and temperature, often leads to higher permeability.

In this thesis we have mainly focused on the water vapor permeability through the coated papers. The WVTR values were determined as per the standard TAPPI 448 and ASTM E96, with a Permatran-W (Model 3/34, Mocon Inc., MN, USA). The testing conditions were kept constant with a temperature of 23 °C and 50% RH, until specified otherwise. The results were further compensated to 100% RH with was N₂ at a flow rate of 12 SCCM used as carrier gas. The sample was prepared by cutting a paper specimen of 20 x 20 mm² that was masked in an aluminum sheet with a 6 mm diameter opening at the center of the sample. Permeability values were calculated by equation 8 and reported in g.μm/m².day.Pa.

$$Permeability = \frac{WVTR \ value \times thickness}{water \ vapor \ pressure \ difference}$$
 (Eq. 8)

3.3.2.3 Oil or grease resistance

The oil or grease resistance is defined as the tendency of the coated paper to resist oil/grease. The oil resistance is found to be dependent on the polarity and crystallinity of the polymer that paper is coated with. The oil/grease resistance can be determined by Kit test. Kit test is performed to quantify the performance of paper or paper boards that are used in the food packaging applications. Kit test is offered by the Technical Association of the Pulp and Paper Industry (TAPPI), under the standard test no. TAPPI T559, in which the paper surface is subjected to solutions with different concentrations of castor oil, toluene and heptane. The highest number solution (kit rating No. 12) is considered to be the most aggressive that remains on the surface without penetrating through the paper. The solutions are numbered from 1 to 12 and are put on a small piece of paper specimen for 15 s. After 15 s the drop is wiped off and is checked for a stain. If the solution leaves a stain on the paper, the specimen is considered to fail the test and if there is no stain after 15 s, the test is considered to be passed for that solution. Kit rating no.1 through 12 implies the increasing resistance of the paper towards oil/grease. Another test offered by TAPPI for oil/grease resistance is Turpentine test (TAPPI T454). However, this test is mainly applied to greaseproof, glassine or vegetable parchment and is not useful for paper and paper boards.

3.3.3 Mechanical properties

The strength of the paper is important when it comes to the applications of paper products in daily life. The mechanical properties of the paper reflect morphology, structure of fibers and network and intrinsic chemistry of the paper in both machine direction (MD) or cross direction (CD). The standard TAPPI test methods used to determine the mechanical properties of the paper includes tensile strength, bending strength, tearing resistance and compression strength on the

edge. The mechanical properties of the paper are known to change on modification/coating of the paper. For example, for polymers like starch, plasticizers added can improve the mechanical properties of the paper. ¹² **Table 3.1** comprises the standard tests and conditions required for them. The tests have been carried out in both cross-machine (CD) and machine direction (MD).

Table 3.1: Instruments and TAPPI standards used to measure tensile strength, compressing strength, bending stiffness and tearing resistance of uncoated and coated papers.

Mechanical properties	Instrument	TAPPI standard	units
Tensile strength	Instron testing machine	T 494	lbs/in
Compressing strength on the edge	TMI crush tester	Т 822	lbs
Bending stiffness	Taber stiffness tester	T 489	g cm
Internal tearing resistance	Elmendorf-type tearing tester	T 414	g

Tensile strength represents the strength due to the morphology of the paper. It is dependent on the quality of the network of fibers. Paper made with long fibers has higher strength than of short fibers. For carrying the tensile test, the specimen is cut into 1" x 11" dimensions attached to two clamps with a gap of 7.1" between the clamps. The specimen is then stretched at a constant rate of 0.5 in/min. The tensile strength is calculated by dividing the maximum tensile load with the width of the specimen. A plot of the load versus width of the cross section was obtained with the Bluehill software package (Instron, MA, USA).

Compressing strength on the edge is used to determine the compression strength of strip formed into a ring. For this a strip of paper specimen is cut into dimensions 0.5" x 6" and slid into a ring sample holder and the load is applied on the edges of the paper from top. These tests were performed following the TAPPI T822 protocol with a TMI crush tester (Model, 1210, Instron,

MA, USA). The RCT value was recorded in lbs units, as the load required to crush the paper sample in both MD and CD direction.

Bending stiffness (BS) was measured by cutting the paper into a 1.5" x 2.75" dimensions, following TAPPI T489 protocol, with a Taber Stiffness Tester (Model 150-D, Teledyne Taber, NY, USA). The specimen was clamped from one side to the tester and the other side was bent by 15° with a force of (500 Taber stiffness units). The bending stiffness was reported as the average of left and right values on the tester in both MD and CD direction.

Tearing resistance measures the internal resistance of the paper. It is the measure of the force perpendicular to the plane of the paper that is necessary to tear a single sheet of paper through a specified distance after the tear has been started. It was studied using an ME-1600 Manual Elmendorf-type tearing tester (Oakland Instrument Co, MN, U.S.) following the TAPPI T414 protocol in both MD and CD direction.

3.3.4 Recyclability

Recyclability is one of the most important aspect that need to be examined for the paper-based products. As is being mentioned before, paper products are becoming popular due to their easy recyclability. However, the recyclability of coated paper depends on the material that paper is being coated with. The synthetic polymers that papers are coated with generally ends in landfills, and some laminates are known to remain in the pulp that makes the recycled paper of no further use. A general recycling procedure being used on industrial scale includes repulping of the paper by soaking into warm water for around 30 min, purification that involves washing the pulp with appropriate solvent and manufacturing the paper back from the pulp.

3.3.5 Basis weight, coating load and material thickness

As mentioned before, all the properties of the coated papers depend on the coating load of the material and the thickness of the coating, therefore it is important to determine the basis weight, coating load and material thickness of coated papers. The basis weight of coated and uncoated paper was measured as per ASTM D646 protocol. The sample was prepared by cutting the paper specimen into $12 \times 12 \text{cm}^2$ size. The weight of the specimen was recorded before and after coating and basis weight before and after coating was calculated by dividing the weight of the specimen by the area as given in **Equation 9**. The grammage/ coating load was calculated by **Equation 10** and was reported in g/m^2 . The material thickness was measured with an auto micrometer (Testing Machine Inc., New Castle, DE, USA), reported in μm .

Basis weight =
$$\frac{weight(g)}{area(m^2)}$$
 (Eq. 9)

Coating load = Basis weight (coated – uncoated) (Eq.
$$10$$
)

3.3.6 Scanning electron microscopy (SEM)

Uncoated paper has large porous network that allows the diffusion and penetration of liquid and gas through it. The pores are masked after coating and hence helps in improving the resistance of the paper towards liquids. SEM images were taken of all the uncoated and coated papers in order to understand the change in the surface morphology after coating the papers. The SEM images were recorded with a JEOL 6610 SEM (JOEL Ltd., Japan) system that has an accelerating voltage of 15 kV. The samples for SEM characterization were prepared by mounting the paper specimen onto aluminum stubs with a carbon double-sided tape. The stubs were subsequently exposed to a 15 mm thick layer of gold using a sputtering coating equipment.

3.3.7 Thermogravimetric analysis (TGA)

The paper samples were also studied for their thermal stability after coating. Since the paper products are exposed to heating especially in microwave usable applications, the samples were tested using a Q-50 thermogravimetric analyzer (TA Instruments, New Castle, DE). For preparing the sample a small piece of paper weighing around 6-10 mg was placed in an aluminum pan in the instrument. The samples were then heated under a nitrogen atmosphere at a flow rate of 40 mL/min from 23 to 600 °C at a constant heating rate of 10 °C/min. The DTG curves were also plotted as a first derivative of TGA curve.

3.3.8 Attenuated-Total-Reflection Fourier-Transform Infrared ATR-FTIR analysis

For characterizing the coating on the paper surface ATR-FTIR analysis was done for looking at the characteristic peaks of the coating chemicals. The instrument used for ATR-FTIR analysis was a Shimadzu FTIR spectrometer IR-Prestige21 (Shimadzu Co., Columbia, MD), equipped with an attenuated-total-reflection (ATR) part (PIKE Technologies, Madison, WI). The ATR-FTIR spectrum for all the samples tested were obtained with an average of 25 scans over a 4000-400 cm⁻¹ wavenumber range at a resolution of 4 cm⁻¹.

3.3.9 Gel permeation chromatography (GPC)

Gel permeation chromatography is a type of size exclusion chromatography that works on the principle of separation of the polymer chains based on their size. The number average molecular weight (M_n) , weight average molecular weight (M_w) , viscosity, average molecular weight (M_v) and polydispersity index (PDI) of the synthesized polymers was done using GPC technique. Waters Corp. (Milford, MA, USA) instrument was used, equipped with a Waters 1515 isocratic pump, a Waters 717 autosampler, Waters Styragel columns including HR4, HR3, and

HR2 (300 mm x 7.8 mm (I.D)) columns, as well as a Waters 2414 refractive index detector. The columns were maintained at 35 °C using THF as the eluent at a flow rate of 1 mL/min. The GPC system was calibrated using polystyrene standards with molecular weights ranging from 500 to 2.48 x 10⁶ Da. To prepare the samples, about 2 mg of each polymer sample was dissolved in 1 mL of THF solvent in a 5 mL vial. The solution was filtered and transferred to a GPC vial. The obtained data were analyzed using Breeze software (version 3.30 SPA, 2002: Waters, Milford, MA).

3.3.10 Differential scanning calorimetry (DSC)

DSC technique is a thermo-analytical technique where the heat required to heat the sample and reference is measured. The glass transition temperature of the elastomers is important to study as it gives the information about the temperature where the rubbery state changes to the glassy state and vice versa. The T_g values of the synthesized polymers can be determined by DSC. The DSC instrument used was a Q100 instrument (TA Instruments, New Castle, DE). The samples were prepared by weighing about 6-10 mg of the polymer in a DSC pan. The samples were then passing through two heating cycles. In the first cycle, the samples are heated from -70 to 200 °C at a ramp rate of 10 °C/min. Subsequently, the samples were cooled to -70 °C and reheated to 200 °C at the same ramp rate. The glass transition temperature (T_g) was determined using Universal Analysis 2000 software, V4.5 (TA Instruments, Delaware).

3.3.11 Nuclear magnetic resonance

¹H NMR spectra of the synthesized polymers were recorded using a 500 MHz NMR spectrometer (Agilent, USA). The samples were prepared by dissolving about 5 mg of each sample in 0.5 mL of CDCl₃.

REFERENCES

REFERENCES

- 1. Huhtamäki, T., Tian, X., Korhonen, J. T. & Ras, R. H. A. Surface-wetting characterization using contact-angle measurements. *Nat. Protoc.* **2018**, *13*, 1521–1538.
- 2. Tian, D., Song, Y. & Jiang, L. Patterning of controllable surface wettability for printing techniques. *Chem. Soc. Rev.* **2013**, *42*, 5184–5209.
- 3. Liukkonen, A. Contact angle of water on paper components: Sessile drops versus environmental scanning electron microscope measurements. *Scanning* **2006**, *19*, 411–415.
- 4. Dourado, F., Gama, F. M., Chibowski, E. & Mota, M. Characterization of cellulose surface free energy. *J. Adhes. Sci. Technol.* **1998**, *12*, 1081–1090.
- 5. Garnier, G. & Glasser, W. G. Measuring the surface energies of spherical cellulose beads by inverse gas chromatography. *Polym. Eng. Sci.* **1996**, *36*, 885–894.
- 6. Shen, W., Sheng, Y. J. & Parker, I. H. Comparison of the surface energetics data of eucalypt fibers and some polymers obtained by contact angle and inverse gas chromatography methods. *J. Adhes. Sci. Technol.* **1999**, *13*, 887–901.
- 7. Kim, D., Pugno, N. M. & Ryu, S. Wetting theory for small droplets on textured solid surfaces. *Sci. Rep.* **2016**, *6*, 1–8.
- 8. Murakami, D., Jinnai, H. & Takahara, A. Wetting transition from the cassie-baxter state to the wenzel state on textured polymer surfaces. *Langmuir* **2014**, *30*, 2061–2067.
- 9. Zilles, J. U. Characterization of coated papers: Wettabilities and Surface Tensions of Different Paper Types *Application report: AR221e* **2000**.
- 10. Marmur, A. Solid-Surface Characterization by Wetting. *Annu. Rev. Mater. Res.* **2009**, *39*, 473–489.
- 11. Morris, B. A. Barrier. *The Science and Technology of Flexible Packaging* **2017**, 259–308 (Elsevier, 2017)
- 12. Caulfield, D. F., Gunderson, D. E. Paper Testing and Strength Characteristics. TAPPI Press **1988**, 31-40.

Chapter 4: FOOD-SAFE CHITOSAN-ZEIN DUAL-LAYER COATING FOR WATER-AND OIL-REPELLANT PAPER SUBSTRATES

A version of this chapter is published as:

Kansal, D., Hamdani, S. S., Ping, R., Sirinakbumrung, N., Rabnawaz, M. Food-safe chitosan-zein dual-layer coating for water- and oil- repellent paper substrates. ACS Sustainable Chem. Eng. **2020**, *8*(*17*), 6887-6897.

4.1 Summary

Herein we report a unique approach that relies on 100% biobased and biodegradable food-safe materials for water- and oil-resistant paper. A 35-liner paper was coated with an oil-resistant chitosan solution, and subsequently by a hydrophobic zein solution. The resultant chitosan-zein-coated paper showed remarkable water resistance (Cobb 60 value of 4.88 g/m²) and oil repellency (Kit rating 12/12). Scanning electron microscopy (SEM) analysis was used to determine the changes in the surface texture of the paper before and coating treatment. The excellent mechanical properties of the coated paper were retained after the coating treatment. In addition, the pulp was recycled from the chitosan-zein-coated paper to validate the recyclability of this novel approach.

4.2 Experimental

4.2.1 Materials

Chitosan of molecular weight $M_n = 50,000\text{-}190,000$ g/mol (100% deacetylated, see ¹H NMR in Figure S1) and zein (96%) were purchased from Sigma. Ethanol (95%) was purchased from Koptec. Deionized (DI) water was used in all experiments described herein. Glacial acetic acid was purchased from Macron Fine Chemicals. All the chemicals were used without further purification. Paper (35 liner Kraft) was purchased from Uline (United States).

4.3 Methods and Characterization

4.3.1 Preparation of chitosan and zein stock solutions

Chitosan stock solution: A chitosan stock solution (4%, w/v) was prepared by dissolving 4 g of chitosan in 2% (v/v) acetic acid to provide a total volume to 100 mL, and this solution was stirred for 24 h at ambient temperature. Further dilutions were made from 4% (w/v) stock chitosan solution to make 0.5%, 1%, 2%, 3% (w/v) chitosan solutions. For example, to prepare 5 mL of a

2% (w/v) chitosan solution, 2.5 mL of 4% (w/v) chitosan solution was mixed with 2.5 mL of 2% (v/v) acetic acid solution under continuous stirring. The solution was stirred for another 10 min to provide a homogeneous solution.

Zein stock solution: A stock zein solution (40%, w/v) was prepared by dissolving 40 g of zein powder in an ethanol/water (85/15%, v/v) mixture to a total volume of 100 mL. The solution was stirred overnight at room temperature. Further dilutions were performed from the 40% (w/v) zein solution to provide 20% and 10% (v/v) solutions of zein. For example, to make 5 mL of a 20% (w/v) zein solution, 2.5 mL of the 40% (w/v) solution was mixed with 2.5 mL of an 85% (v/v) ethanol solution. The solution was stirred for another 10 min prior to use.

Coating Preparation: The paper substrates were coated by a bar coating technique using K303 Multi Coater (RK PrintCoat Instruments Ltd, UK,). For each layer, a 5.0 mL solution was applied on ~29 cm x 21 cm Kraft paper. The first layer of chitosan was applied as a solution and dried for 24 h at room temperature before applying the zein solution. After applying the zein solution, the bilayer coated paper was dried at room temperature for another 24 h. These coated paper substrates were then pre-conditioned at 23 °C under 50% relative humidity (RH) before performing further studies. The same procedure was used for the single-layer coated paper (e.g., chitosan-coated paper) where the coating solution was applied and was dried at 24 h at room temperature.

4.3.2 Characterization

Basis weight, coating load, material thickness: The basis weight or mass per square meter of unmodified paper (U-p), chitosan-coated paper (C-p), zein-coated paper (Z-p), chitosan and zein mix-coated paper (CZ-mix-p), as well as the chitosan and zein bilayer-coated paper (CZ-p)

were measured in accordance with the ASTM D646 protocol. The paper was cut into 12 x 12cm² sections. The basis weight, coating load and material thickness were recorded as per the procedure mentioned in Chapter 3, section 3.3.5.

Water vapor transmittance rate (WVTR) and Water absorption capacity (Cobb 60 value): WVTR values for U-p, C-p, Z-p and CZ-p were recorded with a Permatran-W (Model 3/34, Mocon Inc., MN, USA) at a temperature of 23 °C and relative humidity (RH) of 50%. The permeability was measured using **Equation 8**, mentioned in Chapter 3, section 3.3.2.1.

The water absorptiveness values of U-p, C-p, Z-p, and CZ-p were determined as Cobb 60 values following a TAPPI standard T441 om-09 protocol. For these measurements, a Cobb sizing tester (Büchel BV Inc., Utrecht, Netherlands) was used to allow the paper substrate to be in contact with 100 mL of distilled water for 60 s. The Cobb 60 values were calculated using **Equation 6**, Chapter 3, section 3.3.2.2.

Grease resistance: Grease resistance of U-p, C-p, Z-p, and CZ-p were studied following the TAPPI T 559 pm-96 standard protocols. The detailed procedure and kit rating solution preparation has been detailed in Chapter 3, section 3.3.3.

Contact angles (CAs) and Sliding angles: The water and oil (castor oil) contact angles (CAs) of U-p, C-p, Z-p and CZ-p were measured with a VCA 2000 (Video Contact Angle System, AST Products, INC., USA). Droplets with volumes of approximately 10 μL were placed onto the paper specimen and the value was recorded after 30 s. Three replicates were recorded for each sample.

Water and oil sliding angles were determined by fixing the specimen onto a movable wood plate. A droplet with a volume of 100 µL was placed on the specimen, and the wood plate was tilted at a constant speed of (2°/s) until the water/oil droplet started to slide. The angle was recorded for three replicates each for U-p, C2-p, Z20-p, and C2Z20-p.

Attenuated-Total-Reflection Fourier-Transform Infrared (ATR-FTIR) Spectroscopy: The ATR-FTIR analysis of the paper substrates U-p, C-p, Z-p and CZ-p were recorded using a Shimadzu FTIR spectrometer IR-Prestige21. (Section 3.3.8, Chapter 3)

Thermogravimetric Analysis (TGA) and Scanning Electron Microscopy (SEM): TGA data for U-p, C-p, Z-p, and CZ-p samples were recorded with a Q-50 thermogravimetric analyzer (TA Instruments, New Castle, DE). Detailed procedure for TGA has been mentioned in Chapter 3, section 3.8. SEM images were recorded with a JEOL 6610 SEM (JEOL Ltd., Japan) system with an accelerating voltage of 15 kV to study the surface texture of the U-p, C-p, Z-p and CZ-p samples (Chapter 3, section 3.3.7).

4.3.3 Recyclability

The recyclability of the different coated papers (C-p, Z-p, and CZ-p) were determined via a repulping approach. For this experiment, 3.0 g of coated paper (C2Z20, chitosan 2wt% first layer, Zein 20 wt% as top layer) was weighed and cut into 2 x 2 cm² pieces, and repulped using a blender after soaking in distilled water for 30 min. The pulp was divided into four parts. The first three parts were washed with DI water, 2% (v/v) acetic acid solution, and 85% (v/v) ethanol solution separately three times each. The fourth part was first washed with 2% (v/v) acetic acid solution, subsequently with 85% (v/v) ethanol solution, and finally with distilled water. All of these parts were filtered onto a mesh, pressed, and ironed to obtain the paper. The obtained paper was

subsequently dried overnight in an oven at 55 °C. The uncoated and coated paper samples that were obtained after repulping were subsequently analyzed via ATR-FT-IR spectroscopy for characteristic peaks corresponding to zein and chitosan.

4.3.4 Mechanical Properties

Paper samples (35 liner Kraft) were coated with chitosan (2% w/v), zein (20% w/v), and bilayers of chitosan and zein (C2Z20) polymers. Each test was performed in both cross-machine direction and machine-direction three times to study the effect of the coatings on the paper substrate.

Tensile Strength (TS), Ring Crush Tests (RCTs), Bending Stiffness (BS), Internal Tearing Resistance (ITR) tests were performed via the TAPPI standards as described in Chapter 3, section 3.3.3.

4.4 Results and Discussion

To develop a plastic-, PFAS- and siloxane-free approach for water- and oil-resistant paper, we came up with a novel approach through which the paper is coated with biodegradable biopolymers that not only impart the coated paper with 100% biodegradability, but also ensure that the pulp can be conveniently recycled by washing the coating away in an appropriate benign solvent such as a water/ethanol mixture. A dual-layer approach was utilized in this study. The first layer of the coating was composed of chitosan, which is easily derived from chitin and is fully biodegradable. Meanwhile, the second coating layer is composed of zein, which is an agricultural by-product derived from corn. The coating materials are biodegradable and food-safe, which thus ensures that the coated paper is also biodegradable and food safe.

Paper is made up of cellulose, which is highly polar and hence renders the paper hydrophilic. Due to the porous nature of paper and the resultant capillary action that takes place, paper also readily absorbs of oils and water. Our aim was to render paper both water and oil repellent using biodegradable materials. Figure 4.1 displays several possible hypothesized scenarios in which zein and chitosan are used to coat paper. For example, zein is hydrophobic, and therefore zein-coated paper will only be water-resistant (Figure 4.1a). Meanwhile, chitosan is oleophobic but also hydrophilic. Therefore, chitosan-coated paper will only exhibit oil repellent properties (Figure 4.1b). A chitosan-zein blend will have poor water and oil resistance due the concurrent exposure of the hydrophilic chitosan and oleophilic zein (Figure 4.1c). Finally, a duallayer coated paper with zein forming the top layer and chitosan comprising the bottom layer will be both water and oil repellent (Figure 4.1d). Zein layer was chosen as the top layer on account of its hydrophobic nature, so that when paper encounters water, the water does not become absorbed or permeate into the paper. Chitosan was selected as the bottom layer because of its excellent oil repellency due to its hydrophilic nature. Consequently, when oil encounters the zein layer, the oil may pass through that outer layer as zein lacks oil repellency. However, the oil will be repelled by the inner chitosan bottom layer, and thus the coated paper will be protected against contamination by the oil.

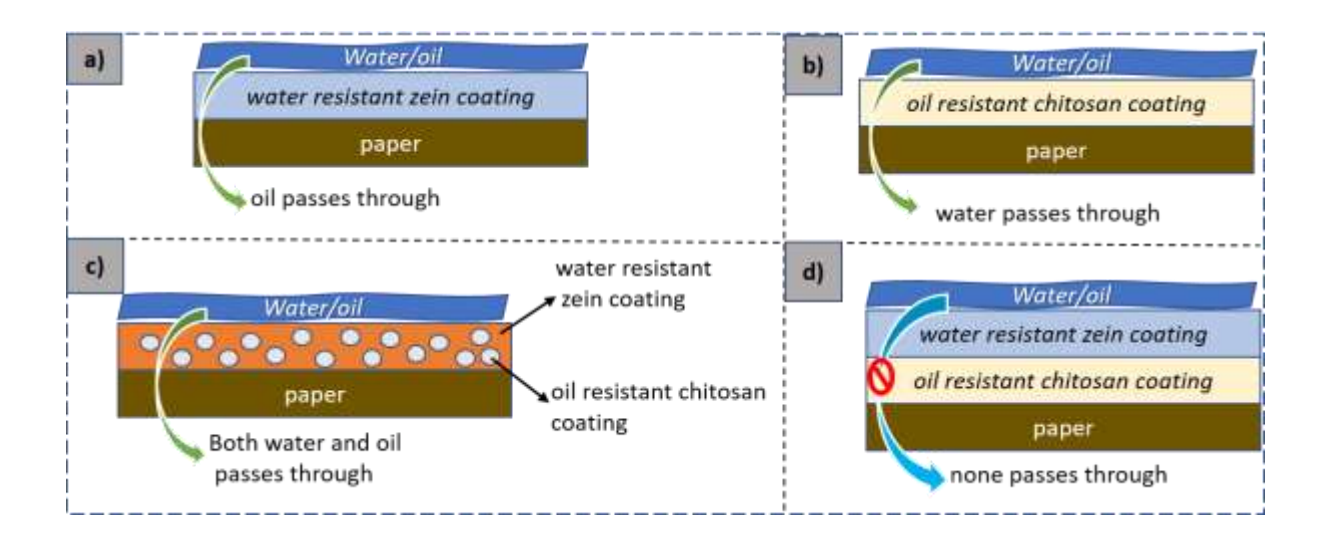


Figure 4.1: Illustration of various coatings on paper with respect to their water and oil repellency.

a) Zein-coated paper exhibits water resistance but prone to permeation by oils; b) Chitosan-coated paper is oil resistant but allows the passage of water; c) a zein and chitosan blend coating allows the passage of both water and oil; and d) a dual-layer coating (with a chitosan bottom and zein top layer) prevents the passage of both water and oils.

To prove the hypotheses depicted in **Figure 4.1**, Kraft paper substrates were coated with different coatings (see **Table 4.1**), and their water and oil repellencies were determined. After the application of the coating, the coated paper was dried overnight at room temperature. Prior to the water and oil repellency tests, coated paper samples were pre-conditioned at room 23 °C and 50% relative humidity (RH) for 24. As shown in Table 1, the zein-coated paper was only water resistant, while the chitosan-coated paper was only oil repellent. The paper that was coated by a blend of zein and chitosan exhibited poor water and oil resistance owing to the exposure of both hydrophilic and hydrophobic groups on the surface of the coated paper. In the case of our novel combination, where zein comprised the top layer, and chitosan formed the bottom layer, the coated paper showed remarkable water and oil resistance. A firm interaction between chitosan and zein layers is

essential for practical applications of chitosan-zein coated paper. A good interaction between zein and chitosan is expected as zein had 45% hydrophilic functional groups, ¹⁻³ which is evident from the fact that we did not observe any delamination of the zein from the dual-layered coated paper. Also, though, the chitosan layer was ambiently dried for 24 h before applying the zein layer, but as zein was applied as an ethanol/water solution. The ethanol/water solution readily wets the chitosan surface, and subsequently swells chitosan, thus allowing the zein and chitosan polymer chains to entangle at the interface. In one case, zein was applied as the bottom layer and chitosan was applied as the top layer. The paper bearing this coating had an excellent kit rating due to the presence of the chitosan top layer, but it also had poor water resistance as water was absorbed by the chitosan layer.

Table 4.1: Comparison of the Cobb 60 values and Kit ratings for various coated paper substrates

Sample	Cobb 60 (g/m ²)	Kit Rating
U-p (control)	29.34	0
Z20-p (Figure 1a)	9.38	5.66
C2-p (Figure 1b)	25.5	12
C2 and Z20 blend (Figure 1c)	20.35	6
C2Z20-p (Figure 1d)	4.88	12
Z20C2-p (control)	26.4	12

After validation of our hypothesis that the use of chitosan as the bottom layer and zein as the top payer provides the best combination, then we conducted systematic studies on various formulations that were obtained by varying the concentrations of zein and chitosan. Different coating loads of zein and chitosan were studied to identify optimal performance, such as minimum

coating load and best cobb and kit values. The data obtained from these tests with various formulations tested are shown in **Table 4.2**. In some cases, only one layer was applied to the paper substrate as controls in this study. The thickness of the uncoated paper was found to be 181 μ m whereas for single-layer coated paper, e.g., C1, C2, Z10, Z20 the thicknesses were found to be in the range of ~197-199 μ m, implying that the coating covering the paper substrate had a thickness of ~20 μ m. For the bilayer-coated paper, the thickness was found from 208 to 210 μ m, which again fall in agreement that the second coating is ~10 μ m thick.

Table 4.2: Basis weight, thickness and coating load of uncoated and coated paper

Sample Name	Material Thickness (μm)	Basis Weight (g/m²)	Coating Load (g/m²)
U-p	181	-	-
C1-p	199	132.05±0.83	2.57 ± 0.19
Z10-p	197	142.084±1.51	14.35 ± 1.04
Z20-p	198	152.66±2.09	23.86 ± 2.74
C1Z10	210	142.84±5.39	14.37±1.62
C1Z20	210	154.58±6.42	21.99±1.62
С2-р	205	131.11±2.62	3.65 ± 0.28
C2Z10	207	145.83±4.85	14.58±1.23
C2Z20	208	154.80±4.29	23.61±2.82

C represents Chitosan, Z represents Zein, while the number denotes the concentration in %(w/v). For example, C1Z10 represents a dual-layer coating of 1% chitosan (bottom) and 10% zein (top) solutions. Z20-p represents single-layer coated paper that is coated with 20 w/v% zein solution. C2Z20-p represents bilayer coated paper, where firstly paper is coated with 2w/v% chitosan solution, then the paper is dried at room temperature for 24 h, and subsequently coated with 20w/v% zein solution, and then dried at room temperature for 24 h.

The coated paper was characterized by ATR-FTIR spectroscopy. **Figure 4.2** shows the ATR-FTIR spectra of uncoated paper as well as paper samples that had been coated by chitosan (C2), zein (Z20) and a bilayer of chitosan and zein (C2Z20). Chitosan and zein show characteristic peaks in the region of 1400-1700 cm⁻¹. The uncoated paper (U-p) did not exhibit any peaks in that region. Meanwhile, the 2% chitosan-coated paper (C2-p) exhibited peaks in the range of 1500-1600 cm⁻¹, which can be attributed to C=O and N-H stretching vibrations. In the spectrum of 20% zein-coated paper (Z20-p), two broad peaks are seen in the region from 1500-1700 cm⁻¹ corresponding to different C=O and N-H peaks belonging to the amide moieties in zein, while C-H stretching peaks in the range of 2900-3000 cm⁻¹ are also observed. The dual-layer-coated paper (C2Z20-p) exhibited peaks in the same region, indicating that both zein and chitosan are present in this coating.

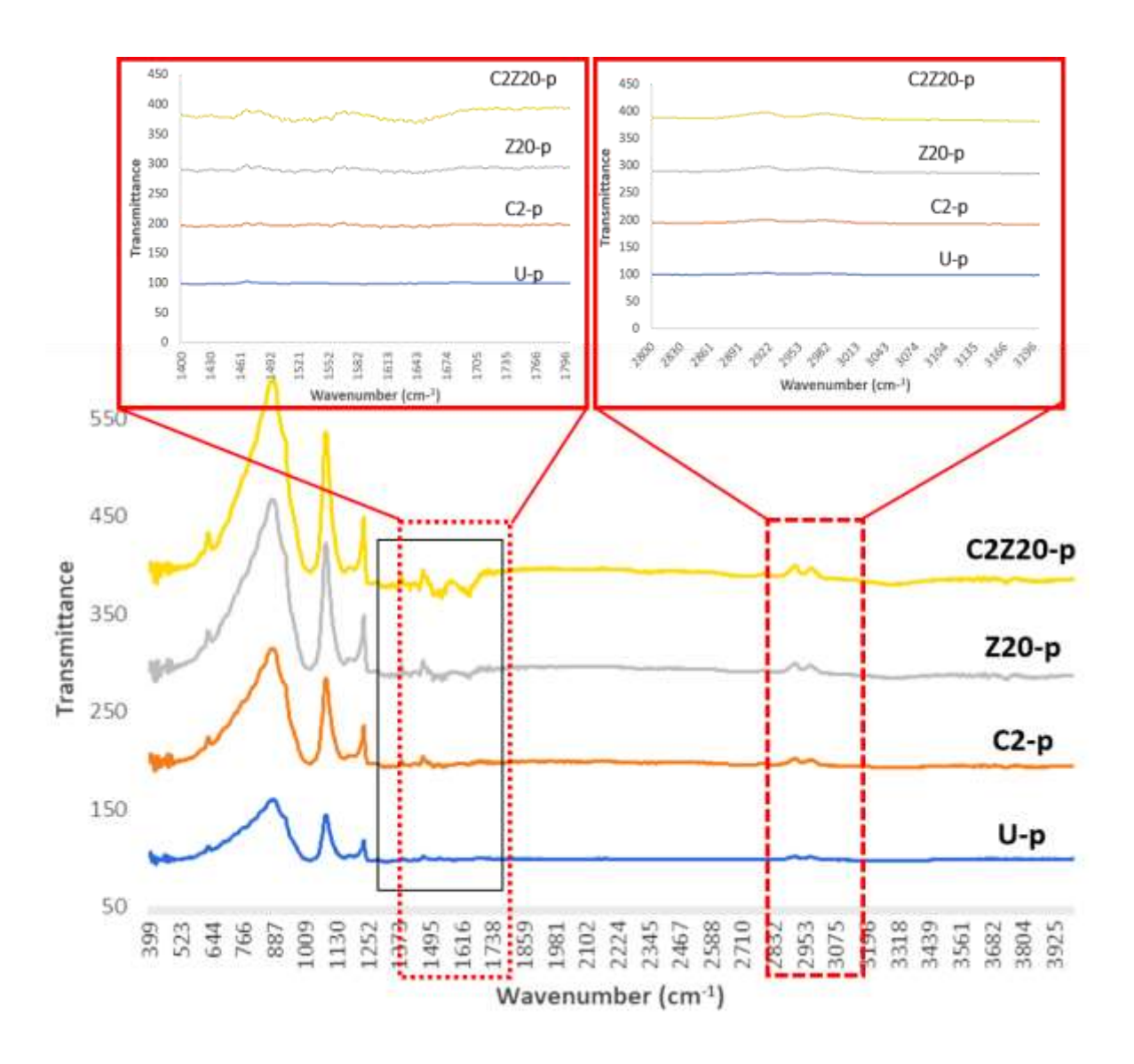


Figure 4.2: ATR-FTIR spectra of uncoated paper (U-p), 2% chitosan-coated paper (C2-p), 20% zein-coated paper (Z20-p), and dual-layer-coated paper (C2Z20-p). Two IR portions are zoom-in for clarity.

Both uncoated and coated paper samples were studied to evaluate their tolerance toward water vapor and liquid water as probes. The tolerance toward liquid water was reported as the Cobb 60 value, while the WVTR corresponded to the resistance toward water vapor (see **Figure 4.3**). From the Cobb 60 values, a reduction of the water absorbency by 13% was observed for the

paper that was coated with 2% (w/v) chitosan solution (C2) in comparison with the uncoated paper (U-p). This reduction was due to the pores of the paper becoming covered by the coating, thus impeding the passage of water to some extent. However, only a modest reduction was observed, which suggested that the coating offered only modest water resistance. On the other hand, when the paper was only coated with 10% (Z10) and 20% (Z20) (w/v) zein solution, reductions of 52% and 68% were respectively observed as compared to the uncoated paper. The drastic reduction in the Cobb 60 value that was provided by the zein coating as opposed to the chitosan coating can be attributed to the chemical compositions of these materials. Chitosan has polar hydroxy and amino groups on the surface that interact with water through hydrogen bonds, and thus chitosan is more hydrophilic. In contrast, zein possesses a smaller number of polar groups on its surface so that it is more hydrophobic in nature, and hence it repels water to a greater extent. The Cobb 60 value for the dual-layer-coated paper indicated that the water repellency decreased by 83.3% relative to uncoated paper, as indicated for the Cobb 60 value of 4.88 g/m² for C2Z20 versus 29.34 g/m² for uncoated paper. This can be explained based on the SEM images of the dual-layer-coated paper (C2Z20) and will be discussed later. As can be seen, there were no open pores remaining on the dual-layer-coated paper, and also, the hydrophobic nature of the zein imparted the paper with a high degree of water resistance.

To understand the effect of zein on the water absorbency of the dual-layer coating, two different sets of coated papers were prepared, CxZ10 and CxZ20, where x can be 1% or 2% chitosan solution. A 48% reduction of the Cobb 60 value was observed when the concentration of zein was increased from 10% to 20% (w/v) for C2Z10 (9.46 g/m²) to C2Z20 (4.88 g/m²). This decrease in the Cobb 60 value can be attributed to the hydrophobic nature of zein. The difference

between Cobb 60 values of Z20-p (9.38 g/m2) and C2Z20-p (4.88 g/m2) is due to the better masking of the pores in the case of C2Z20-p. C2Z20-p is a dual-layer coated paper with more coating load, and no visible pores, which is also evident from the SEM images. In addition, chitosan (the bottom layer) has excellent film-forming properties in the case of C2Z20-p and hence can mask pores effectively. In addition, because the 20% solution yields a thicker coating, it tends to fill the bottom chitosan layer effectively from water, and thus helped to improve the water-resistance of the paper.

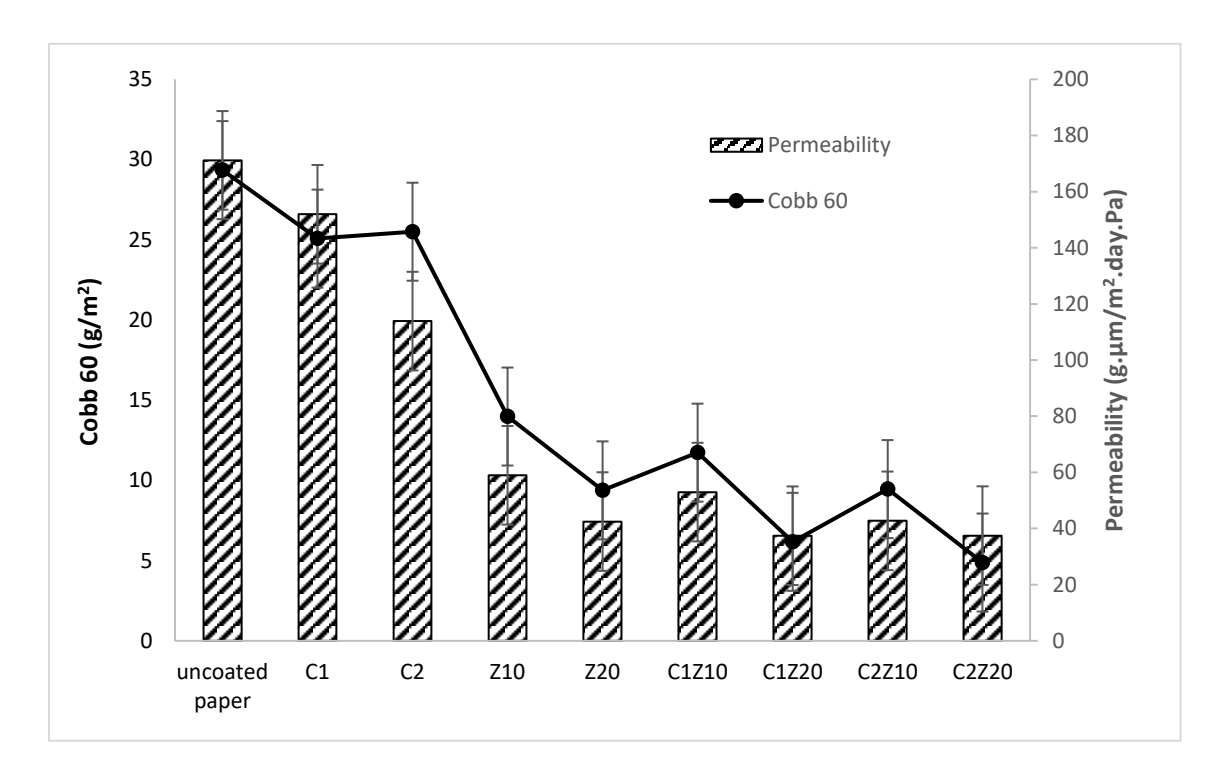


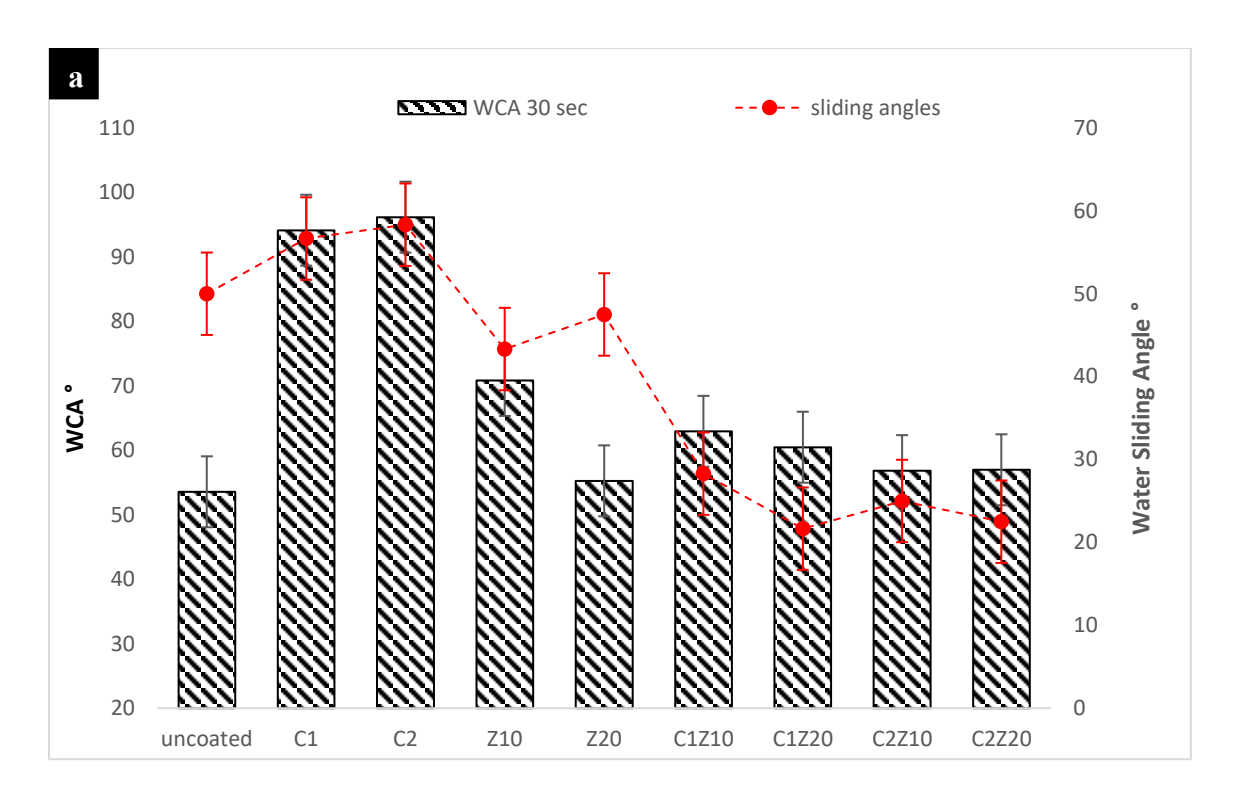
Figure 4.3: Permeability $(g \cdot \mu m/m^2 \cdot day \cdot Pa)$ and Cobb 60 values (g/m^2) of coated and uncoated paper samples at 50% RH and 25 °C. The average thickness of all coated papers was ~ 200 μm .

Water vapor permeability data also showed a similar trend for the coated paper. C1 (1% chitosan)- and C2 (2% chitosan)-coated paper showed a very high-water vapor permeability, but when the chitosan-coated paper was also coated with Z10 and Z20 the permeability decreased

considerably. CxZ10 and CxZ20, where x can be 1% or 2% (w/v) of chitosan, also showed a decrease in the permeability as the concentration of the zein solution was increased from 10% to 20% (w/v). This was again observed due to the filling of the pores of the paper and the hydrophobic nature of zein, which absorbs less water vapor, and hence reduces the water vapor permeability. Overall, the zein concentration affects the water vapor barrier properties, while chitosan does not have a significant effect.

The wettability of the coated paper was also explored via contact angle measurements at 30 s, as shown in Figure 4.4a. The water contact angle (WCA) of the uncoated paper at 30 s was found to be $53.5 \pm 1.3^{\circ}$, due to the roughness of the paper. For the paper that had been coated with a 2% (w/v) chitosan solution, a WCA of 96.1±5.8° was obtained at 30 s. Meanwhile, the paper samples that had been coated with a 20% (w/v) zein solution exhibited a WCA of $55.2 \pm 2.6^{\circ}$ at 30 s, while the value was also found to decrease for the samples bearing the dual-layer coating of C2Z20 from $56.9 \pm 4.2^{\circ}$. In the case of paper as substrates, the contact angles depend on surface energy, roughness, and porosity. The decreasing order of water contact angles is C2>C1Z20> C2Z10> C2Z20 ≈Z20, and the trend is exciting. C2 paper has the maximum contact angle due to the excellent masking of the pores along with very rough surfaces of the C2 coated paper (see SEM images described later). C1Z20 showed a higher contact angle relative to C2Z10, C2Z20, and Z20 because of higher hydrophobic zein content and better masking of the pores with chitosan. In the case of C2Z10, better masking of pores due to chitosan but zein coating load is low relative to C1Z20 and therefore has a lower WCA than C1Z20. The contact angles for C2Z20 and Z20 are almost equal due to the two opposite factors, such as Z20 is rough but porous while C2Z20 is nonporous but smooth. The excellent performance of the dual-layer coating is also evident from the

fact that the sliding angles were very impressive for the dual-layer-coated (C2Z20) paper (e.g., 22.5°) compared to the paper samples that had been coated with 2 wt% chitosan (58.3°). These low water sliding angles are also in agreement with the excellent Cobb 60 values for the C1Z10-, C2Z10-, C2Z10-, and C2Z20-coated paper.



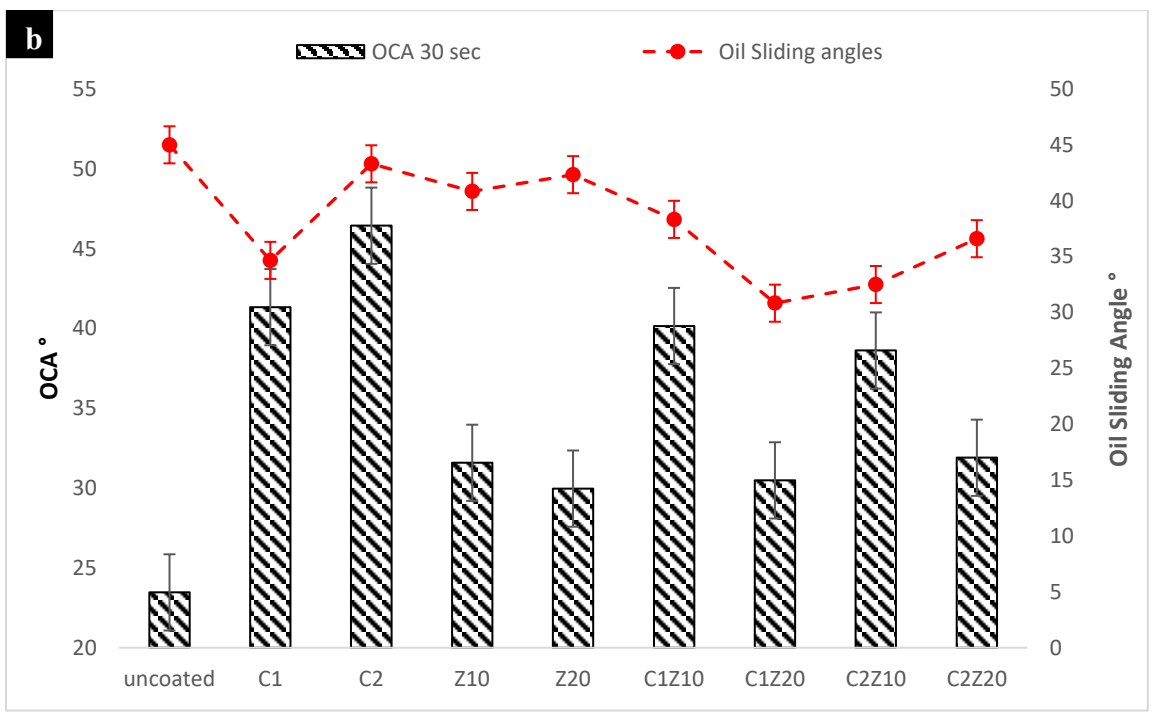


Figure 4.4: Sliding angles and CAs (after 30 s) of: a) water b) castor oil.

To test the resistance of the uncoated and coated paper towards castor oil, oil contact angles, sliding angles and "Kit Ratings" were also determined (See Figure 4.4b, and 4.5). An oil contact angle of $23.6 \pm 2.2^{\circ}$ at 30 s was observed for uncoated paper. For the 2% chitosan-coated paper, a contact angle of $46.4 \pm 0.83^{\circ}$ was obtained at 30 s. Meanwhile, the 20% zein-coated paper exhibited an oil contact angle of $29.9 \pm 2.6^{\circ}$ at 30 s. The reduction in the oil contact angle from those observed with C2 to Z20 was due to the increased surface smoothness of the zein-coated paper as compared to the chitosan-coated paper. In the case of the dual-layer-coated paper C2Z20, an oil contact angle of $31.9 \pm 3.6^{\circ}$ was obtained. Based on the above observations it can be stated that, although the water and oil contact angles of the dual-layer-coated paper samples were lower than those of the 2% chitosan-coated and uncoated papers, but they had excellent sliding angles. The lower contact angles, despite good water repellency of the dual-layer coated paper, corresponds to their smooth surface (described in SEM later). This finding implies that the water or oil droplets do not diffuse through the pores and suggests that this coating may be suitable for various practical applications.

Paper samples that had been coated with various formulations were also subjected to kit rating tests (**Figure 4.5**). The 'kit rating' values showed that the coated paper had a higher resistance towards oil with the kit rating values reaching up to 12/12 and as opposed to the uncoated paper that had a value of 0/12. C2-p and Z20-p were found to have kit ratings of 12 and 5.66, respectively, indicating that zein itself has a poor resistance towards oil while chitosan has better repellency against oil because of its hydrophilic nature. Meanwhile, the dual-layer-coated paper C2Z20-p exhibited a kit rating of 12, implying that although the oil passes through the zein

top layer on this paper, the bottom chitosan layer still acts as a barrier preventing the passage of the oil through the coated paper.

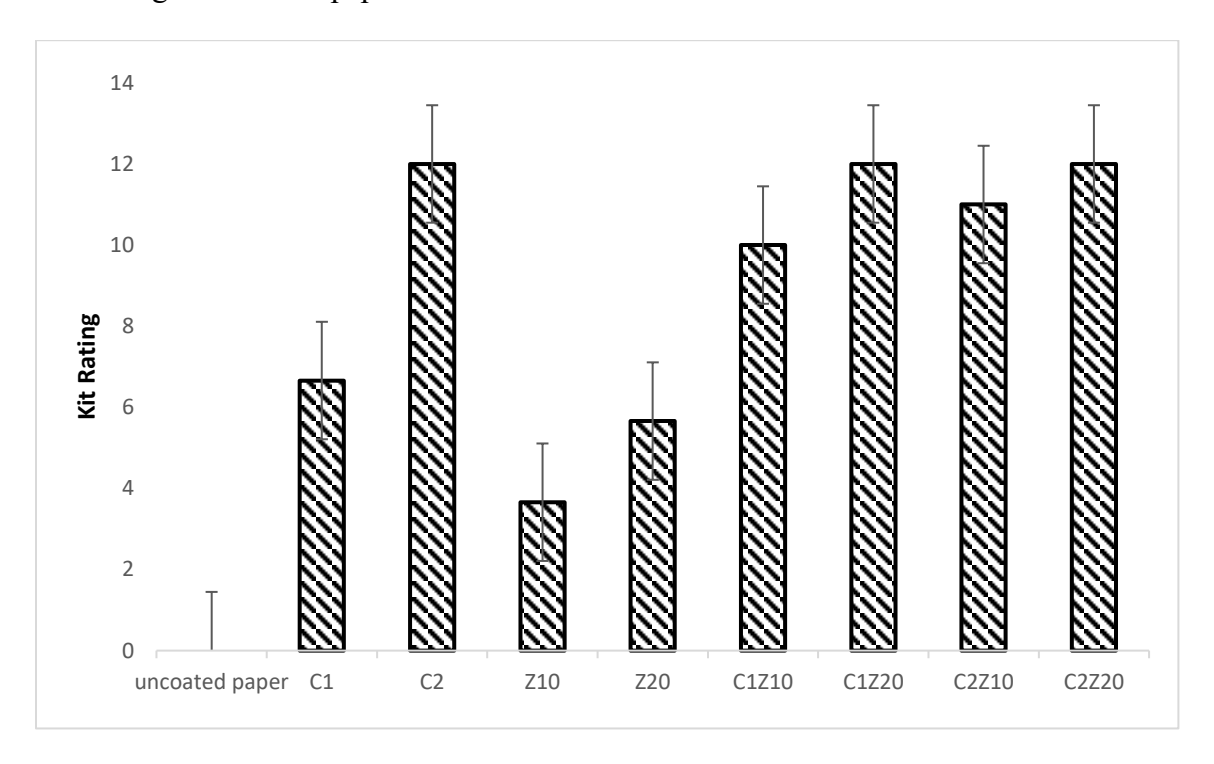


Figure 4.5: Kit ratings of coated and uncoated paper samples. A kit rating of '12' corresponds to the maximum oil-resistance, while a value of '0' corresponds to a complete lack of oil resistance.

To understand the behavior of the coated paper at the microscopic level, SEM images of U-p, C2-p, Z20-p, C2Z20-p were recorded (**Figure 4.6**). As can be seen in **Figure 4.6a**, the uncoated paper possesses a high density of pores that permit the passage of water and oil, and hence the paper has poor resistance against these liquids. **Figure 4.6b** shows the SEM image of the chitosan-coated paper (C2-p), where most of the pores are masked. However, due to the hydrophilic nature of chitosan, it forms hydrogen bonds with water and hence absorbs an enormous amount of water. On the other hand, chitosan is oleophobic and hence the surface of this paper is able to repel oil. The SEM image of zein-coated paper (Z20-p) is shown in **Figure 4.6c**, where

again, most of the pores are covered by zein. Due to the hydrophobic nature of zein, the surface of the zein-coated paper is more repellent to water but less repellant to oil. The surface of the dual-layer-coated paper C2Z20 is smooth, and the pores on the paper are coated with chitosan and zein (see **Figure 4.6d**). It is evident from the SEM images that the dual-layer coating has the least surface roughness, which explains one of the key reasons (along with porosity and surface energy) why lower contact angles were observed for the dual-layer-coated paper despite their superior water and oil resistance.

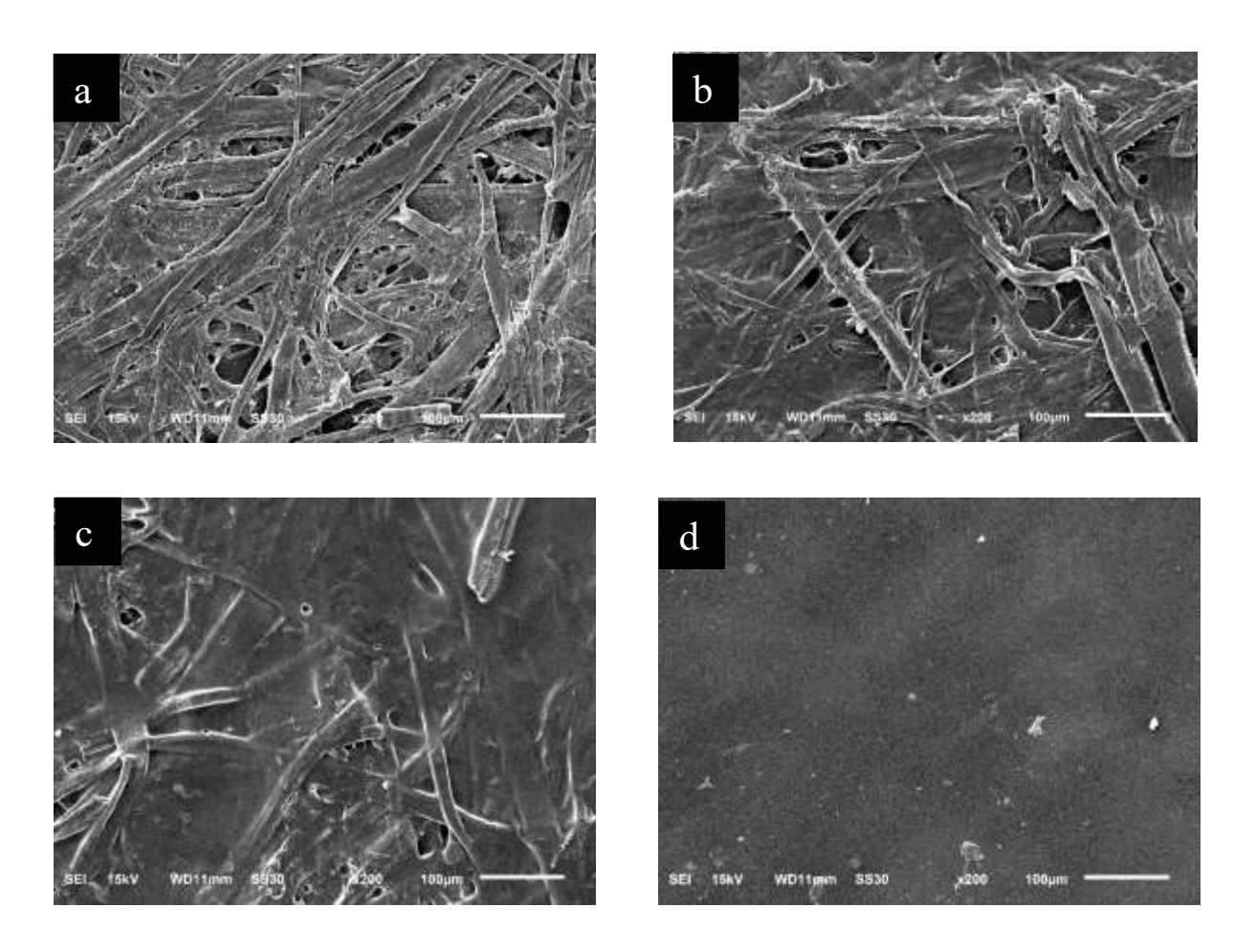


Figure 4.6: SEM images (200×) of unmodified paper U-p (a), chitosan-coated paper C2-p (b), zein-coated paper Z20-p (c), as well as the chitosan and zein bilayer-coated paper C2Z20-p (d).

The thermal stabilities of the U-p, C-p, Z-p, and C2Z20-p samples were evaluated via TGA. Since the coating load was minimal, therefore no significant changes were observed in the TGA plots for coated and uncoated paper. Therefore, free-standing films of chitosan and zein were prepared to gain insight with regard to the weight loss of chitosan and zein. It was observed that the paper substrate decomposed between 200 and 400 °C (Figure 4.7). Chitosan showed three weight loss regions in the graph. The first weight loss occurred below 150 °C and was due to the removal of water/moisture from the chitosan. The second weight loss was observed ~ 180 °C, which was likely due to the removal of the acetic acid that had been used for chitosan dissolution. Lastly, the third weight loss occurred in the range of 220-400 °C and due to the degradation of the chitosan polymer chain. A.5 Zein also showed two weight loss regions. The first one was observed in the range of 90-150 °C due to water loss, and the second occurred in the range of 200-350 °C.6 As there no degradation was observed below 200 °C, our findings indicate that the coated paper is thermally stable and could be suitable for dual oven applications (e.g., conventional oven and microwave).

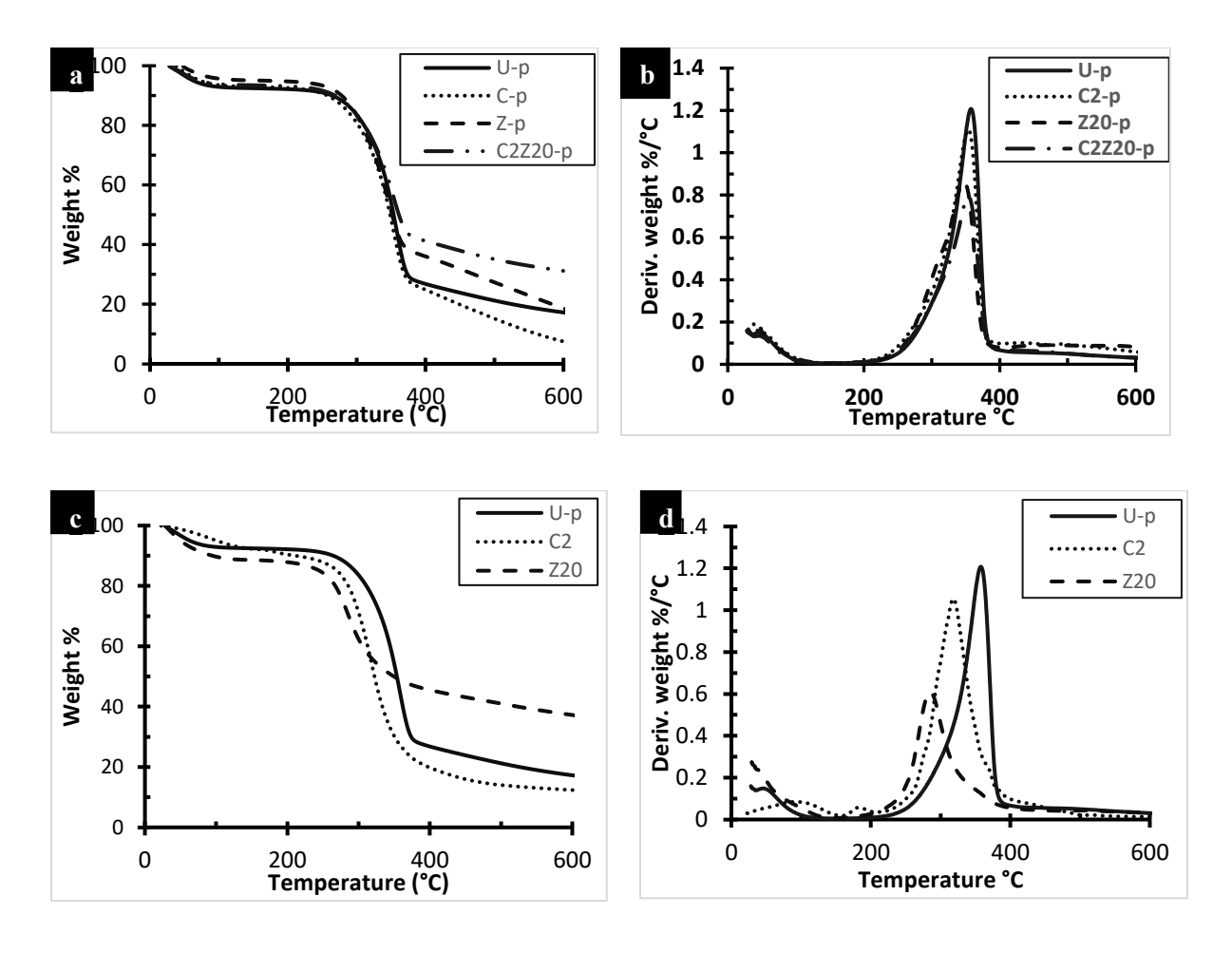


Figure 4.7: TGA (a) and DTG (b) plots of uncoated paper (U-p) and coated paper (C2, Z20, C2Z20). Also shown are TGA (c) and DTG (d) plots of the chitosan coating (C2), Zein coating (Z20), and unmodified paper (U-p).

The mechanical properties of the coated paper samples were also evaluated. In particular, tensile strength (TAPPI T494), bending stiffness (TAPPI T489), ring crush tests (TAPPI T822), and internal tearing resistance (TAPPI T414) experiments were performed on U-p, C-p, Z-p and C2Z20 (**Figure 4.8**). The tensile strength data indicated that in the cross-direction, the strength of U-p and C2-p were 29.05 and 32.38 lbs/in, which increased rapidly to 42.2 lbs/in for zein-coated paper (Z20) possibly due to the stiff and rigid nature of zein material. In the case of the dual-layer-

coated paper, the tensile strength decreased back to 28.01 lbs/in, which is close to that of the uncoated paper. A similar trend was observed with regard to the machine-direction for all of the paper samples (**Figure 4.8a**). This behavior implied that even though a single coating of zein increases the stiffness of the paper, the presence of the dual-layer coating has no drastic effect on the tensile strength of the paper.

Ring crush tests showed that with single zein coating on the paper, the value increased drastically for Z20-p to 38.73 lbs in both CD and MD from 22.13 and 31.2 lbs, respectively, for U-p due to the rigid zein material. However, the performance decreased slightly to 32.97 and 29 lbs for C2Z20 in CD and MD, respectively. The coated paper showed an overall increase in its ring crush strength. Bending stiffness in the cross-direction increased from 25.4 g cm for U-p to 29.35 g cm for C2Z20-p, whereas in the machine-direction, U-p showed a value of 52.35 g cm which decreased to 42.6 g cm for C2Z20-p. Internal tearing resistance was found to increase as one progressed from uncoated paper to coated paper with a value of 146.67 to 158.67 g for U-p and C2Z20-p, respectively, in the cross-direction of the paper. In the machine-direction, it was observed that internal tearing resistance decreased slightly from 146.67 g to 142.67 g for U-p and C2Z20-p, respectively. Overall, the mechanical properties of various paper substrates indicated that the application of a single layer of the zein coating onto the paper had a dramatic effect on the tensile strength, bending stiffness, ring crush force and internal tearing. In contrast, the presence of a bilayer coating exhibited only a modest effect on the mechanical properties of the paper. We suspect that this behavior (e.g., zein improved the mechanical properties) might be due to the stiff and brittle nature of zein materials relative to chitosan. The stiffness of zein is also evident from the excellent performance of Z20 in the ring crush test.

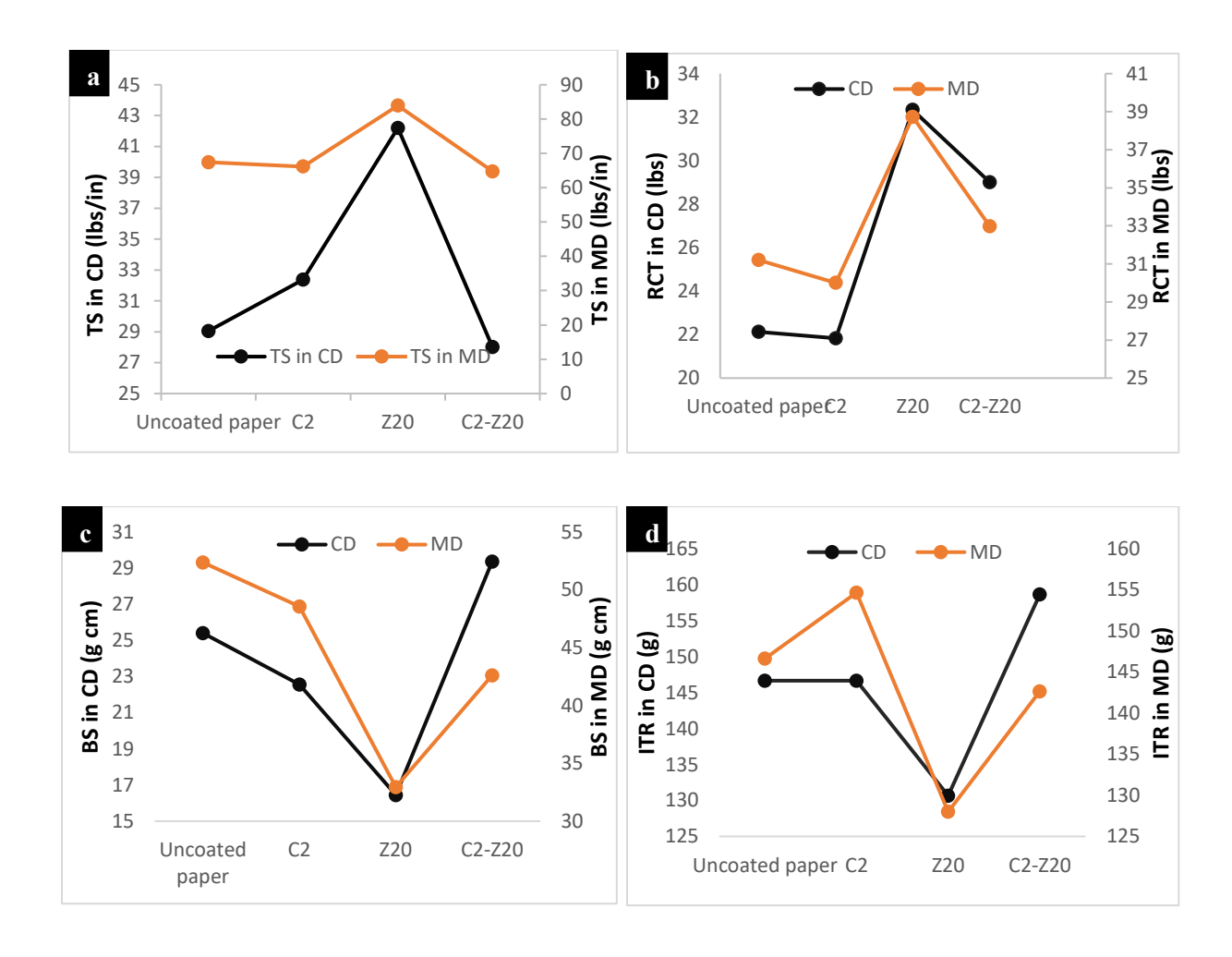


Figure 4.8: Mechanical properties of the uncoated paper (U-p), and coated paper (C2, Z20 and C2Z20). Tensile strength (a), ring crush test (b), bending stiffness (c), and internal tearing resistance (d).

One of the key benefits of our dual-layer coating is that it can be applied via the physical grafting approach, which enables the separation of the coating from the paper on demand and hence facilitates pulp recovery. Photographs of the paper pulp that were recovered from the dual-layer coated paper using various washing treatments are shown in **Figure 4.9**. When the pulp was washed with distilled water and 2% acetic acid separately, zein was left behind in the form of yellow precipitates, as this polymer is dark yellow and insoluble in water or aqueous acetic acid

solutions. The dark brown color revealing the presence of zein disappeared after the pulp had been washed with a water/ethanol mixture, which indicates the successful recovery of pulp from the coated paper. Further confirmation for the removal of zein and chitosan from the dual-layer-coated paper was obtained via FTIR analysis, which indicated that zein and chitosan had been completely removed from the pulp after washing with ethanol/water and acetic acid/water mixtures (**Figure A** in Appendices). This repulpability confirmed two key benefits of this coating approach, namely, the recovery of pulp and the recovery of the coating materials.

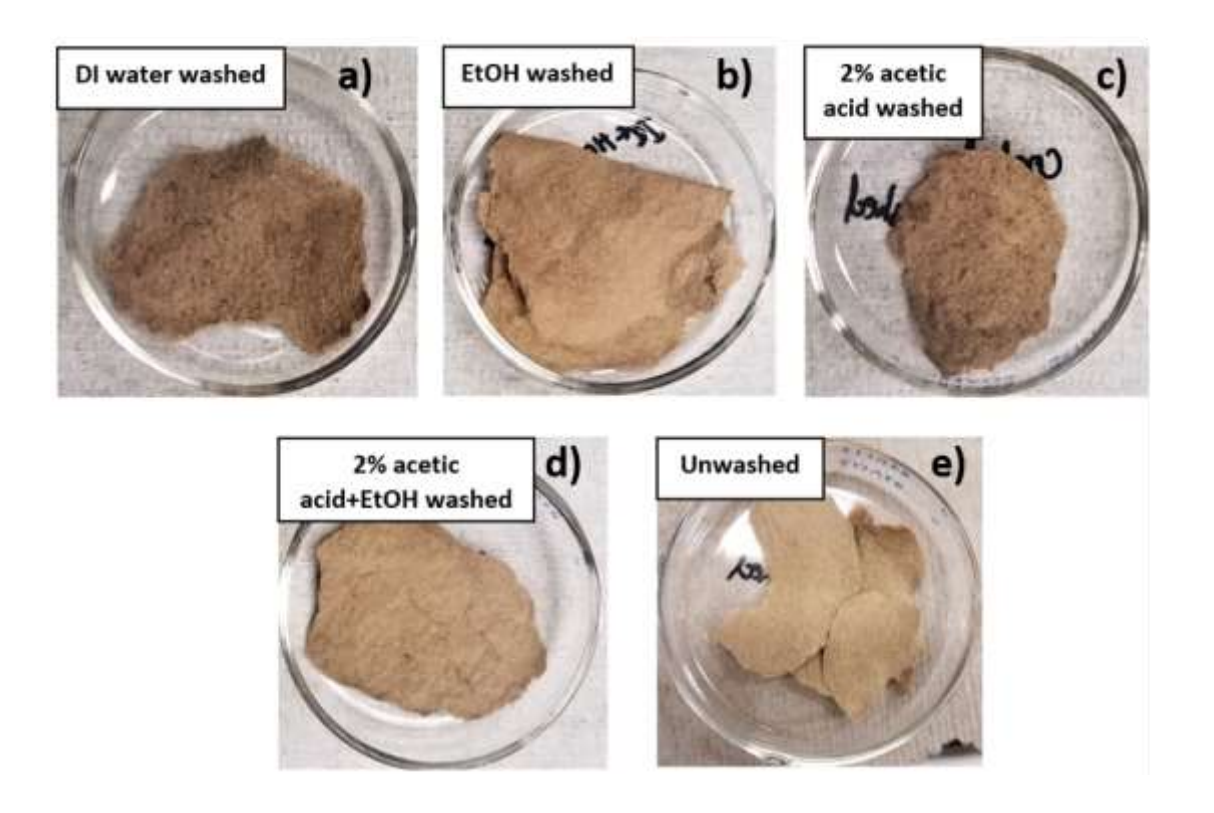


Figure 4.9: Photographs of repulped paper samples after various washing treatments. (a) Pulp washed with distilled water; (b) pulp washed with 2% acetic acid solution; (c) pulp washed with 85% ethanol solution; (d) pulp washed with first with 2% acetic acid and then with 85% ethanol; and e) unwashed pulp. The brown color of the paper is primarily due to the use of unbleached Kraft paper.

4.5 Conclusions

In summary, we have developed a novel dual-layer approach to fabricate water- and oil-resistant paper. The dual-layer-coated paper exhibited excellent water resistance (with a Cobb 60 value of 4.88 g/m²) and grease resistance (with a kit rating of 12/12). The water and oil contact angle of the dual-layer-coated paper were relatively low due to the smoothness of paper surface, but the sliding angles of this paper for water and oil were superior to that of the uncoated and

chitosan-coated paper. SEM analysis verified the surface texture of the coated and uncoated paper and the rationale for the low contact angles exhibited by the dual-layer-coated paper. The coated paper has excellent thermal stability and good mechanical properties. In addition, the pulp recovery from the coated paper was also validated. This food-safe paper coating that is derived from by-products (zein and chitosan) will offer several economic and environmental benefits related to packaging and non-packaging sectors, while also helping the environment.

REFERENCES

REFERENCES

- 1. Kasaai, M. R. Zein and Zein -Based Nano-Materials for Food and Nutrition Applications: A Review. *Trends in Food Science and Technology* **2018**, *79*, 84–197.
- 2. Parris, N. & Dickey, L. C. Extraction and Solubility Characteristics of Zein Proteins from Dry-Milled Corn. *J. Agric. Food Chem.* **2001**, *49* (8), 3757-3760.
- 3. Argos, P., Pedersen, K., Marks, M. D. & Larkins, B. A. A Structural Model for Maize Zein Proteins. *J. Biol. Chem.* **1982**, *257* (17), 9984–9990.
- 4. Liu, H.; Wei, Z.; Hu, M.; Deng, Y.; Tong, Z.; Wang, C. Fabrication of Degradable Polymer Microspheres via PH-Responsive Chitosan-Based Pickering Emulsion Photopolymerization. *RSC Adv.* **2014**, *4* (55), 29344–29351.
- 5. Cárdenas, G. & Miranda, S. P. FTIR and TGA Studies of Chitosan Composite Films. *J. Chil. Chem. Soc.* **2004**, *49* (4), 291–295.
- 6. De Almeida, C. B., Corradini, E., Forato, L. A., Fujihara, R. & Filho, J. F. L. Microstructure and Thermal and Functional Properties of Biodegradable Films Produced Using Zein. *Polimeros.* **2018**, *28*, 30–37.

Chapter 5: STARCH AND ZEIN BIOPOLYMERS AS A SUSTAINABLE REPLACEMENT FOR PFAS, SILICONE OIL AND PLASTIC-COATED PAPER

A version of this chapter is published as:

Kansal, D., Hamdani, S. S., Ping, R., Rabnawaz, M. Starch and zein biopolymers as a sustainable replacement for PFAS, silicone oil, and plastic-coated paper. ACS Ind. Eng. Chem. Res. **2020**, *59*(*26*), 12075-12084.

5.1 Summary

Here we are reporting an inexpensive approach for preparing recyclable water and oil repellent paper products using biobased materials such as starch and zein. The application of dual-layer coatings of starch and zein onto a Kraft paper yielded a "Cobb 60" value of 4.81 g/m². In addition, the coated paper exhibited excellent grease resistance with a kit rating of 12/12. Scanning electron microscopy characterization confirmed that the dual-layer coating filled the pores of the paper substrate. The mechanical properties, as well as the thermal stability of the paper, were maintained after the coating treatments, and thus this coated paper has potential for widespread use in our daily lives while also minimizing the environmental footprint of packaging materials.

5.2 Experimental

5.2.1 Materials

Corn starch was acquired from Sigma as whiter powder corn starch with ~15% moisture, while GMO-free zein was obtained from Sigma as yellow-brown powder. Ethanol (95%) was acquired from Koptec. Deionized water was used to make all of the solutions described in this study. Glacial acetic acid was purchased from Macron Fine Chemicals. Meanwhile, 35-liner paper was purchased from Uline, United States.

5.3 Methods and Characterization

5.3.1 Solution preparation of starch and zein and coating method

Starch stock solution: To prepare a starch solution with a concentration of 5% (w/v), 5 g of starch powder was mixed with 15 mL of deionized water and 80 mL of distilled water before it was heated to 90 °C for 10 min. After the water was heated, the starch solution was mixed with hot water under constant stirring and the heating was continued another 20 min at 90 °C. When

the solution became turbid, the heating was stopped, and it was cooled back to room temperature prior to use.

Zein stock solution: To prepare a 20% (w/v) zein stock solution, 20 g of zein powder was mixed with 80 mL of 85% (v/v) ethanol solution. The solution was stirred continuously for 2 h at room temperature. A further dilution to 10% (w/v) was performed from the above prepared 20% (w/v) stock zein solution. For example, a 10% (w/v) zein solution was prepared by taking 20 mL of the above prepared 20% (w/v) zein solution and adding 20 mL of 85% (v/v) ethanol solution with constant stirring at room temperature.

Coating method: A bar coater K303 Multi Coater (RK PrintCoat Instruments Ltd, UK) with rod number 8 was used to coat the paper substrates. ~5 mL of the coating solution was applied on ~29 cm x 21 cm size Kraft paper. The first layer of starch solution was applied and dried for 24 h at room temperature. After that, the second layer of zein solution was applied on top. The bilayer coated paper was dried at room temperature for another 24 h. The coated paper substrates were pre-conditioned at 23 °C and 50% relative humidity (RH) before performing further studies. The same procedure was followed for controls i.e. single layer starch, zein coated papers where the coating was dried for 24 h at room temperature and then pre-conditioned under same conditions.

5.3.2 Characterization

Basis weight, coating load, material thickness: The uncoated paper (U-p), starch-coated paper (S5-p), zein-coated paper (Z10-p, Z20-p) and bilayer coated paper (S5Z10-p, S5Z20-p) were tested for the basis weight, coating load and material thickness. The detailed procedure for basis weight, coating load and material thickness has been described in Chapter 3,

section 3.3.5. The basis weight and coating load of the coated paper were calculated and reported in g/m^2 . Material thickness was recorded in μm .

Water vapor transmittance rate (WVTR) and Water absorption capacity (Cobb 60 value): The water vapor transmission rate and Cobb 60 value were recorded for uncoated paper (U-p) and all of the coated paper samples (S-p, Z-p, SZ-p). WVTR was recorded at 23 °C and at 50% relative humidity (RH). Cobb 60 values or water absorptiveness has been reported as an average of three experimental values along with standard deviations have been reported. A detailed procedure has been described in Chapter 3, section 3.3.2.2.

Grease Resistance: Grease resistance was reported following the TAPPI standard T 559 pm-96 (Chapter 3, section 3.3.2.3) for uncoated paper (U-p) and coated paper samples (S-p, Z-p, SZ-p). The data reported is an average of experiments performed in triplicates.

Contact angles (CAs) and sliding angles: Water and oil contact angles were measured using a VCA 2000 system (Video Contact Angle System, AST Products, INC., USA). A droplet of $\sim 10~\mu L$ was placed onto the paper and the contact angle was recorded after 30 s and 5 min. Three replicates were taken for every paper substrate and were reported as the average of these values.

Water and oil sliding angles for uncoated paper (U-p) and coated paper samples (C-p, Z-p, CZ-p) were recorded by attaching the paper substrate to a movable wood plate. A droplet of \sim 100 μ L was placed on the paper. The wood plate was tilted slowly at a constant speed of (2°/s) until the water or oil droplet started to slide down. The angle was reported as the average of three replicate measurements.

Attenuated Total Reflectance FTIR, Thermogravimetric analysis (TGA), Scanning electron microscopy (SEM) analysis: The FTIR, TGA and SEM analysis were carried out for uncoated paper (U-p), and coated paper samples (S-p, Z-p, SZ-p), using procedures mentioned in Chapter 3 section 3.3.8, 3.3.7 and 3.3.6.

5.3.3 Recyclability

The Uncoated paper (U-p) and coated paper samples (S-p, Z-p, SZ-p) were tested for recyclability by the repulping approach. Paper (3.0 g, S5Z10-p and uncoated) were cut separately into 2x2 cm² pieces. The uncoated and coated paper samples were soaked in distilled water for 30 min and blended to yield the pulp. This pulp was divided into three equal portions. The first portion was washed with distilled water, the second portion was washed with an 85% (v/v) ethanol solution, and the third portion was washed first with 85% ethanol and subsequently with distilled water. All of these washing treatments were performed 3 times. The washed pulps were then filtered onto a mesh, pressed and ironed to yield the paper. The obtained paper was dried overnight in an oven at 50 °C. All of the repulped paper samples were examined by ATR-FTIR spectroscopy with regard to the possible disappearance of characteristic peaks corresponding to starch and zein.

5.3.4 Mechanical Properties

The uncoated and coated paper samples were also tested for any changes in the mechanical strength after coating. All of the mechanical tests were performed in both the cross-machine direction and the machine-direction and the results are reported as an average of three measurements that were recorded for each test. The tensile testing, bending stiffness, ring crush test and internal tearing resistance has been evaluated following the procedure described in section 3.3.3 of Chapter 3.

5.4 Results and Discussion

To develop a food-safe and an inexpensive biobased paper coating that would be suitable for water and oil repellent applications, starch and zein were employed as bottom and top layer, respectively. The dual-layer coating approach was applied onto 35-liner Kraft paper substrates in this study. The paper substrate was first coated with a starch solution and dried for 24 h at room temperature, which was followed by the addition of zein solution. After the application of the zein solution, the sample was dried for another 24 h at room temperature. No heat treatment was applied at any stage of the coating process. The dual-layer-coated paper was then pre-conditioned at 50% RH for 24 h prior to performance analysis.

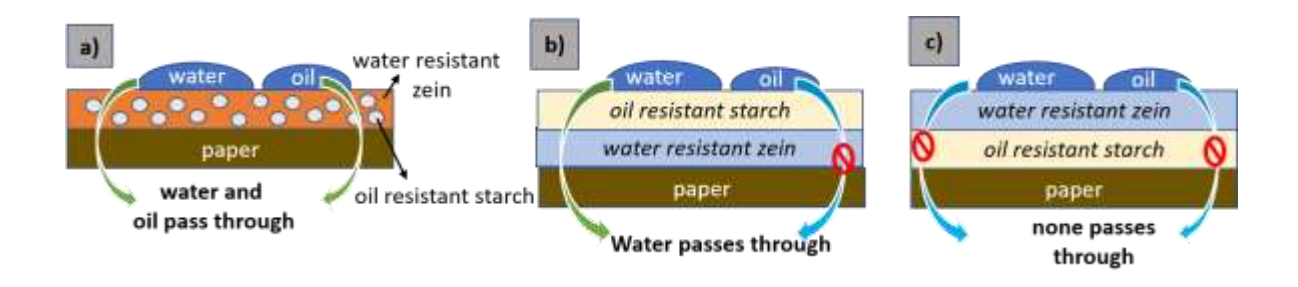


Figure 5.2: Illustration of various coating on paper substrate and their anticipated water and oil repellencies. a) A zein-starch blend coating allows the passage of both water and oil. b) A dual-layer coating with zein comprising the bottom layer and starch forming the top layer only retains oil but permits the passage of water. c) A dual-layer coating in which starch comprises the bottom layer and zein forms the top layer offers a barrier against both oil and water.

To validate our hypothesis depicted in **Figure 5.1**, we prepared three coated paper samples (see **Table 5.1**). Samples coated with a blend of zein and starch showed poor water and oil repellency owing to the exposure of both hydrophilic starch (a water absorber) and oleophilic zein (an oil absorber). Meanwhile, paper samples were also coated with a dual-layer film in which zein

comprised the bottom layer and starch formed the top layer. These samples showed excellent oil resistance (with a 12/12 kit rating) due to the oleophobic starch top layer, but they had poor water repellency with a Cobb 60 value of 20.91 g/m². In contrast, excellent performance was achieved when the ordering of the layers within the dual-layer coating was reversed. When zein was employed as the top layer, while starch served as the bottom layer, excellent oil resistance (12/12) was obtained, and this coating also offered remarkable water barrier performance (Cobb values 6.2 g/m²). Uncoated paper was used as a control, which exhibited both poor water and oil resistance. These findings validated our hypothesis.

Table 5.1: Comparison of Cobb 60 values and kit ratings for S5Z10-coated paper, reverse coated Z10S5 paper and mix coated S5Z10 paper

Sample	Cobb 60 (g/m ²)	Kit Rating
Uncoated paper (control)	29.3	0
S5 and Z10 mix	55.0	0
Z10S10-p	20.9	12
S5Z10-p	6.2	12

After validation of our hypothesis that a dual-layer in which starch comprises the bottom layer and zein forms the top layer offers the best water and oil repellency, the next objective was to identify the concentrations of starch and zein that would provide the optimum Cobb 60 and kit rating values. For this purpose, coatings were prepared with the use of different starch and zein concentrations. Once the optimal formulations for starch and zein were identified (e.g., S5Z10 and S5Z20), further analysis of paper samples that had been coated with these optimized formulations was carried out. **Table 5.2** represents the material thickness, basis weight, and coating load of

S5Z10 and S5Z20 as well as various controls. The coatings were found to be homogeneous, with thicknesses varying from 220±5.35 μm for S5Z10 to 226.6±2.86 μm for S5Z20.

Table 5.2: Coating content and thickness of uncoated and coated paper

Sample Name	Material Thickness (μm)	Basis Weight (g/m²)	Coating Load (g/m²)
U-p	180±1	-	-
S5-p	203±2	137	5
Z10-p	207±2	152	20
Z20-p	205±2	155	23
S5Z10-p	220±5	154	22
S5Z20-p	226.6±3	159	27

'S' represents Starch; 'Z' represents Zein; the number denotes the concentration %(w/v), for example, S5Z10 represents bilayer coating of 5% starch and 10% zein.

The coated paper samples were characterized by ATR-FTIR analysis to confirm the presence of starch and zein on the substrate. **Figure 5.2** shows the ATR-FTIR spectra of uncoated paper, as well as starch-coated, zein-coated, and starch-zein bilayer-coated paper samples. The uncoated paper that is made up of cellulose shows characteristic peaks in the range of 2900-3000 cm⁻¹ corresponding to for C-H stretching vibrations, and at 1100-1150 cm⁻¹ for C-O stretching. Starch and cellulose are similar in structure except that starch has alpha linkages, while cellulose has beta linkages. Therefore, the ATR-FTIR spectrum of starch-coated paper (S5-p) showed identical peaks to that of the uncoated paper. The spectrum of 10% (w/v) zein-coated paper (Z10-p) displayed two broad peaks in the region from 1500-1700 cm⁻¹, which can be assigned to different C=O and N-H peaks belonging to the amide moieties in zein. Meanwhile, the peak in the

range of 2900-3000 cm⁻¹ can be assigned to the stretching of the C-H groups found in zein.

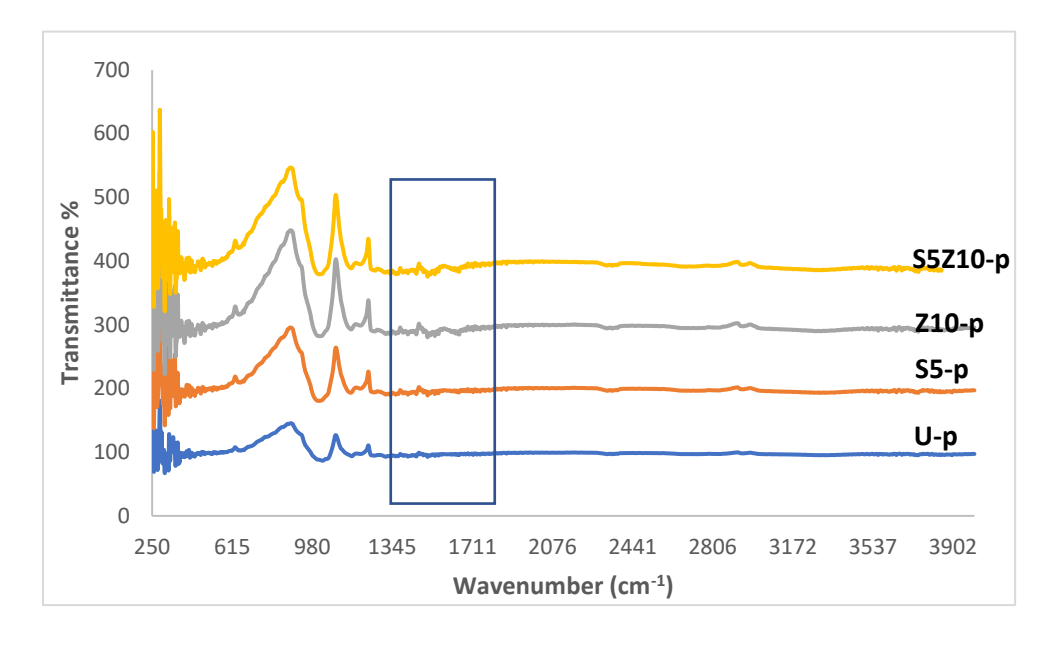


Figure 5.1: ATR-FT-IR spectra of uncoated paper (U-p), 5% (w/v) starch-coated paper (S5-p), 10% (w/v) zein-coated paper (Z10-p), and bilayer-coated paper (S5Z10-p).

Next, we studied the interactions of the uncoated and coated paper substrate with water. In this regard, Cobb 60 and permeability values were recorded to evaluate the repellencies of these samples against liquid water and water vapor, respectively (**Figure 5.3**). From the Cobb 60 value, it was observed that the water absorbency of the paper increased by 29% for starch-coated (S5) paper with a Cobb 60 value of 37.9±1.4 g/m² in comparison with the uncoated paper, which had a Cobb 60 value of 26.9±0.3 g/m². This increase is due to the polar hydroxyl groups of starch that render this paper more hydrophilic and thus cause it to absorb more water. In contrast, a decrease of 59% was observed when the paper was coated with zein (Z20-p) with a Cobb 60 value of 3.05±0.2 g/m². This can be due to the filling of the cellulosic pores of the paper and due to the hydrophobic nature of zein, which helps it to repel water.

The effect of increasing the zein concentration on the water absorbency of the paper substrate was also investigated. As can be seen, the Cobb 60 value increased from 3.05±0.2 to 10.9±0.2 g/m² in response to a decrease in the zein concentration from 20% to 10% (w/v). This is due to a more complete filling of the papers' pores, which thus prevented the passage of water. A similar trend was observed for two different dual-layer-coated papers (S5Z10 and S5Z20), where the Cobb 60 values were found to decrease from 6.18±0.3 g/m² for S5Z10 to 2.6±0.5 g/m² for S5Z20. Based on these experiments it was concluded that the Cobb 60 value was dependent on the top layer of the bilayer-coated paper, which was zein in this case.

A similar trend was observed when the paper samples were tested against water vapor. The permeability values were found to increase from 91.2 g· μ m/m²·day·Pa for U-p to 113.1 g· μ m/m²·day·Pa for the starch-coated (S5) paper, due to the presence of some unfilled pores that allowed the passage of water vapor. In contrast, when the paper was coated with Z20 (permeability value 43.9 g· μ m/m²·day·Pa) and Z10 (permeability value 61.9 g· μ m/m²·day·Pa), the permeabilities were found to decrease from that observed with uncoated paper. These reductions were observed due to the filling of more pores with increases in the zein concentration. In the case of the bilayer-coated paper, the permeability of water vapor was observed to decrease as one progressed from S5Z10 to S5Z20 for the same reason.

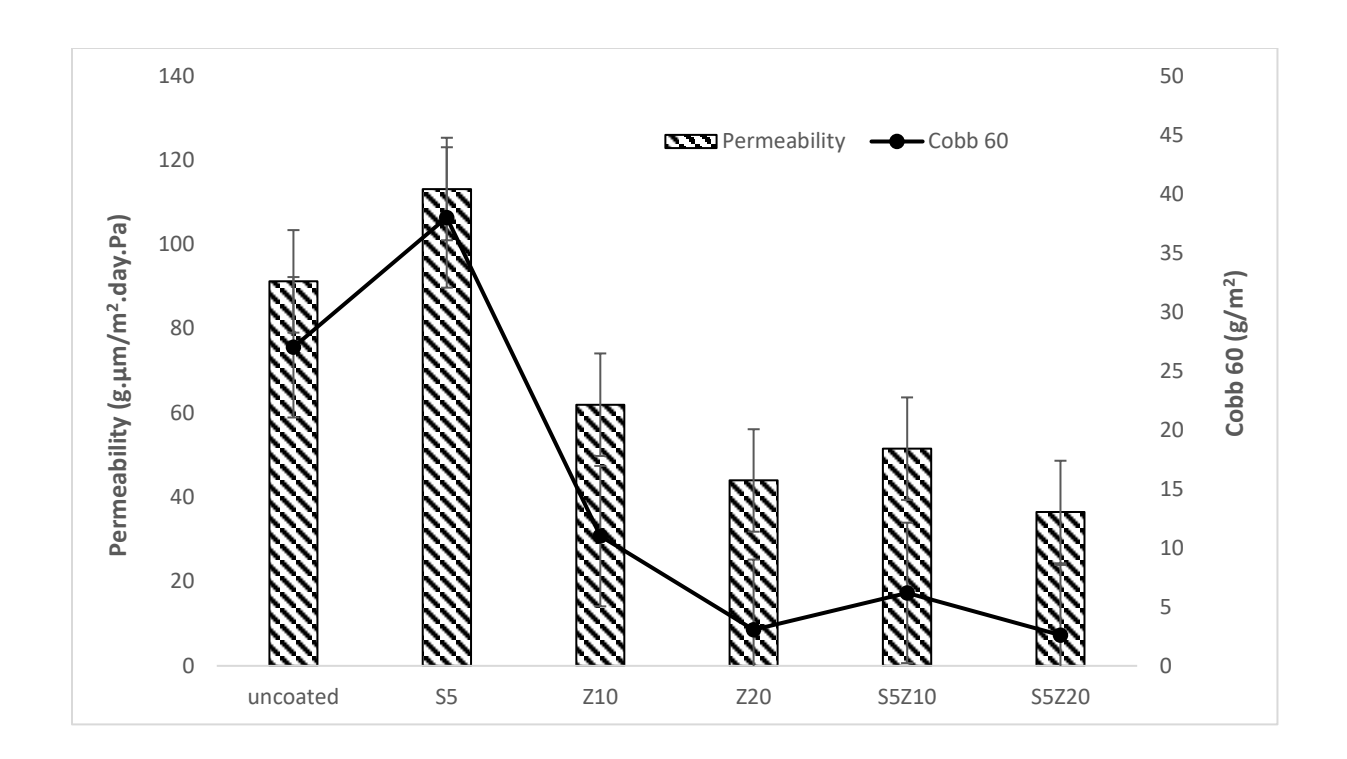


Figure 5.2: Permeability (g·μm/m²·day·Pa) and Cobb 60 values (g/m²) of coated and uncoated paper samples at 25 °C and 50% RH.

Contact angles were also taken to evaluate the response of the coated surface toward water and oil (see **Figure 5.4**). It was observed that the uncoated paper exhibited a contact angle of 53.5±1.4° at 30 s, which decreased to 0° after 5 min due to the water permeating into the cellulosic pores on the surface of the paper. When the surface was coated with S5, an increase in the contact angle to 77.5±2.1° at 30 s was observed. This higher contact angle can be explained based on SEM observations demonstrating the surface roughness of the starch-coated paper, as will be discussed later. In contrast with the behavior on the uncoated paper, the contact angle only decreased moderately to 47.4±7.4° at 5 min due to the filling of the paper's pores by the starch coating. Among the Z10- and Z20-coated paper samples, it is noteworthy that the respective contact angles at 30 s were 78.0±3.6° and 64.0±6.9°. This trend is due to an increase in the smoothness of the

surface on the coating that was derived from the 20% (w/v) zein solution. A similar trend was observed with the paper samples that were covered by the dual-layer coatings S5Z10 and S5Z20, where the top layer of the coating was the deciding factor in determining the contact angles. Since Z10 comprised the top layer of S5Z10, this coating exhibited a contact angle of 71.7±4.1° at 30 s, which closely matched that of Z10. Likewise, the contact angle of 62.5±9.5° that was exhibited by S5Z20 closely matched that of Z20.

Water sliding angles for uncoated paper and S5-coated paper were found to be 80.0±0.0°, implying that the surface was not smooth to allow the droplets to slide down. When the paper was coated with Z10 and Z20, the sliding angles were found to be 55.0±0.8° and 24.6±2.5°, respectively. A smaller sliding angle was observed for Z20 due to the increased smoothness of the surface. For a similar reason, the paper samples that were coated with S5Z10 and S5Z20 showed respective sliding angles of 40.6±4.2° and 35.0±0.0°.



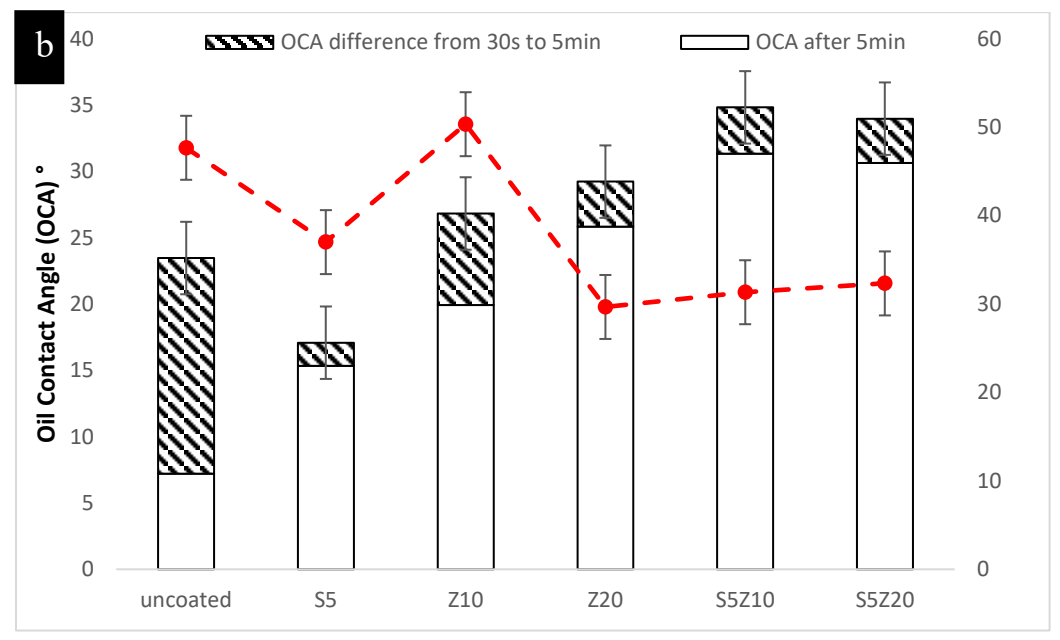


Figure 5.3: Contact angles (at 30 s and 5 min) and sliding angles of a) water b) castor oil. [WCA: Water contact angle and OCA: Oil contact angle]

Oil contact angles were also measured with the use of castor oil droplets. The oil contact angles showed a similar trend to that observed with the water contact angles. An oil contact angle of 23.4±2.2° was observed for uncoated paper at 30 s that decreased to 7.2±0.7° at 5 min after the droplet had been placed on the surface. Meanwhile, the S5-coated paper exhibited a contact angle of 17.1±1.5° at 30 s, which had decreased to 15.3±1.2° at 5 min. The Z10- and Z20-coated paper samples exhibited oil contact angles of 26.8±1.5° and 29.2±3.0°, respectively, at 30 s that subsequently decreased to corresponding values of 19.9±0.5° and 25.8±1.6° at 5 min. It is noteworthy that the changes in the contact angles observed at 5 min from those observed earlier at 30 s were smaller for the coated paper samples in comparison with the uncoated samples. Also, because starch is more oleophobic than zein, the S5-coated paper shows a smaller decrease in its oil contact angle at 5 min from that observed at 30 s, implying that this surface exhibited a stronger and longer-lasting oil repellency. The samples bearing the dual-layer coatings S5Z10 and S5Z20 exhibited respective oil contact angles of 34.8±1.6° and 33.9±2.4° at 30 s, which exhibited very modest decreased to corresponding values of 31.3±0.6° and 30.6±0.1° after 5 min. The oil repellency of the dual-layer-coated paper samples is mainly due to the presence of the oleophobic starch-based bottom layer.

The "kit rating" data (see **Figure 5.5**) showed that the uncoated paper has no tolerance towards oil, with a kit rating number of 0/12, due to the cellulosic pores that allow the passage of oil. The S5-coated paper exhibited a kit rating of 6.3/12, while that for the Z10-coated paper was 3.0/12. This can be explained based on the nature of starch and zein, particularly when one keeps in mind that a higher kit rating implies stronger repellency against oil. In particular, starch bears polar hydroxyl groups that render it oleophobic, whereas 45% of zein's composition consists of

alkyl groups so that it is less oleophobic. However, dual-layer-coated paper such as those coated by S5Z10 and S5Z20 were found to have a high kit rating number of 12/12 despite the presence of zein as the upper layer. There are two reasons for the high oil repellency of these dual-layer coatings. Firstly, more of the paper's pores become filled by the dual-layer coating. Secondly, although the oil passes through the top layer of zein, it eventually reaches the bottom layer of starch which is more oleophobic and is impermeable to the oil, and hence the paper still repels the oil.

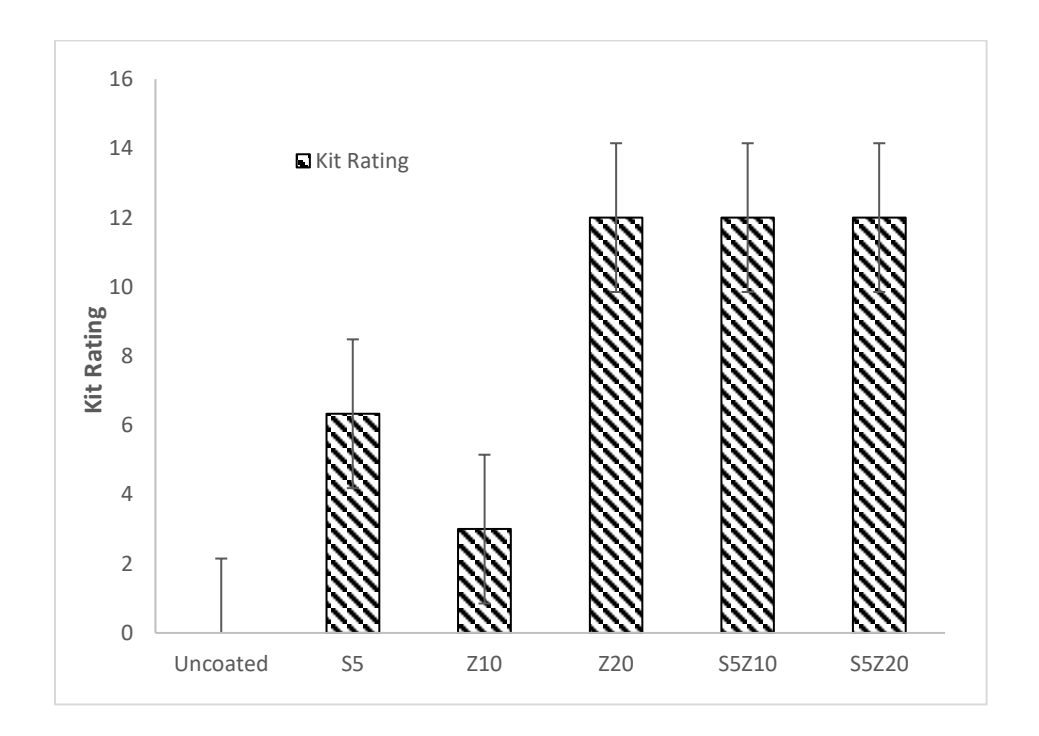


Figure 5.4: Kit ratings of coated paper and control. Higher number denotes higher oil-resistance and vice versa.

SEM analysis was performed to investigate the surface texture of the paper at the different stages of fabrications as shown in **Figure 5.6**. SEM images are shown for the uncoated paper (U-p), as well as the S5-coated, Z10- and S5Z10-coated paper samples. It can be seen that the uncoated

paper possessed numerous pores (**Figure 5.6a**), whereas most of the pores were covered in the case of the S5-p sample (**Figure 5.6b**). This masking of the pores along with the oleophilic nature of starch is the likely reason for the good oil repellency of starch-coated paper. **Figure 5.6c** shows the zein-coated paper, where some pores remain visible. Meanwhile, no pores are visible S5Z10-p sample (**Figure 5.6d**). In addition, the dual-layer-coated paper is much smoother than its counterparts, as the fibers are well-covered with a thick coating, which is due to the high amount of total coating load (starch + zein).

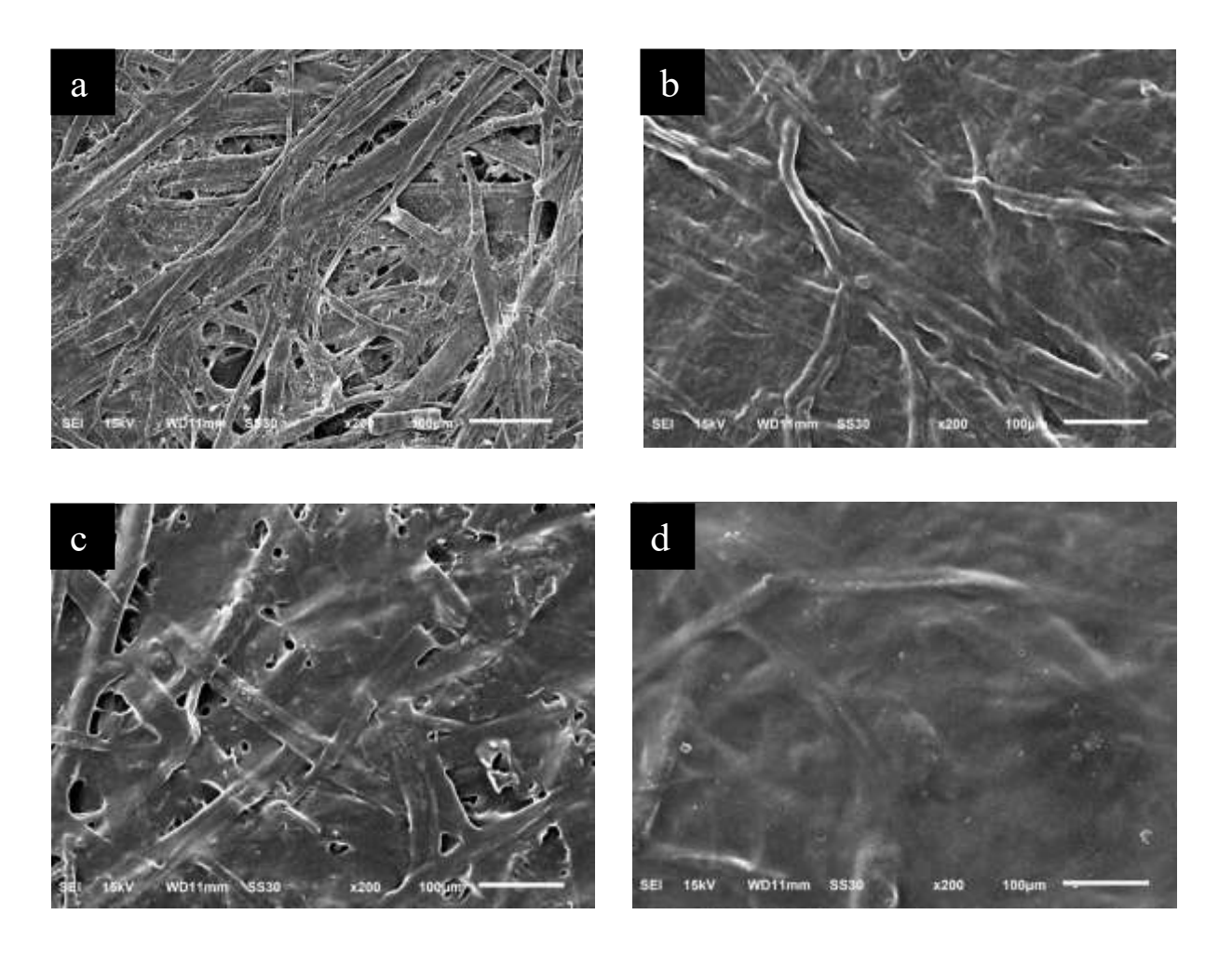


Figure 5.5: SEM images (200×) of: (a) unmodified paper (U-p); (b) starch-coated paper (S5-p); (c) zein-coated paper (Z10-p); and (d) starch-zein dual-layer-coated (S5Z10-p).

Mechanical properties are important factors that influence the applicability and durability of a material, and thus the mechanical strength of the coated paper was also evaluated. In particular, we evaluated the tensile strength, bending strength, we performed ring crush tests, and measured the internal tearing force in both the machine and cross-machine direction. It was observed that in the machine direction (MD), the tensile strength of the starch-coated paper increased considerably by 33.6% to a value of 64.88±1.6 lbf for S5-coated paper as compared to 43.02±4.51 lbf for uncoated paper. Meanwhile, when the paper was coated with Z10, an increase of 11% over that of the uncoated paper was observed, with a value of 48.07±1.26 lbf. For the S5Z10-coated paper, again a slight increase to 50.02±0.43 lbf was observed, which ensures that the paper can withstand more tension before breaking. A similar trend was observed in the cross-machine direction (CD), with the tensile strength for the S5Z10-coated paper reaching 20.77±0.51 lbf versus 18.53±0.41 for the uncoated paper (Figure 5.7a). The Z10-coated paper showed a great increase in crush resistance to a value of 43.09±0.45 lbs in the MD and 36.60±3.45 lbs in the CD versus 31.20±2.4 lbs in the MD and 22.13±4.01 lbs in the CD for uncoated paper. S5Z10 did not deviate much, indicating that the strength of bilayer coated paper is as good as of uncoated paper as shown in Figure 5.7b.

The strength required to bend the paper was observed to increase for Z10-p but remained similar for the S5Z10-coated paper in both the MD and CD. However, an increase of 22% in the MD and 9% in the CD was observed for the zein-coated paper versus the uncoated paper as shown in **Figure 5.7c**. The internal tearing force showed different trends in the MD and the CD. In the MD, the force was found to decrease for the S5Z10-coated paper versus that of the uncoated paper.

Whereas in the CD, the force was found to increase by 7% from that of the uncoated paper, as shown in **Figure 5.7d**.

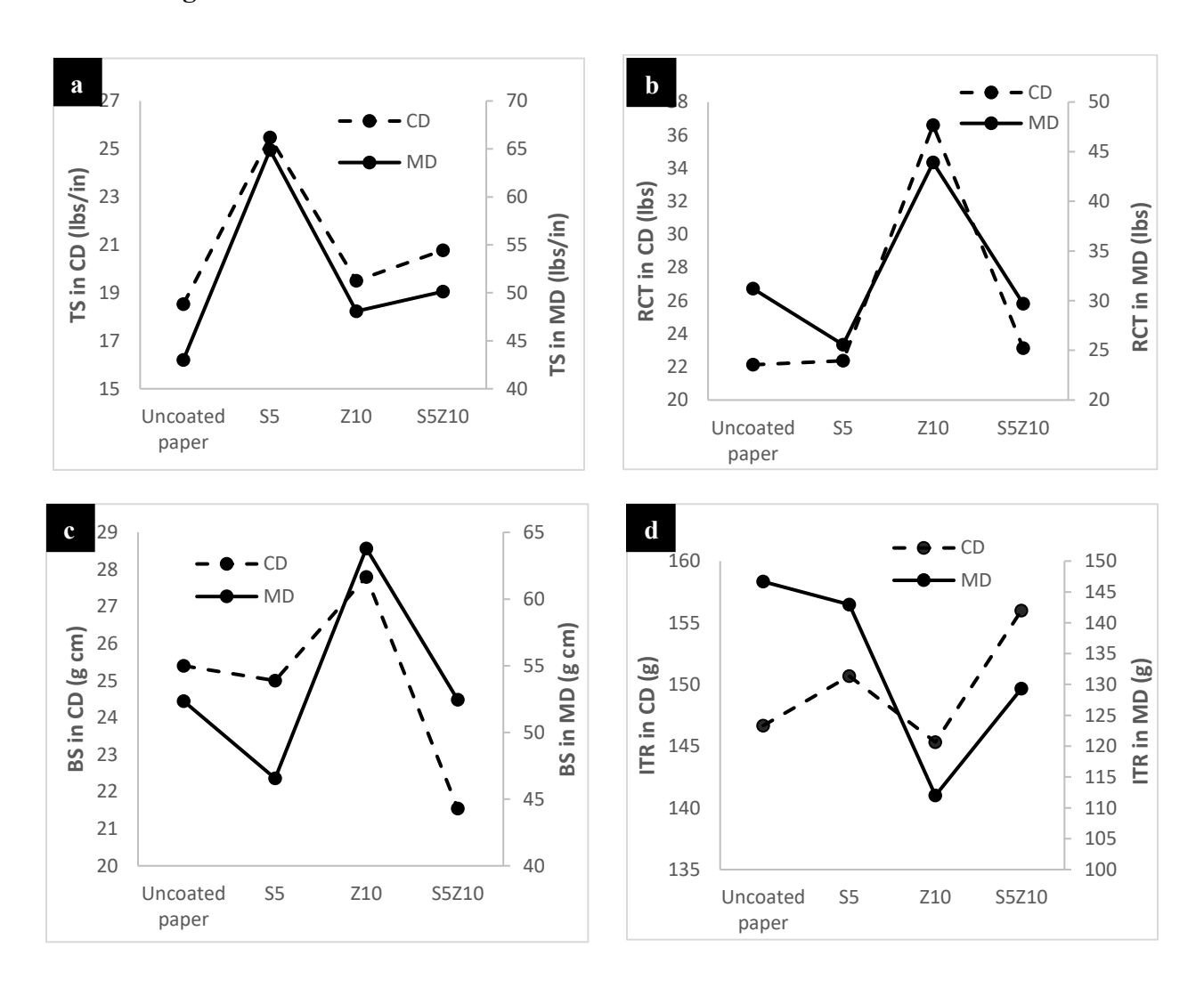


Figure 5.6: Mechanical properties of the uncoated paper (U-p), and coated paper (S5, Z10 and S5Z10) including a) The tensile strength, b) ring crush test, c) bending stiffness, and d) internal tearing.

The thermal stability of the coated and uncoated paper samples were also evaluated via TGA measurements. **Figures S4a** and **S4b** (see SI) display the TGA curves of U-p, S5-p, Z10-p, and S5Z10-p. However, due to the low coating load on the paper, no appreciable change in the

thermal degradation was observed. For this reason, films of starch and zein were prepared in the absence of paper substrates to investigate the thermal behavior of these materials. In the case of the starch film (**Figure S4c** and **S4d**) (see SI), the first loss was observed at ~150 °C, which corresponded to the loss of water. The second loss was observed at ~320 °C, which indicated the breaking of the amylose and amylopectin chains in starch.³ For the zein films, the first loss at ~100 °C is again due to loss of water, and second loss at ~ 300 °C was due to the thermal rupture of protein chains.⁴ The % weight loss graph indicates that starch-zein dual-layer coated paper can be used for various practical applications without becoming damaged.

Finally, it was important to study the recyclability of the coated paper, in order to determine whether coated paper can be recycled. To achieve this, the repulping approach was used, where the paper was soaked in water first and subsequently washed with various solvents in order to remove the coating from the paper. Photographs of S5Z10-coated paper samples that were taken after various various stages of the repuling process are shown in **Figure 5.8**. For comparison, uncoated paper was also repulped and washed with water. The color of the S5Z10 paper that had been washed with only water is slightly darker in color due the presence of zein, as zein is brown in color and insoluble in water. Meanwhile, the S5Z10-coated paper sample that had been washed with 85% ethanol/water (v/v) has a similar color to that of uncoated paper pulp, indicating the removal of the S5Z10 coating from this paper. We also analyzed from FT-IR (**Figure B** in the appendices) that the successful repulping of the coated paper.

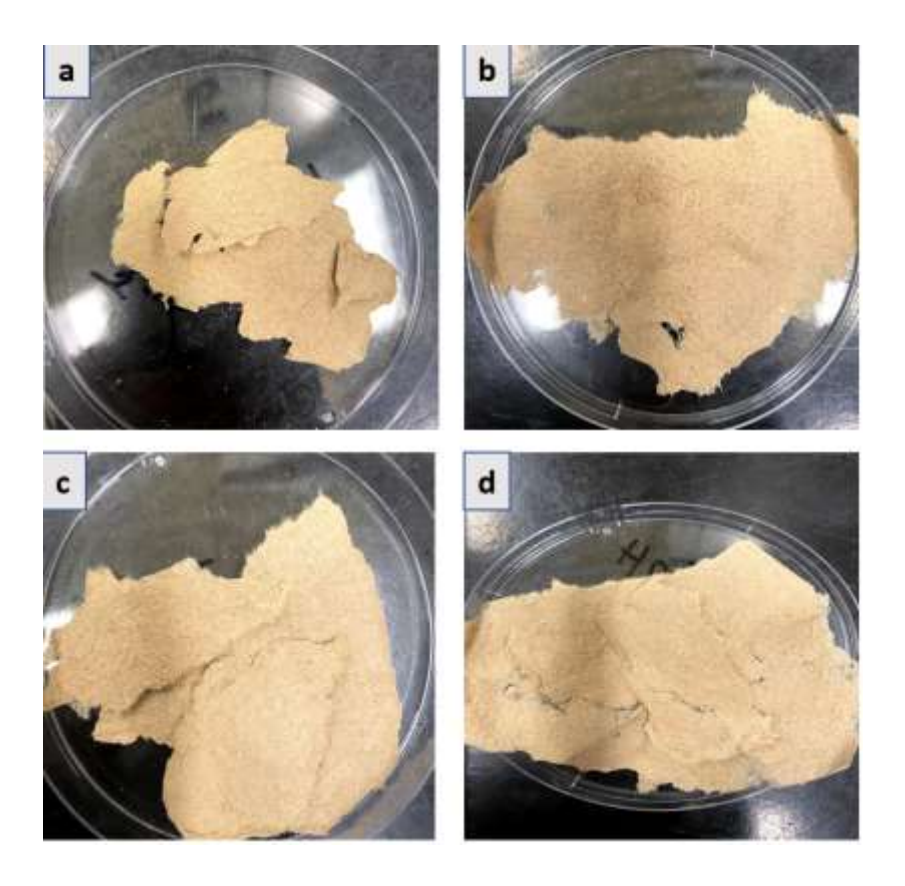


Figure 5.7: Photographs of repulped paper samples after various washing treatments. (a) Uncoated paper pulp that had been washed with distilled water; (b) S5Z10-coated paper pulp that had been washed with distilled water; (c) S5Z10-coated paper pulp that had been washed first with distilled water and then with an 85% ethanol solution; and (d) S5Z10-coated paper pulp that had washed with first with distilled water and then with 85% ethanol.

5.5 Conclusion

In summary, we have developed an innovative dual-layer coating strategy to impart both water and liquid repellency to paper substrates simultaneously. Starch was used as the bottom layer, while zein was used as the top layer. These coatings exhibited excellent resistance against both water (e.g., Cobb 60 value of 6.18±0.26 g/m² for S5Z10-p) and oil with kit ratings reaching up to

12. This improvement in the property was explained from the insights gained from SEM analysis, where the cellulosic pores of uncoated paper were found to be masked by the coating material that led to an increase in water contact angle and a decrease in the Cobb 60 value. The mechanical analysis showed that the dual-layer-coated paper had comparable strength to that of its uncoated counterparts, and thus it would be suitable for practical applications. The recyclability data also shows that after washing the coated paper with the appropriate solvents, the coating material can be readily removed so that the paper can be recovered for future use. The cost-competitive supply of food-grade zein will be key for the commercialization of this technology for large-volume applications.

REFERENCES

REFERENCES

- 1. Kizil, R., Irudayaraj, J. & Seetharaman, K. Characterization of Irradiated Starches by Using FT-Raman and FTIR Spectroscopy. *J. Agric. Food Chem.* **2002**, *50*(14), 3912–3918.
- 2. Halsall, T. G., Hirst, E. L. & Jones, J. K. N. Structure of starch and cellulose. *Nature* **1947**, *159*, 97.
- 3. Liu, X., Yu, L., Liu, H., Chen, L. & Li, L. Thermal Decomposition of Corn Starch with Different Amylose/Amylopectin Ratios in Open and Sealed Systems. *Cereal Chem.* **2009**, *86*, 383–385.
- 4. De Almeida, C. B., Corradini, E., Forato, L. A., Fujihara, R. & Filho, J. F. L. Microstructure and thermal and functional properties of biodegradable films produced using zein. Polimeros 2018, 28, 30–37.

Chapter 6: FABRICATION OF OIL- AND WATER-RESISTANT PAPER WITHOUT CREATING MICROPLASTICS ON DISPOSAL

A version of this chapter is published as:

Kansal, D., Rabnawaz, M. Fabrication of oil- and water- resistant paper without creating microplastics on disposal. Journal of Applied Polymer Science, **2020**, *138(3)*.

6.1 Summary

Herein we report a plastic-free paper coating derived from chitosan and sunflower oil. Chitosan grafted sunflower oil paper coatings were prepared via the ring opening of the partially epoxidized sunflower oil with chitosan. The product of these reactions was characterized by nuclear magnetic resonance (NMR) and infrared (IR) spectroscopy techniques. The sunflower oil grafted chitosan solution was coated onto a Kraft paper. The Cobb 60 and kit rating values were determined to be 8.00 g/m² and 7.66 respectively for the optimal formulations. Meanwhile, the water contact angle was found to be 94.0±1.6° after 30 s. Scanning electron microscopy analysis was employed to gain insight regarding the changes that occurred on the paper surface at the microscopic level.

Scheme 6.1: Depection of interaction of chitosan-g-sunflower oil with paper substrate

6.2 Experimental

6.2.1 Materials

Chitosan and sunflower oil were purchased from Sigma-Aldrich. The molecular weight (M_n) of chitosan was 50,000-190,000 g/mol. 3-Cloroperbenzoic acid was purchased from Sigma-Aldrich with a purity >77%. Meanwhile, glacial acetic acid was purchased from Macron Fine

Chemicals. Dichloromethane and acetone solvent of ACS reagent grade were purchased from Sigma. Deionized (DI) water was used for all the experiments. All chemicals were used as received without any further purification.

6.3 Methods and Characterization

6.3.1 Synthesis of epoxidized sunflower oil (ESO)

Epoxidized sunflower oil (ESO) was prepared by dissolving SO in dichloromethane in a round-bottom flask. 3-Chloroperbenzoic acid (*m*-CPBA) was dissolved in dichloromethane as a separate solution. This *m*-CPBA solution was subsequently added to the sunflower oil solution under constant stirring. The solution was stirred for 1 h at room temperature. The crude product was extracted with water and dried over Na₂SO₄. The dichloromethane was subsequently removed via rotary evaporation. The final product was obtained as a light yellow oil (2.64 g, 88% yield for ESO1 and 2.7 g, 90% yield for ESO3) and characterized by ¹H NMR spectroscopy. The protocols employed for the preparation of the two ESOs (namely ESO1 and ESO2) are outlined in **Table 6.1**.

Table 6.1: Amounts of the different starting materials.

Sunflower oil (g)	m-CPBA (mg)	Solvent (dichloromethane, mL)	Product
3	50	15	ESO1
3	200	15	ESO2

6.3.2 Preparation of the chitosan stock solution

Chitosan stock solution was prepared by dissolving chitosan powder in a 2% v/v acetic acid aqueous water solution. The 2% v/v acetic acid solution was prepared by dissolving 2 mL of

glacial acetic acid in 98 mL of distilled water, and this solution was thoroughly mixed prior to use. For example, a 4% (w/v) solution was prepared by dissolving 2 g of chitosan powder in 98 mL of a 2% aqueous acetic acid solution. The solution was stirred overnight at room temperature until all of the solids had dissolved and a uniform solution was obtained.

6.3.3 Synthesis of chitosan-graft-sunflower oil

Chitosan-*graft*-sunflower oil (CS-*g*-SO) was prepared by pre-dissolving ESO (from Table 1) in acetone, and subsequently adding this solution to a chitosan solution in different ratios (as described in the Results and Discussion section) at room temperature with constant stirring in a 20 mL glass vial. The solution was subsequently heated to 75 °C for 3 h with continuous stirring and left stirring at room temperature for another 12 h. These CS-*g*-SO solutions were used as coatings for paper substrates without any purification.

6.4 Coating Procedure

The papers were coated using a bar coater machine, K303 Multi Coater (RK PrintCoat Instruments Ltd, UK) with a coating rod. First, the paper was fixed on the coating machine with the rod on top, and around 5 ml of solution to be coated was put on the top. The solution was coated evenly with the rod. After coating, paper was dried at room temperature for 24 h and then conditioned at 50% relative humidity and 23 °C for another 24 h before carrying out any tests.

6.5 Characterization

Basis weight, coating load and material thickness: Basis weight, coating load and material thickness were calculated for uncoated paper (U-p), 2 wt% chitosan-coated paper (CS2-p), and chitosan-g-sunflower oil-coated papers (CS-g-SO1-p and CS-g-SO2-p). With regard to the abbreviations in the previous sentence, the term "-p" refers to a paper sample that is covered by

the respective coating, while the numbers denote concentration of the coating solutions in wt%. The basis weight and coating load are reported in g/m^2 and the thicknesses of samples were reported in μm as an average of three values. The detailed procedure has been described in Chapter 3, section 3.3.5.

Water vapor transmittance rate (WVTR) and water absorption capacity (Cobb 60 value): WVTR and Cobb 60 values were recorded for U-p, CS2-p, CS-g-SO1-p, and CS-g-SO2-p to understand the transmittance of water vapor through paper and water absorption respectively over time. All Cobb 60 values and WVTR were reported in units of g/m²·day. The permeability values were calculated using **Equation 8**, mentioned in section 3.3.2.2 of Chapter 3.

Grease resistance: U-p, CS2-p, CS-g-SO1-p, and CS-g-SO2-p samples were tested to evaluate their grease resistance following the TAPPI standard T 559 pm-96 protocol (Chapter 3, section 3.3.2.3). Three values were recorded for each sample, and the values reported herein corresponded to their average.

Contact angles (CAs) and sliding angles: Water contact angles (WCAs) and oil contact angles (OCAs) were recorded using a VCA 2000 (Video Contact Angle System, AST Products, Inc., USA) instrument. Distilled water was used for the WCA measurements, while castor oil was employed for the OCA measurements. The WCAs and OCAs were respectively recorded for U-p, CS2-p, CS-g-SO1-p, and CS-g-SO2-p, at 30 s by placing a ~10 μL droplet of water or castor oil on the paper substrate.

Water and oil sliding angles were recorded for U-p, CS2-p, CS-g-SO1-p, and CS-g-SO2-p by fixing the paper samples on a movable wooden plate. A droplet of \sim 10 μ L was placed on the

surface of the paper, and the wooden plate was tilted at constant rate of 2°/s until the water or oil droplet began to slide along the surface.

IR, Thermogravimetric, Scanning electron microscopy analysis: U-p, CS2-p, CS-g-SO1-p, and CS-g-SO2-p were studied for FT-IR, TGA and SEM analysis following method described in section 3.3.8, 3.3.7 and 3.3.6 of Chapter 3.

Nuclear magnetic resonance (NMR): ¹H NMR spectra were recorded using a 500 MHz NMR spectrophotometer (Agilent, Santa Clara, CA, USA) over a chemical shift range from 0 to 14 ppm.

6.6 Results and Discussion

A two-step synthetic procedure was employed to prepare CS-g-SO. First, sunflower oil was epoxidized using *m*-CPBA as the oxidizing agent (**Scheme 6.2**). Two epoxidized SOs were prepared, and they were respectively denoted as ESO1 and ESO2. As can be seen in the ¹H NMR spectra (**Figure 6.1**), ESO exhibited signals at 2.92 ppm (-CHOCH-) and 1.50 ppm (-CH₂-CHOCH-CH₂-). The degree of epoxidation was calculated to be 3.3% for ESO1 and 5.1% for ESO2.^{2,3} (see appendices for calculation of the degree of grafting). ATR-FTIR spectra of ESO1 and ESO2 were also recorded, and the peak appearing at 843 cm⁻¹ was assigned to C-O-C stretching of the epoxide ring.

Scheme 6.2: Synthetic route toward the epoxidized sunflower oil.

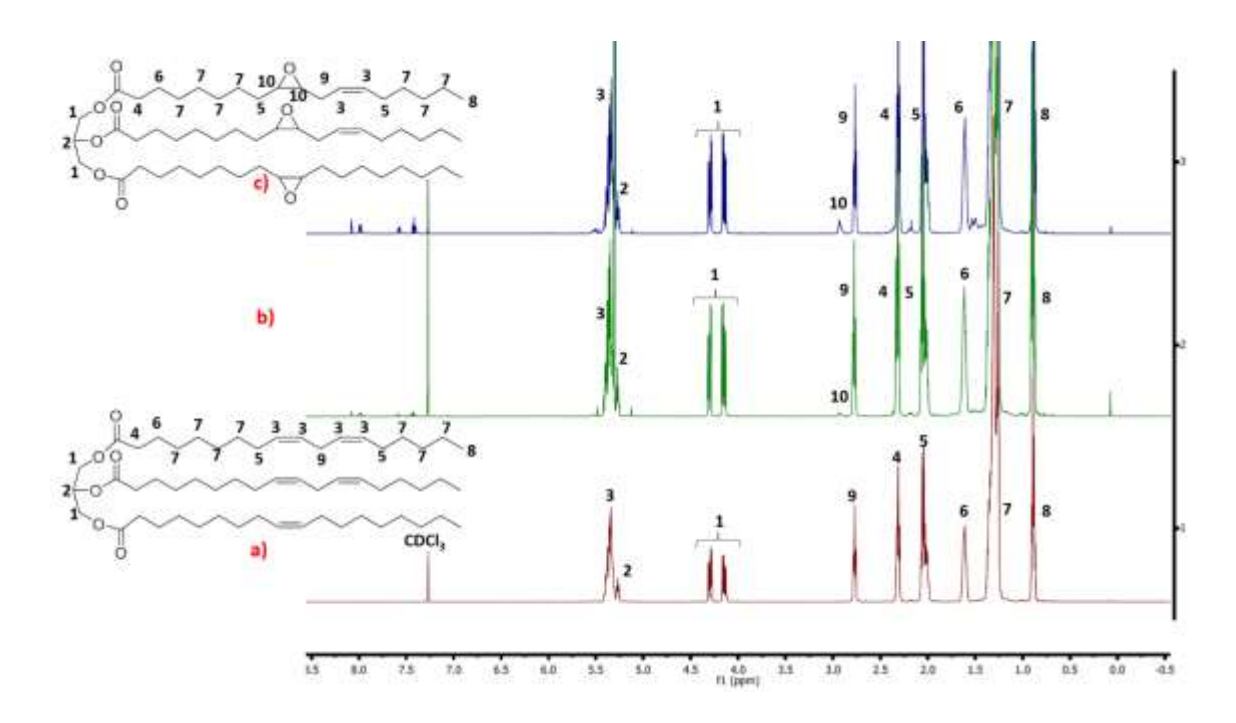


Figure 6.1: ¹H NMR spectrum of sunflower oil **(a)** before epoxidation. Also shown are ¹H NMR spectra of epoxidized sunflower oil, including **(b)** ESO1 and **(c)** ESO2.

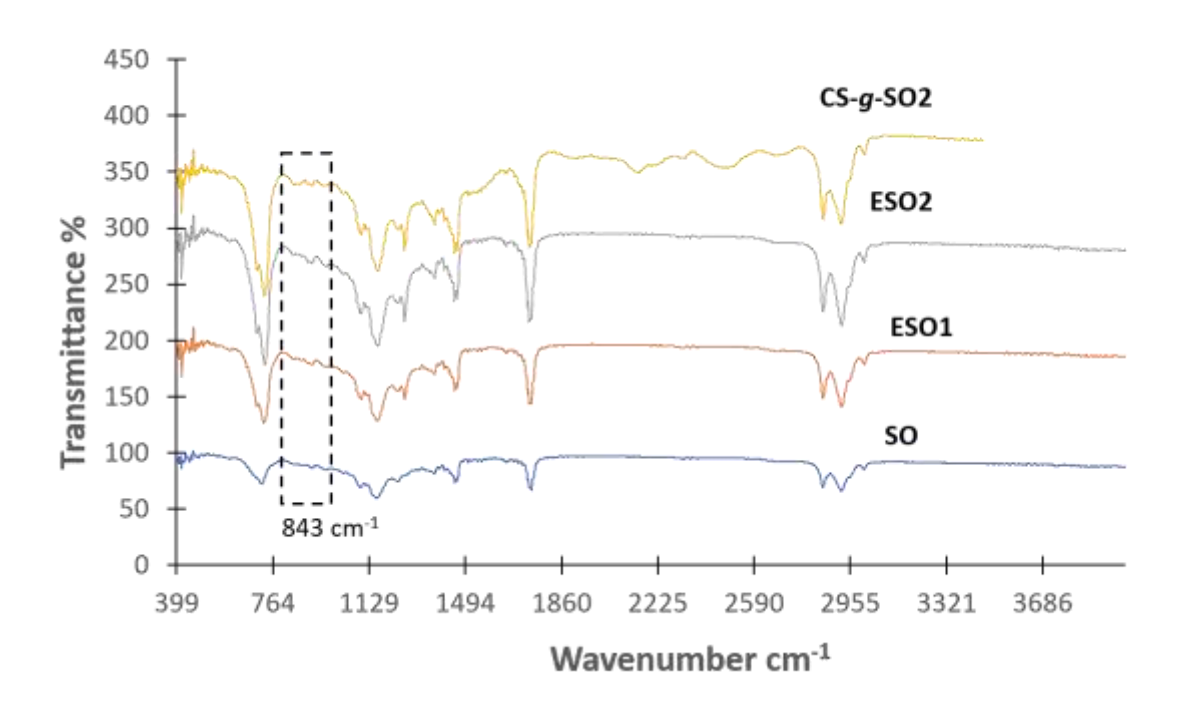


Figure 6.2: ATR-FTIR spectra of un-epoxidized sunflower oil (SO), epoxidized sunflower oil (ESO1 and ESO2), and chitosan-g-sunflower oil (CS-g-SO2).

After it was confirmed that the epoxidation of sunflower oil was successful, the next step was to graft ESO onto chitosan. ESO was grafted onto chitosan in an acid catalyzed nucleophilic ring-opening reaction targeting the epoxy ring (**Scheme 6.3**). The epoxide ring initially becomes protonated by acetic acid that is present in the medium, and then the amino group of chitosan attacks the epoxy ring to open it and form a stable C-N bond. In the ¹H NMR spectrum of CS-g-SO, the disappearance of the epoxide peak (C-O-C) at 2.92 ppm was expected (**Figure 6.3**). However, chitosan exhibits broad peaks in the ¹H NMR spectrum, and thus the disappearance of the peak at 2.92 ppm was not readily apparent and therefore it was difficult to confirm whether or not the grafting had taken place. In the FT-IR spectrum of chitosan-g-SO, it was expected that the C-O-C stretching vibration of the epoxide peak would disappear or reduce in the intensity and a

peak corresponding to C-N-C stretching would appear after the -NH₂ attack on epoxide ring (**Figure 6.2**). The peak at 843 cm⁻¹ corresponding to the C-O-C vibration of the epoxide was found to disappear from the FT-IR spectrum of CS-*g*-SO, while a doublet was observed at 1050 cm⁻¹ that was attributed to a C-N-C stretching vibration (**Figure 6.2**).⁴ Thus, FT-IR spectroscopy confirmed the disappearance of the epoxy ring.

Scheme 6.3: Proposed opening of oxirane ring of epoxidized sunflower oil with chitosan to form chitosan-*g*-sunflower oil.

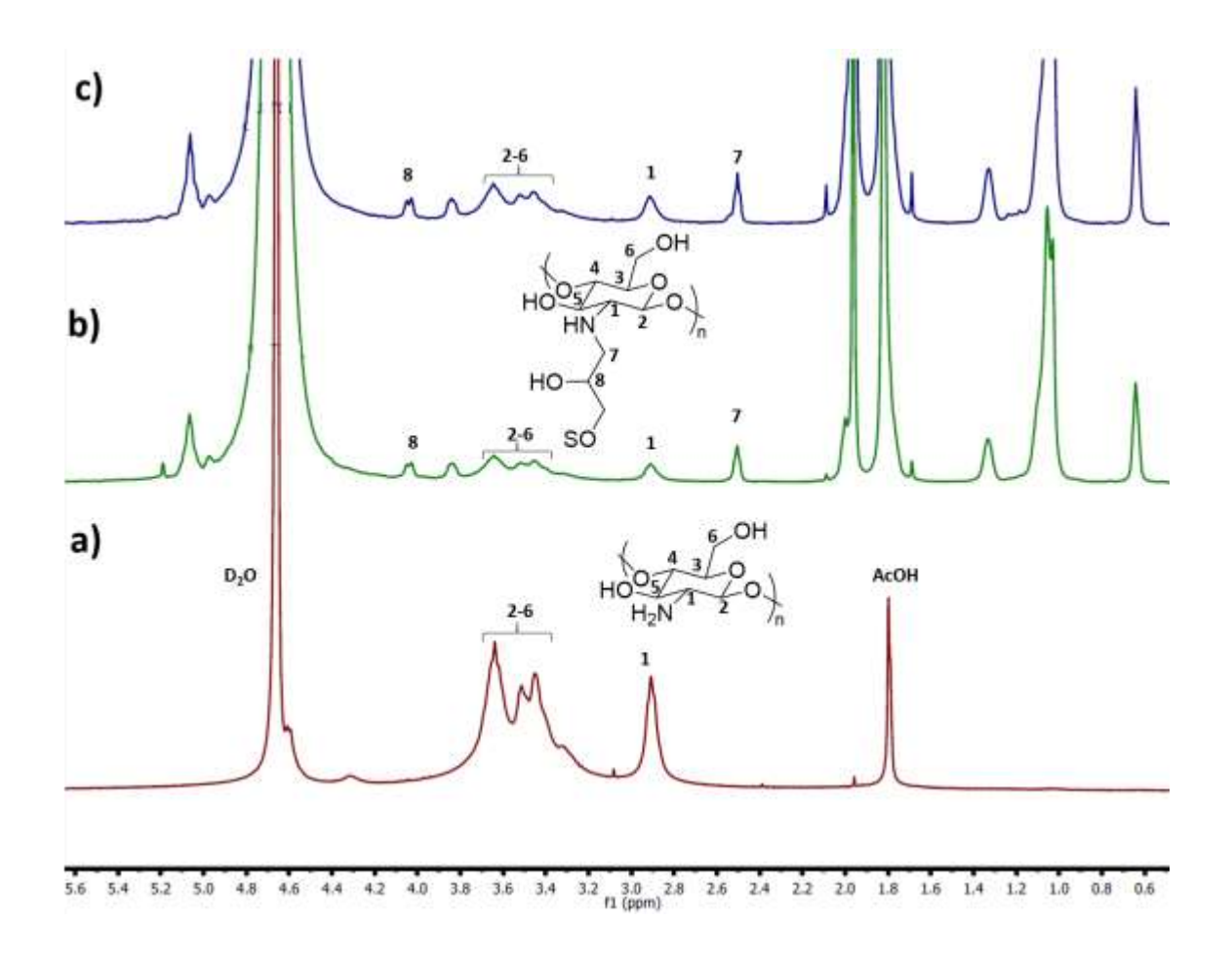


Figure 6.3: ¹H NMR spectra of: (a) 2 wt% chitosan, (b) chitosan-*g*-SO1 after heating at 70 °C for 3 h, and (c) chitosan-*g*-SO2 after heating at 70 °C for 3 h.

ESO and chitosan were reacted together at various ratios to obtain a series of CS-g-SO copolymers (see **Table 6.2**). Cobb 60 and kit rating values were recorded to evaluate the behavior of our coatings on paper substrates, and these results are summarized in **Table 6.2a** and **6.2b**, respectively. With a chitosan:ESO ratio of 1:8(w/w), gel formation occurred, possibly due to dense crosslinking. Among the copolymers that were prepared at chitosan:ESO ratios of 1:1, 1:2, and 1:4, the best Cobb 60 and kit values were exhibited by the copolymer prepared at a ratio of 1:4.

Furthermore, the best Cobb 60 value of ~10 was achieved when the concentration of the chitosan solution was 2 wt%, and these samples also exhibited high kit ratings (>6).

Table 6.2: (a) Cobb 60 (g/m²) and (b) kit ratings of paper samples bearing CS-g-SO copolymers with various compositions.

Ratios (w/w)	For CS:ESO1		For CS:ESO2	
Chitosan:ESO	Cobb60	Cobb60	Cobb60	Cobb60
	(CS 2 wt%)	(CS 4 wt%)	(CS 2 wt%)	(CS 4 wt%)
1:1	21.2	27.2	18.3	18.9
1:2	13.1	28.1	23.2	18.5
2:1	N/A	31.4	N/A	22.7
1:4	8.1	Gel formation	10.0	Gel formation
1:8	21.3	Gel formation	16.6	Gel formation

Ratios (w/w)	For CS:ESO1		For CS:	ESO2 b
	Kit Rating	Kit Rating	Kit Rating	Kit Rating
	(CS 2 wt%)	(CS 4 wt%)	(CS 2 wt%)	(CS 4 wt%)
1:1	5.6	10.0	4.3	9.3
1:2	3.0	9.3	6.0	7.3
2:1	N/A	8.6	N/A	7.0
1:4	6.0	Gel formation	7.6	Gel formation
1:8	5.3	Gel formation	8.0	Gel formation

Once the best formulation was identified for chitosan and epoxidized sunflower oil, a systematic study was undertaken. Since the properties of the coated paper are known to be dependent on the thickness of the coating and coating load, it was important to first calculate the material thickness and coating load of the coated paper in our case. As shown in **Table 6.3**, it was observed that the material thickness increased from 178.3 µm to 197.0, 198.0, and 197.3 µm for

CS2-, CS-g-SO1-, and CS-g-SO2-coated paper samples. This finding suggested that all of the coated papers had a relatively uniform thickness.

Table 6.3: Material thickness, basis weight and coating load for uncoated and coated paper.

Sample	Material thickness (μm)	Basis weight (g/m²)	Coating load (g/m²)
U-p	178.3	-	-
CS2-p	197.0	131.1	3.6
CS-g-SO1-p	198.0	135.9	5.6
CS-g-SO2-p	197.3	135.8	5.5

'CS2' represents Chitosan, while the number denotes the concentration in % (w/v). CS-g-SO1-p and CS-g-SO2-p denote paper samples that were coated by CS-g-SO, which was synthesized at a 1:4 chitosan:ESO ratio.

The uncoated paper (U-p), as well as paper samples that were coated by chitosan (CS2-p), and chitosan-*g*-sunflower oil (CS-*g*-SO1-p and CS-*g*-SO2-p) were characterized by ATR-FTIR spectroscopy as shown in **Figure 6.4**. Chitosan showed a characteristic peak in the region of ~3200 cm⁻¹ representing the O-H/N-H stretching vibrations. Meanwhile, the absorption bands near ~2900 cm⁻¹ can be attributed to the C-H stretching vibration in chitosan. The band at 1153 cm⁻¹ corresponds to the asymmetric stretching of the C-O-C bridge, while the bands at ~1050 cm⁻¹ correspond to C-O stretching. In contrast, the peaks in the region of 1153 cm⁻¹ were absent from the spectrum of uncoated paper. With regard to the CS-*g*-SO1/CS-*g*-SO2-coated paper, the peak observed at 1730 cm⁻¹ corresponded to the ester group of sunflower oil, implying that the sunflower oil had indeed been grafted onto chitosan.

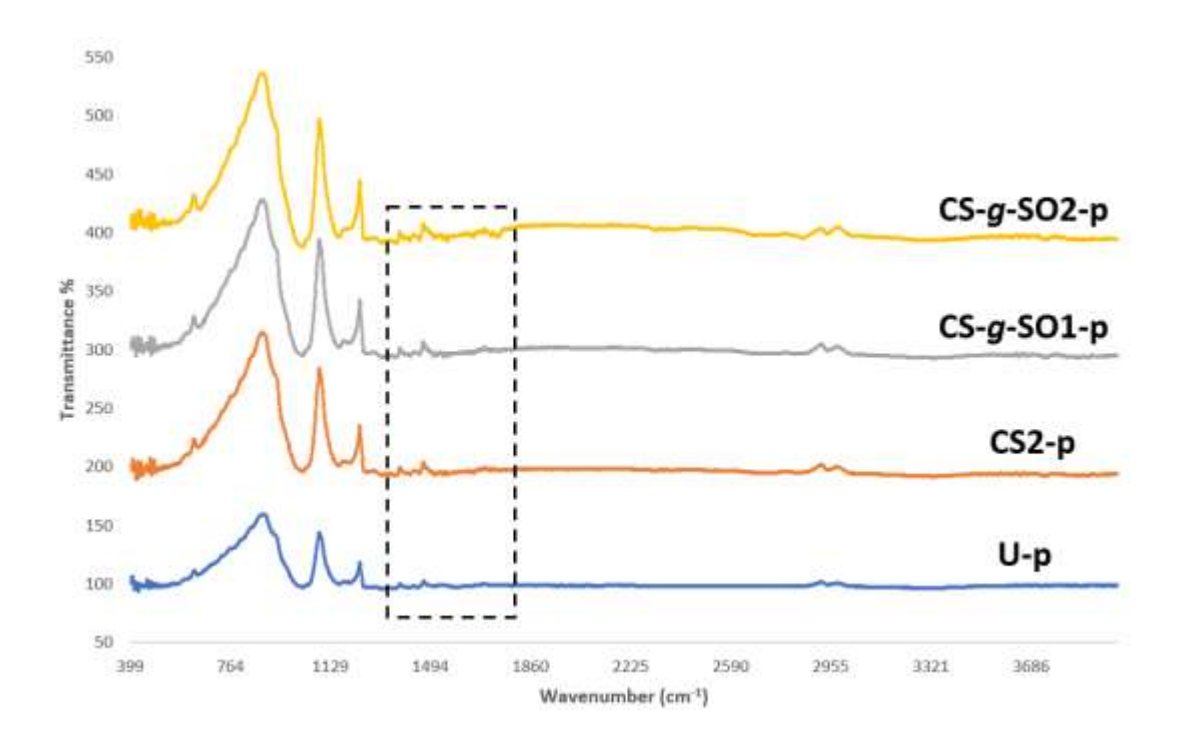


Figure 6.4: ATR-FTIR spectra of uncoated paper (U-p), 2% w/v chitosan-coated paper (CS2-p), and chitosan-g-sunflower oil-coated paper (CS-g-SO1-p and CS-g-SO2-p).

The water resistance (Cobb 60 values) of uncoated paper, chitosan-coated paper, as well as CS-g-SO1- and CS-g-SO2-coated paper samples were evaluated by exposing them to water for 60 s. The Cobb 60 values that were obtained via these measurements are summarized in **Figure 6.5**. It was found that the Cobb 60 value of the uncoated paper was 29.3%, which decreased to 25.5% after the paper had been coated with 2 wt% chitosan. Uncoated paper is cellulosic in nature and it also exhibits a porous structure that allows water absorption. The chitosan-coated paper is non-porous (see SEM images below), but chitosan is very hydrophilic and thus there was no significant improvement in the Cobb 60 values. When paper was coated with CS-g-SO1 and CS-g-SO2, the Cobb 60 values were found to be 8.1 and 10.0 g/m², respectively. A 72% decrease in water absorption for CS-g-SO1-coated paper and 65.7% for CS-g-SO2-coated paper demonstrate

the significant improvement in the water resistance properties. This enhanced water resistance is due to the use of hydrophobic sunflower oil.

The water vapor permeability of uncoated and coated paper substrates was also investigated. Permeability values were measured to analyze the transmission rate of water vapor through paper at 50% RH and at 23°C. Uncoated paper was found to have a permeability value of 90.4 g.µm/Pa.m²·day. In the case of chitosan-coated paper, this value increased to 109.4 g.µm/Pa.m²·day due to the presence of polar groups on the surface of chitosan that rendered it more hydrophilic. These polar groups are able to form hydrogen bonds with water vapor and allows vapor to pass through the chitosan-coated paper. CS-g-SO1- and CS-g-SO2-coated paper showed respective permeability values of 69.2 and 53.4 g.µm/Pa.m²·day under the same conditions. This reduction in the permeability of water vapor can be explained based on the fact that the top surface of the paper is covered by sunflower oil, which is hydrophobic in nature and impedes the passage of water vapor and hence helps to improve the barrier performance against water vapors. It can also be seen that the WVTR value of CS-g-SO2 was lower than that of CS-g-SO1 due to the higher grafting density of sunflower oil onto the chitosan backbone in the latter case. The water vapor permeability for polyethylene films has been reported to be 0.25-1.2 g.µm/m².day.Pa. The low water vapor permeability is due to the formation of uniform layer of PE and absence of polar groups that could otherwise form hydrogen bonds with water. However, it is difficult to achieve such low values for permeability with biobased coating materials. Only biobased material with comparable value for permeability with PE is polyhydroxybutyrate (PHB). The chitosan-gsunflower oil system reported here shows values of as low as 53.4 g.µm/m².day.Pa which is a ~41% reduction in permeability value compared to uncoated paper.

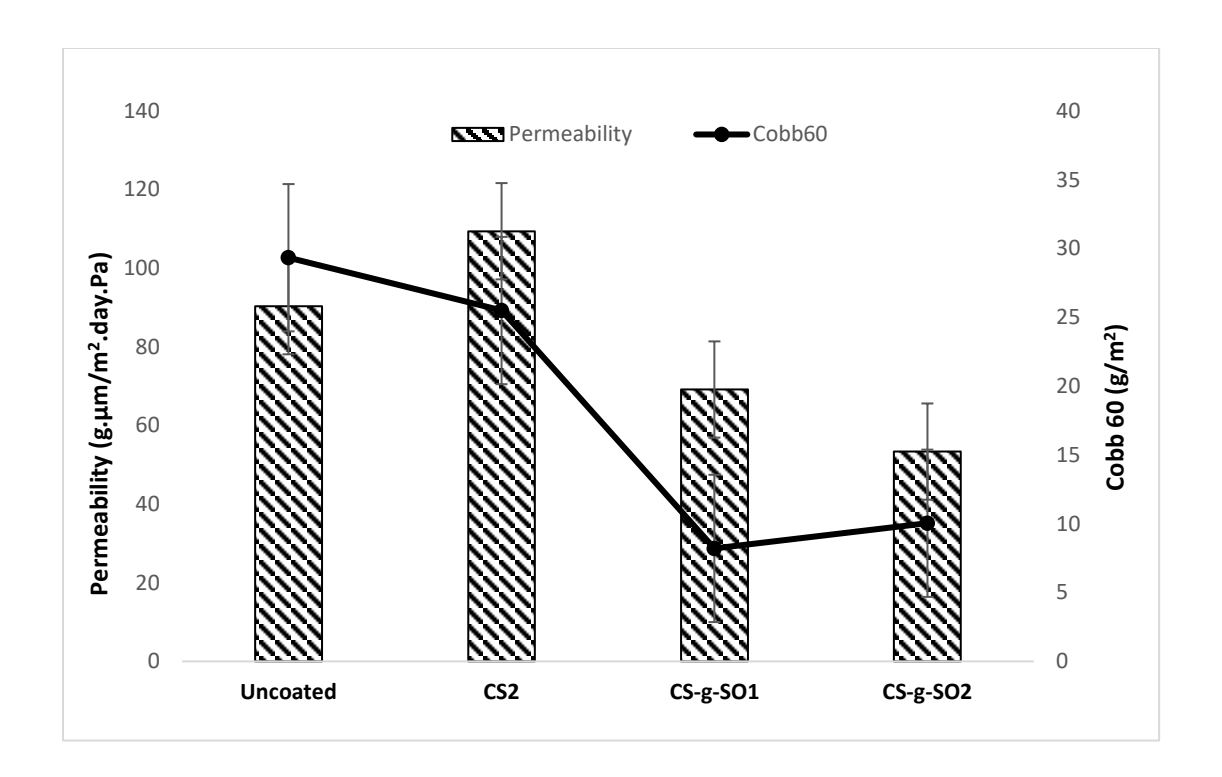


Figure 6.5: Permeability (g·μm/m²·day·Pa) and Cobb 60 values of coated and uncoated paper samples.

Kit ratings provide an indication of oil resistance and therefore these values were recorded for uncoated paper as well as chitosan-, CS-g-SO1- and CS-g-SO2-coated paper to evaluate their oil repellency. The results are summarized in (**Figure 6.6**). The kit ratings of uncoated and chitosan-coated paper were 0 and 12, respectively. Uncoated paper has open pores that allow the passage of oil. However, when paper is coated with chitosan, the pores become filled and since chitosan is oleophobic in nature, oil is repelled by the surface. When paper was coated with CS-g-SO1 and CS-g-SO2, kit ratings of 6.0 and 7.6 were respectively observed. Since sunflower oil is hydrophobic in nature and has a certain affinity toward oil, the oil repellencies of the CS-g-SO1-and CS-g-SO2-coated paper samples were reduced to some extent in comparison with that of

chitosan-coated paper, but were still greater than that of the uncoated paper.

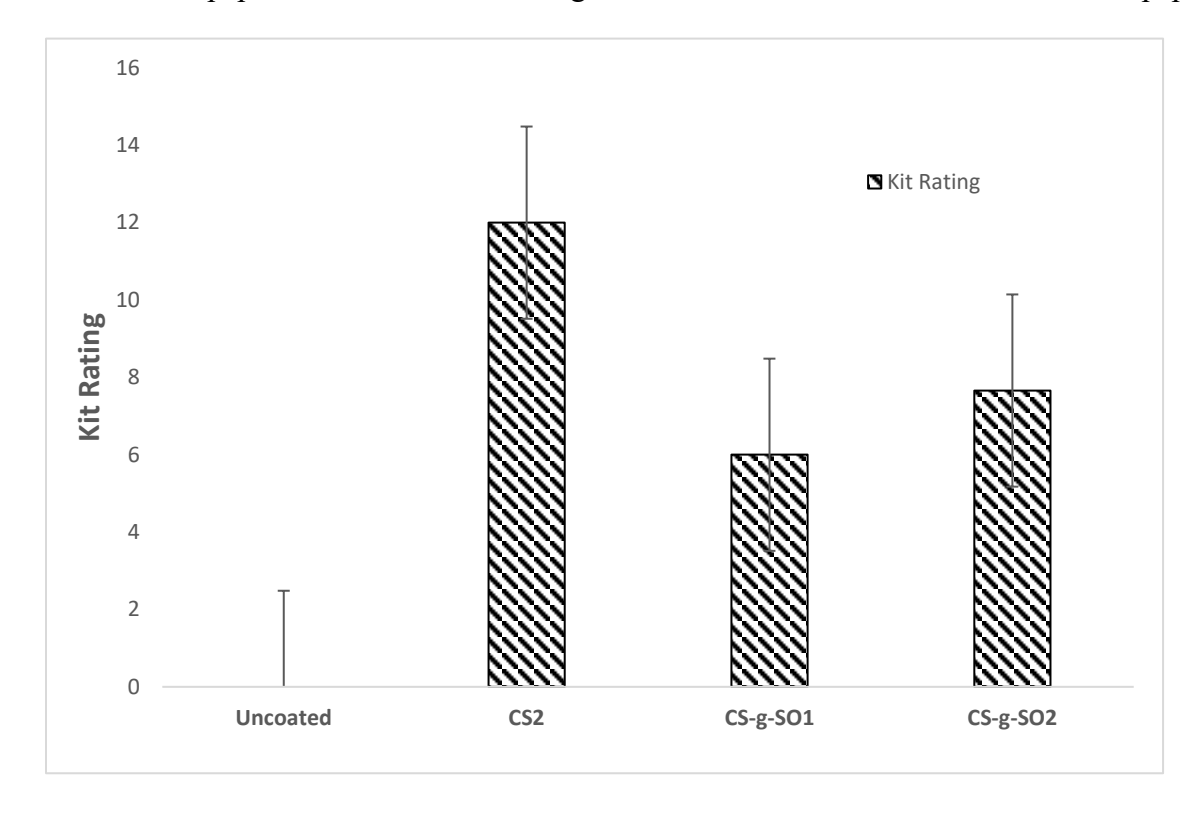


Figure 6.6: Kit ratings of coated and uncoated paper samples.

Water and oil contact angles were also measured to investigate the behavior of coated papers on contact with water. As shown in **Figure 6.7a**, uncoated paper exhibited a WCA of 53.5 $\pm 1.4^{\circ}$ after 30 s, while a WCA of 96.1 $\pm 5.9^{\circ}$ was observed on chitosan-coated paper. The increase in the WCA is due to the lack of permeation by the water droplet into the coated paper. Meanwhile, CS-g-SO1-p showed a WCA of 98.3 $\pm 2.4^{\circ}$ after 30 s. Similar results were obtained with CS-g-SO2-p, with a WCA of 94.3 $\pm 1.6^{\circ}$. The increase in the WCAs beyond 90° indicates the hydrophobic nature of the CS-g-SO-coated paper, which is consistent with their low Cobb 60 values. Similar trends were observed for the oil contact angles (OCAs) as well (**Figure 6.7b**). Uncoated paper showed a lower OCA of 23°, whereas chitosan-coated paper exhibited a higher

OCA with a value of 46. Meanwhile, CS-g-SO1-p and CS-g-SO2-p showed OCAs of 53.1° and 56.9°, respectively.

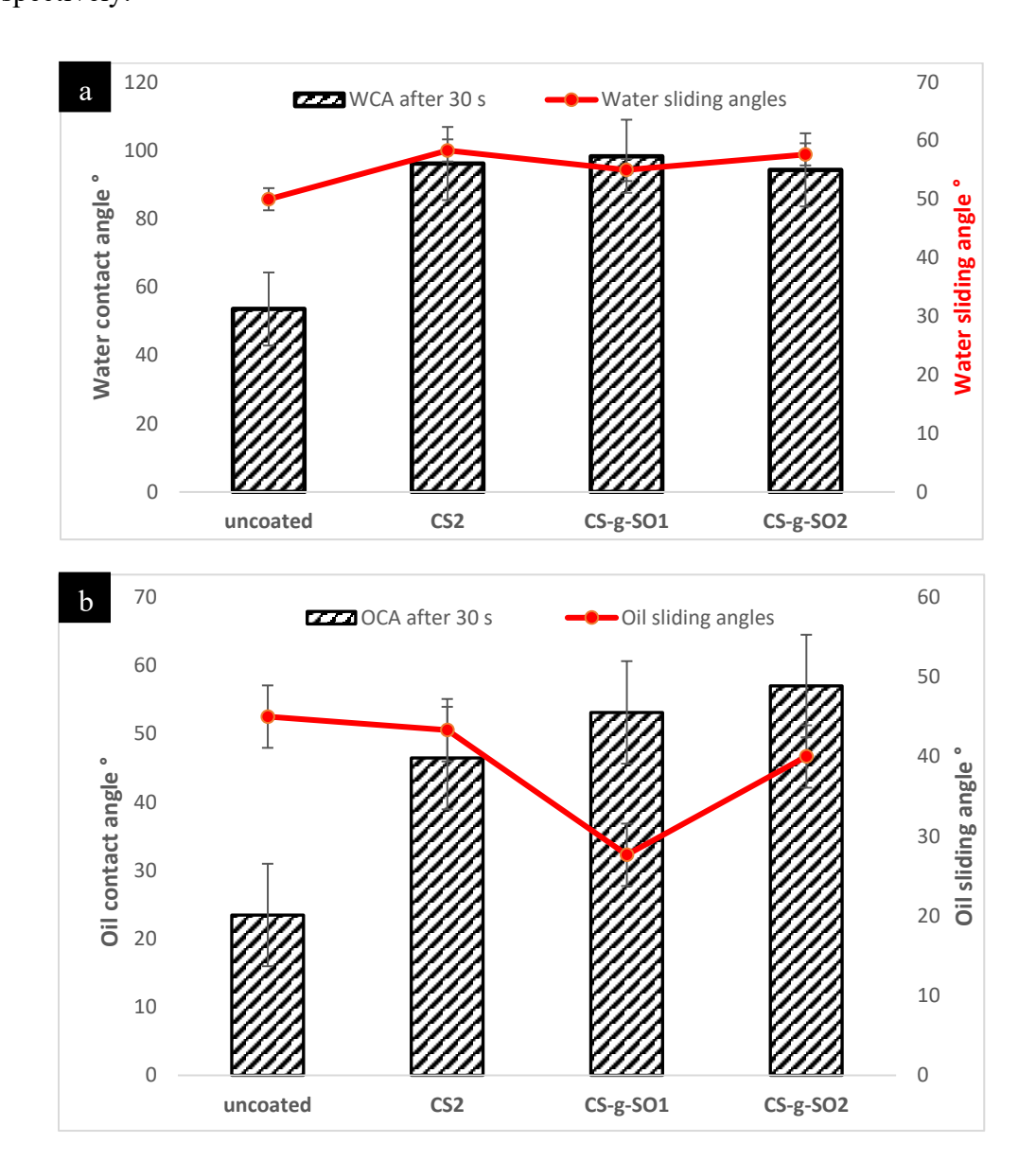


Figure 6.7: (a) Water contact angles and water sliding angles (°) as well as (b) oil contact angles and oil sliding angles (°) of coated and uncoated paper samples. The water and oil contact angles were recorded 30 s after the droplet had been placed on each surface

The thermal degradation of U-p, CS2-p, and CS-g-SO2-p were tested by TGA (**Figure E**). TGA of both paper samples and films was recorded because the coating load on paper was too little to show obvious change, and thus solo materials/film was better for conclusive comparison. Degradation was observed at ~ 250 °C, which can be attributed to the degradation of the paper substrate. The TGA curves of U-p, chitosan film, and ESO are shown. It can be seen that chitosan underwent two thermal degradations, one which occurred below 100 °C and another that took place near 200 °C. The first degradation was due to loss of water and second degradation was due to the degradation of chitosan. Meanwhile, the TGA curve of ESO showed three thermal degradations stages, which occurred at 100, 200, and 400 °C. The first degradation was again due to the loss of water, while the other two correspond to degradation of ESO chemicals bonds.

To understand the surface roughness and its effect on the porosity of our coated samples, SEM images were recorded and are shown in **Figure 6.8**. The uncoated paper is seen to consist of cellulosic fibers, and that explains the penetration of liquids (water or oil) into the pristine paper (**Figure 6.8a**). When the paper was coated with a 2% chitosan solution (**Figure 6.8b**), the pores are filled. However, chitosan is not a good barrier against water because it is hydrophilic in nature. **Figure 6.8c** and **6.8d** show paper samples that had been coated with CS-g-SO1 and CS-g-SO2, respectively. It can be seen that these surfaces are free of pores, which in combination with the hydrophobicity of SO provides these samples with good resistance against water. Some phase separation can also be seen in the CS-g-SO1- and CS-g-SO2-coated paper, which will be studied in detail in the future.

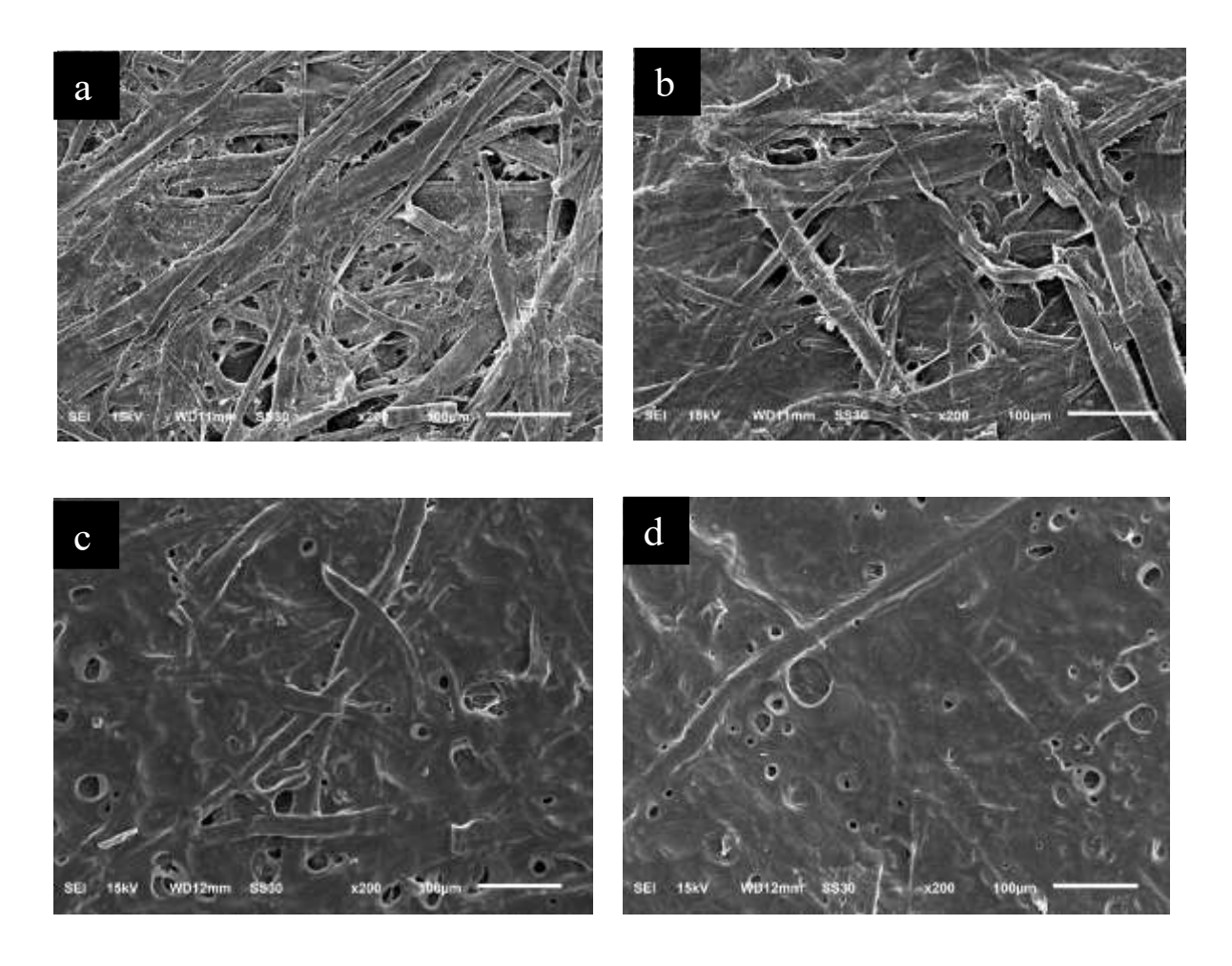


Figure 6.8: SEM images of (a) uncoated paper (U-p), (b) chitosan-coated paper (CS2-p), (c) chitosan-g-SO1-coated paper (CS-g-SO1-p), and (d) chitosan-g-SO2-coated paper (CS-g-SO2-p).

6.7 Conclusions

In summary, we have developed biobased coatings that can provide paper with improves water and oil resistance. Sunflower oil was successfully epoxidized and then grafted onto chitosan to obtain CS-g-SO. NMR and IR analysis were used to validate the chemistry of CS-g-SO and the coated paper. Model studies were used to investigate the grafting chemistry. The Cobb 60 values were found to decrease from 29.3 for uncoated paper to 8.1 for CS-g-SO1-coated paper. The WVTR were also found to decrease from 1608.0 g/m²·day for uncoated paper to 858.0 g/m²·day

for paper samples that were coated with the CS-g-SO2 formulation. The WCA was found to increase as one progressed from uncoated paper to coated papers with SO. SEM analysis validated the masking of pores on paper after the coating. TGA data showed that the coated papers were stable at temperatures reaching up to 250 °C, implying that they are useful for practical applications.

REFERENCES

REFRENCES

- 1. Muturi, P., Wang, D. & Dirlikov, S., Epoxidized Vegetable Oils as Reactive Diluents I. Comparison of Vernonia, Epoxidized Soyabean and Epoxidiinseed Oils. *Prog. Org. Coatings* **1994**, *25*, 85–94.
- 2. Aerts, H. A. J. & Jacobs, P. A., Epoxide Yield Determination of Oils and Fatty Acid Methyl Esters Using ¹H NMR. *J. Am. Oil Chem. Soc.* **2004**, *81(9)*, 841–846.
- 3. Benaniba, M. T., Benaniba, M. T., Belhaneche-Bensemra, N. & Gelbard, G., Epoxidation of Sunflower Oil with Peroxoacetic Acid in Presence of Ion Exchange Resin by Various Processes *Energy Education Science and Technology* **2008**, *21(12)*, 71-82.
- 4. Shimamoto, G. G., Favaro, M. M. A. & Tubino, M., Simple Methods via Mid-IR or1H NMR Spectroscopy for the Determination of the Iodine Value of Vegetable Oils *J. Braz. Chem. Soc.* **2015**, *26*, 1431–1437.

Chapter 7: CONCLUSIONS AND FUTURE OUTLOOK

7.1 Conclusions

Here we have envisioned bio-based and biodegradable coating materials for the paper substrates to minimize existing problems of plastic waste, toxicity and reduced recyclability of coated paper.

In chapter 4, a novel bilayer coating approach has been described to achieve water- and oil- resistancy for the coated paper. The coating materials used were chitosan and zein, which are food-safe. Chitosan is a polysaccharide derived from chitin bio-based and biodegradable. Due to the presence of hydroxyl groups, chitosan becomes oil- resistant. On the other hand, zein is a protein derived from corn. Zein is also bio-based and biodegradable and abundantly available and is a water-resistant material. The dual-layer coating of chitosan and zein showed excellent water-and oil- repellency with Cobb 60 value of 4.88 g/m² and kit rating of 12/12. The SEM images depicted the filling of pores and smoothness of the surface of the coated paper, resulting in a decrease of water and oil contact angle for the dual-layer coated paper. Dual-layer coated paper also showed excellent thermal and mechanical properties, making it useful for practical applications. The repulpability test confirmed the removal of coating material from the repulped paper.

In Chapter 5, dual-layer coating method has been reported with the objective to reduce the cost of the coated paper. The paper was coated with the polysaccharide starch and protein zein. Starch is readily available, relatively cheaper, and chemically similar to chitosan. Starch and zein imparted oil- and water- repellency to the coated paper. The Cobb 60 value for starch and zein

dual-layer coated paper was 6.18 g/m² and kit rating of 12/12. The complete masking of the cellulosic pores of the coated paper was evident from the SEM images. Both mechanical and thermal properties were observed to be excellent. Finally, the repulpability showed that the pulp could be used for further use.

In Chapter 6, a single layer rod coating method has been developed to use downstream oil as the water-resistant coating material. In this method, sunflower oil has been chemically grafted on the backbone of sunflower oil for making the coated paper both water- and oil- resistant. The Cobb 60 was found to be 8.1 g/m², with a reduction in water barrier (WVTR) to 858.0 g/m².day as compared to 1608.0 g/m².day for the uncoated paper. The SEM images showed the covering of the pores, leading to an improvement in the water and oil repellency of the coated paper.

7.2 Future Outlook

The work in this thesis reports the development of water- and oil- resistant coatings for paper substrates. The approach mentioned in this work is thermoplastic and PFAS free and addresses the current challenges associated with the recycling of the paper products. However, there are challenges in the methods developed here and further studies needs to be one.

The Cobb 60 valus reportd here are above 5 g/m2, whereas, the water resistance for the commercially available LDPE coated paper is essentially zero. Therefore, in order to commercialize the coating, the water resistance should be improved further. Another problem faced with the zein coating is the swelling of zein and the solubility of the coating for prolonged time of contact with the liquid.

Another further studies needs to be done in the chitosan grafted oil project. The water and oil resistance of the coated paper is moderate. Therefore, new grafting methods or linkers could be reacted with desired water and oil resistance functional groups to impart better performance to the coated paper.

APPENDICES

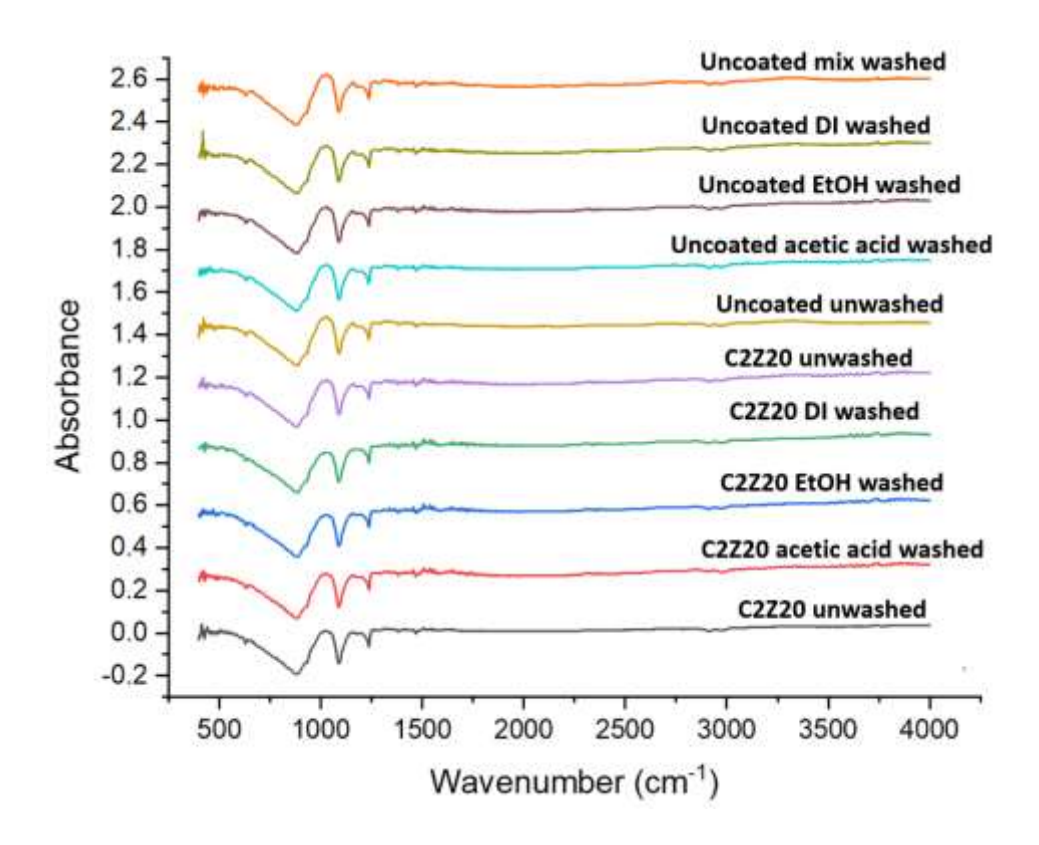


Figure A: FT-IR spectra of paper samples prepared from unwashed U-p as well as C2Z20-p fibers and fibers that had been washed with DI water, 2% acetic acid solution, 85% Ethanol solution for recyclability tests.

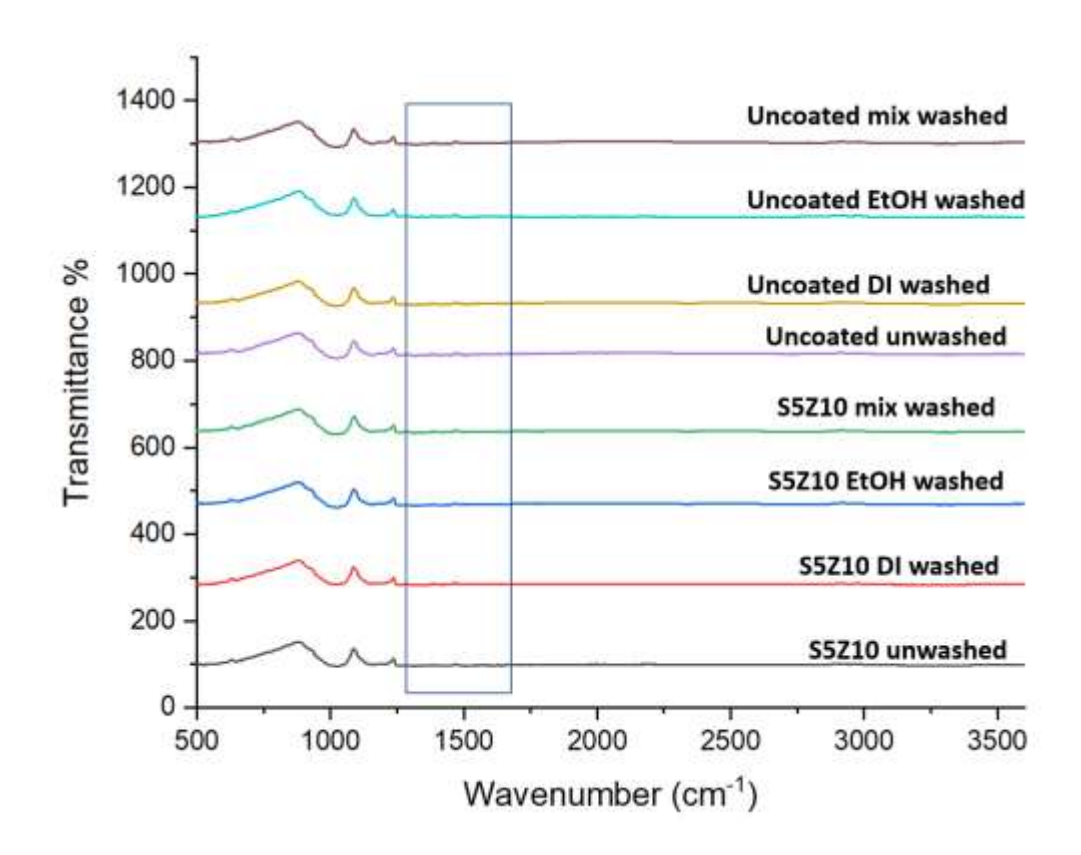


Figure B: ATR-FTIR spectra of paper samples prepared from unwashed U-p as well as S5Z10-p fibers and fibers that had been washed with DI water, 85% Ethanol solution, mixture of DI water and 85% Ethanol solution.

Calculation for degree of epoxidation:

Resonance of proton "a" = 2.01 ppm

Resonance of proton "b" = 1.50 ppm

Resonance of proton "c" = 2.90 ppm

A_{2,t} (peak area at 2.01 ppm in product)

 $A_{2,0}$ (peak area at 2.01 ppm in reactant) = 10.93

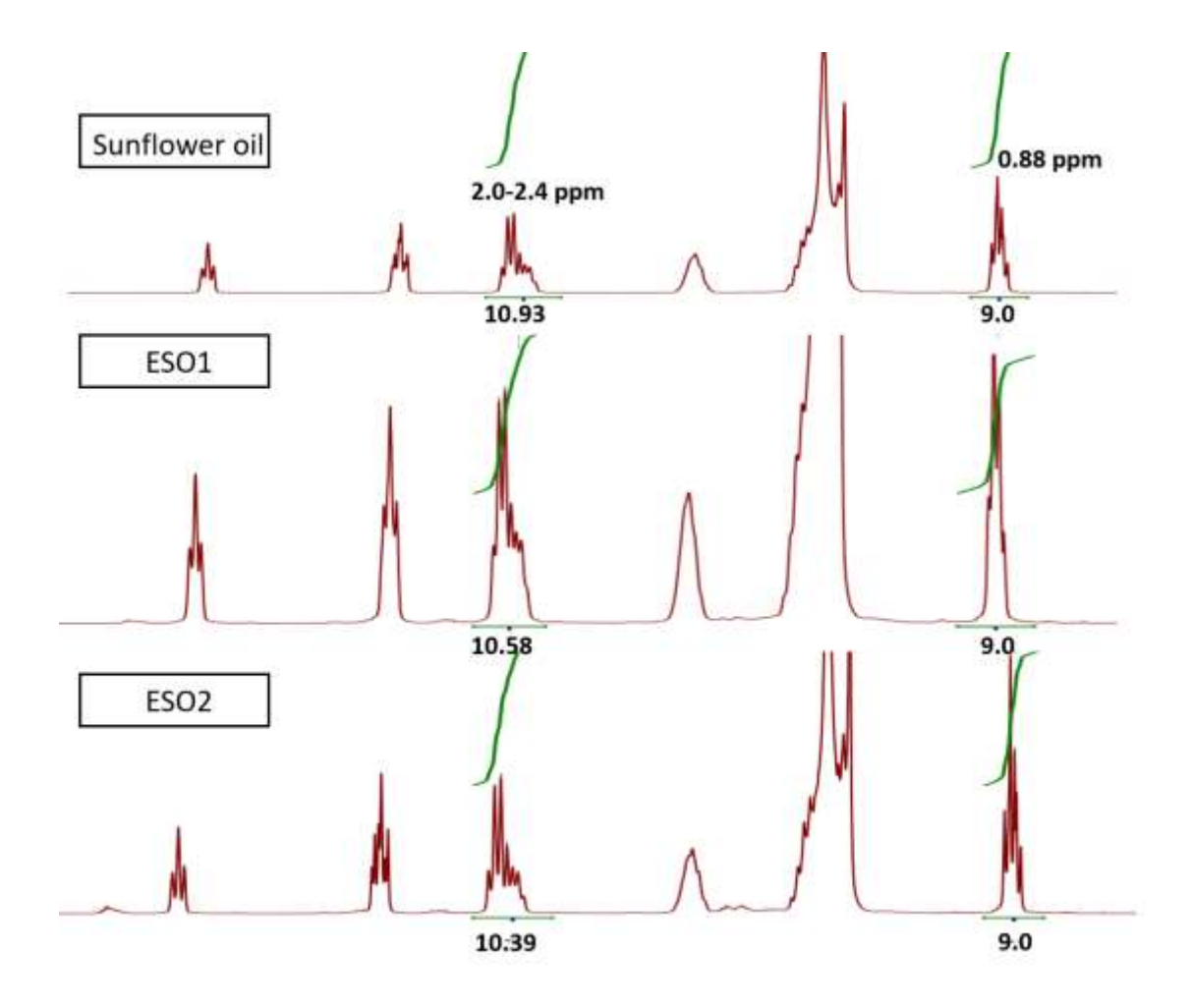
 $A_{s,t}$ (peak area of reference peak [taken for terminal -CH3 groups at 0.88 ppm]) in product = 9

 $A_{s,0}$ (peak area of reference peak at 0.88 ppm in reactant) = 9

 $N_{2.01}$ (number of protons of the signal at 2.01 ppm) = 4

 N_s (number of protons of the signal at 0.88 ppm) = 9

All the above numbers are determined from NMR shown below.



Degree of epoxidation (X) (%) = $100 \times \left[\frac{(N_s.A_{2,0}/N_{2.01}.A_{s,0}) - (N_s.A_{2,t}/N_{2.01}.A_{s,t})}{N_s.A_{2,0}/N_{2.01}.A_{s,0}} \right]$ (equation S1)

(1) Degree of epoxidation for SFO1:

Substituting the values in equation S1with $A_{2,t}$ = 10.58, degree of epoxidation was calculated to be 3.3%

(2) Degree of epoxidation for SFO3:

Substituting the values in equation S1with $A_{2,t}$ = 10.39, degree of epoxidation was calculated to be 5.1%

Model reactions:

We also conducted model reactions in order to investigate the nucleophilic attack of amines on epoxides in aqueous media and confirm the synthesis of CS-g-SO. Ethanol amine was selected as a model molecule for chitosan, and glycidyl methacrylate was utilized as a model compound for ESO. To understand the effect of pH, the reactions were performed at various pH values, including 4, 5, and 6. These pH values were chosen because chitosan is soluble at these pH values. From the ¹H NMR spectra, it was observed that no reactions had occurred at room temperature over a period of 2 h. However, after the temperature had been increased to 70 °C, a new multiplet was observed between 4.2 and 4.4 ppm while the peaks at 4.05 and 4.60 ppm had disappeared (Figure 4a, 4b). In addition, it was confirmed that similar results were obtained when the reactions were performed over the pH range from 4 to 6. We subsequently tried the reaction of ethanol amine with epoxidized sunflower oil at pH 4 and at different temperatures. The C-O-C epoxide peak at 2.92 ppm disappeared from the spectrum of epoxidized sunflower oil after heating at 70 °C for 6 h. Two triplets were observed at 3.87 and 3.11 ppm that respectively represented the newly formed C(H)OH and C(H)NH after the opening of the epoxide ring (Figure 4c and 4d). This confirmed that the epoxide ring opens upon reaction with an amine in water and therefore

one can conclude that the amine groups of chitosan participate in oxirane ring-opening reactions in aqueous acetic acid at $70\,^{\circ}$ C.

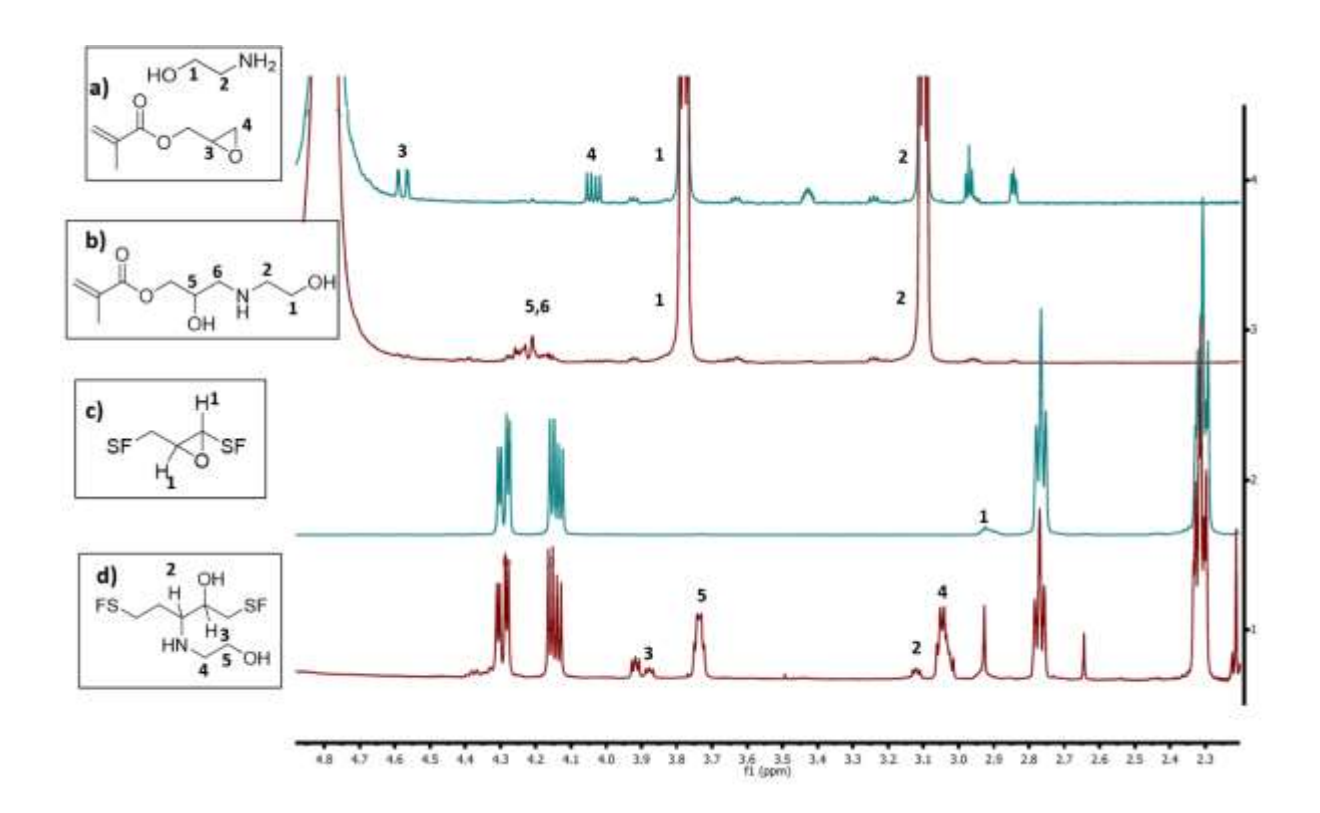


Figure D. ¹H NMR spectra that were recorded for model reactants and after their reactions, including those involving: **(a)** Ethanol amine and glycidyl methacrylate at room temperature, **(b)** ethanol amine and glycidyl methacrylate after heating at 70 °C for 2 h, **(c)** epoxidized sunflower oil (ESO1), and **(d)** ethanol amine-g-sunflower oil after heating at 70 °C for 6 h.

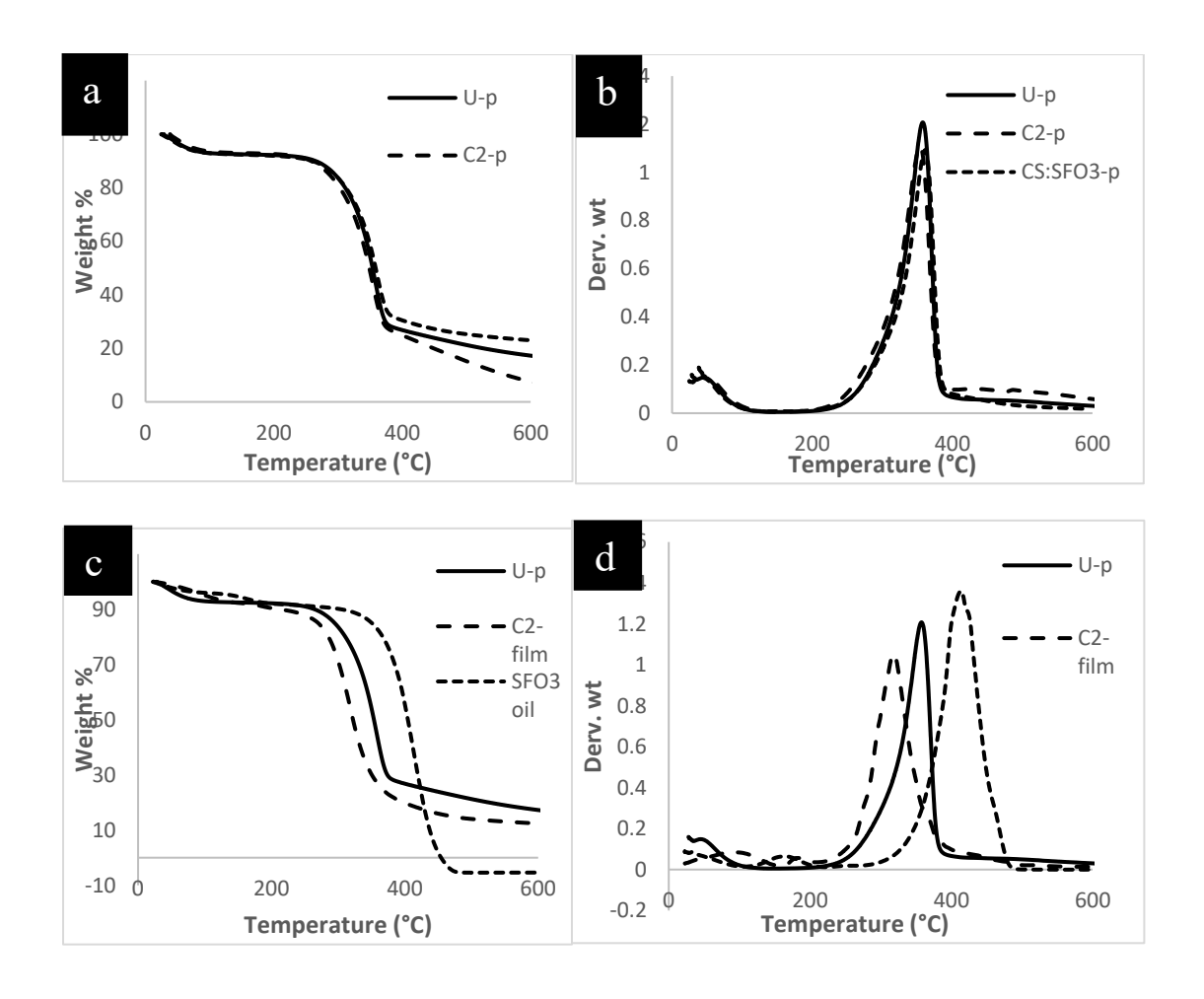


Figure E. (a)TGA and (b) DTG curves for uncoated and coated papers (c) TGA and (d) DTG curves of uncoated paper and material.